IMPLANTABLE DEVICES FOR SENSING AND DRUG DELIVERY IN OPHTHALMOLOGY AND RECONSTRUCTIVE SURGERY

by

Keng-Min Lin

A dissertation submitted to the faculty of
The University of Utah
in partial fulfillment of the requirements for the degree of

Doctor of Philosophy

Department of Mechanical Engineering

The University of Utah

December 2014

Copyright © Keng-Min Lin 2014

All Rights Reserved

The University of Utah Graduate School

STATEMENT OF DISSERTATION APPROVAL

The dissertation of **Keng-Min Lin**

has been approved by the following supervisory committee members:

Bruce Kent Gale	, Chair	**2014/06/09** Date Approved
Jayant Prasad Agarwal	, Member	**2014/06/10** Date Approved
Balamurali Krishna Ambati	, Member	**2014/04/16** Date Approved
Stacy Morris Bamberg	, Member	**2014/04/10** Date Approved
Kenneth LaVaun Monson	, Member	**2014/04/10** Date Approved

and by **Timothy A. Ameel** , Chair/Dean of

the Department of **Mechanical Engineering**

and by David B. Kieda, Dean of The Graduate School.

ABSTRACT

Implantable devices have the potential to solve current challenges in both physiological monitoring and drug delivery by introducing *in situ* measurement and treatment. In this dissertation, two types of implantable devices will be discussed. First, implantable devices for monitoring intraocular pressure (IOP) will be addressed. Second, implantable devices made of both nonbiodegradable and biodegradable materials for bridging a peripheral nerve gap by *in situ* drug delivery will be discussed.

Elevated IOP serves as a major factor that leads to glaucoma, a permanent vision loss disease, and a real-time monitoring implantable IOP sensor with polydimethylsiloxane membrane that was developed. This IOP sensor can be either implanted in the lens capsular bag after cataract surgery or sandwiched between the sclera and the conjunctiva; the latter being more favorable due to easy signal retrieval. For this approach, batch testing data showed a sensitivity of 0.67 mm/mmHg with the range of the device closely matching that expected for glaucoma patients.

Another medical challenge addressed in this dissertation is that peripheral nerve gaps longer than 10mm require special bridging techniques to repair. Autologous nerve grafts are the gold standard to repair peripheral nerve gaps; however, it possesses donor site deficit. Hence, a drug delivery device consisting of a nerve conduit for guided axon growth is proposed, fabricated and verified in this dissertation. Both nonbiodegradable materials and biodegradable materials were used to make the device that can deliver vascular growth factor, nerve growth factor (NGF), bovine serum albumin and polysaccharide. Furthermore, a bioactivity test verified that the NGF released from the

device was still bioactive in promoting axonal outgrowth on chick dorsal root ganglia explants. Two 3-week pilot animal studies in mice and rats also showed that the device is biocompatible with no noticeable inflammatory response. For the release kinetics, the device using diffusion through holes instead of a filter membrane had better consistency in release kinetics. Two mathematical models were also developed to identify the optimal design of the nerve conduit and the model was verified by an in vitro release study. Thus, the model will be used to help determine future nerve conduit designs.

For my family

TABLE OF CONTENTS

LIST OF TABLES

LIST OF FIGURES

LIST OF ABBREVIATIONS

APTES	Aminopropyltriethoxy silane
BSA	bovine serum albumin
BTMSPA	Bistrimethoxysilylpropylamine
Conc.	concentration
DMEM	Dulbecco's modified Eagle's medium
DRG	dorsal root ganglia
ELISA	Enzyme-linked immunosorbent assay
FBS	fetal bovine serum
GDNF	glial cell line-derived neurotrophic factor
GGF	glial growth factor
Hg	mercury
IOP	intraocular pressure
kDa	kilo Dalton
m.	muscle
mg	milligram
mL	milliliter
mm	millimeter
ng	nanogram
NGF	nerve growth factor
OCT	Optical coherence tomography
PANI	polyaniline

PBS	phosphate buffered saline
PCU	polycarbonate urethane
PDMS	Polydimethylsiloxane
PES	Polyethersulfone
pg	pictogram
PGA	polyglycolic acid
PHEMA-MMA	poly(2-hydroxyethyl methacrylate methyl methacrylate)
PLCL	polylactide co-caprolactone
PLGA	polylactic co-glycolic acid
PLLA	poly l-lactic acid
PMMA	Polymethylmethacrylate
PPE	polyphosphoester
PPY	polypyrrole
PU	polyurethane
rhNGF	recombinant human nerve growth factor
μg	microgram
μL	microliter
μm	micron
VEGF	vascular endothelial growth factor

ACKNOWLEDGMENTS

This work is funded by a University of Utah Research Foundation Seed Grant and United States Department of Defense Congressionally Directed Medical Research Program. The author would like to thank Dr. Bruce K. Gale for his continuous support and guidance during this PhD study, and previously during his MS study. This dissertation would not have been possible without his guidance and suggestions. The author also would like to extend his sincere gratitude to his supervisory committee members: Dr. Balamurali K. Ambati, Dr. Jayant P. Agarwal, Dr. Stacy M. Bamberg and Dr. Kenneth L. Monson. The author appreciates Dr. Himanshu J. Sant and Dr. Jill E. Shea for their assistance in this research.

The author would like to acknowledge his colleagues in the State of Utah Center of Excellence for Biomedical Microfluidics for their continuous help in the two projects. For the IOP sensor project, the author appreciates Corey Bishop, Dr. Michael Johnson, Raheel Samuel, Gregory Liddiard, Bonnie Archer, Tadashi Miya, Christina Mamalis and Scott Ho for their assistance. For the nerve conduit project, the author thanks Patti Larrabbee, Bonnie Archer, Dr. Srinivas Chennamaneni, Michael Burr, Dr. William Sanders, Dr. Christi Terry, Scott Ho, Dr. Matt Hockin, Dr. Yuxia He and Dr. Kelly Hewitt for their assistance.

CHAPTER 1

INTRODUCTION

Implantable devices providing *in situ* monitoring and drug delivery can potentially answer current clinical needs in both ophthalmology and reconstructive surgery. In this dissertation, an intraocular pressure (IOP) sensor using microfluidic concepts is presented and a discussion of the design, fabrication and characterization is provided. Then, a nerve conduit made of either nonbiodegradable or biodegradable materials is proposed, manufactured and verified.

Intraocular Pressure Sensors

Glaucoma is the second leading cause of blindness in the United States, and its primary symptom is elevated IOP [1]. Normal IOP is near 10mmHg, whereas higher IOP between 23 to 35mmHg, can cause hypertension inside the eye and result in glaucoma and eventual damage to sensitive eye tissues, leading to blindness.

Due to "white-coat compliance," where patients consume a drug right before visiting an ophthalmologist to ensure their symptoms are minimal [2], [3], detection of lethal-pulse, high IOP is difficult. Current IOP measurement uses a tonometer that measures cornea deflection caused by applied air-flow [4], giving the ophthalmologist an easy, relatively cheap way to estimate IOP. However it lacks accuracy because of assumptions of a "normal" cornea stiffness, while cornea stiffness varies from patient to patient, and has no ability to detect the harmful IOP peak [5]–[7]. Different approaches have been proposed and developed to acquire better accuracy in tonometry [8]–[15] but

none of them can provide accurate real-time IOP measurement.

Several researchers have proposed tonometric-type devices for measuring IOP, though all still rely on consistent and known cornea properties for accuracy. For example, Shaarawy *et al*. reported a wireless IOP monitoring system utilizing a disposable silicone contact lens to measure the change of the cornea curvature and transmit the signal through an antenna to an external device [12]. The change of cornea curvature due to changes in IOP [16] is one of the foundations for contemporary tonometers, and was utilized in this portable device to perform 24-hour IOP monitoring in which the sensor recorded the IOP value every 10 minutes. Another approach by Sahel *et al.* reported a soft contact lens with an embedded resonant gauge to record the change of the cornea curvature [13]. They first simulated the functionality of the contact lens to determine the relationship between the curvature of the cornea to the IOP read-out value, then they placed the lens on porcine cadaver eyes with solution injected to adjust the input IOP value. They also reported that the injection of fluids in the anterior chamber was better than in the posterior chamber because the former could produce small and constant IOP increases [13]. They showed that soft contact lenses could faithfully record the IOP value applied in the cadaver eyes. A third effort in this area by M. Leonardi *et al.* discussed another soft contact lens made of polyimide that could record IOP values based on different cornea curvatures [14], [15]. For the first approach of the device, it was connected to an external power source through wires [14] and was not feasible for daily use. Two pairs of "sensing-resistive strain gauges and compensation-resistive strain gauges" [15] were developed with a microprocessor transferring the curvature difference into IOP value and sending it to an external receiver through an embedded gold antenna

on the soft contact lens [15]. The fabrication process of this lens included microscale fabrication and cast molding. It achieved a 109μV/mmHg sensitivity when tested in porcine cadaver eyes with applied fluids as pressure source [15].

Though several methods have been proposed by Shaarawy, Sahel and Leonardi to improve contemporary Goldmann tonometer, they only changed the tonometer into a portable one so that it could perform 24-hour IOP monitoring. This did not solve the problem that the cornea curvature cannot faithfully transmit IOP value due to varying stiffness in the cornea [5], [6]. Although these sensors might have good sensitivity with low error in a controlled experiment, their success for real IOP measurements in humans is unknown since the stiffness of the cornea cannot be modified before or after the experiment. Thus, there remains a need for an accurate and inexpensive IOP measurement system. Other groups also use tonometer as a sensing mechanism on contact lens-typed IOP sensors [13], [17], but the problem of different cornea stiffness is inevitable.

Other types of IOP sensors that do not rely on cornea deflection have been proposed. These implantable sensors provide real-time IOP monitoring, and the ophthalmologist or the patient can access the IOP reading. Based on the sensing approach, these implantable sensors can be divided into three groups: capacitive pressure sensors, piezoresistive pressure sensors and unpowered pressure sensors.

Capacitive pressure sensors, which are the most wide-spread pressure sensors, convert pressure-induced parallel plate displacement into a capacitance difference associated with a changing distance between or overlapping area of two or more parallel plates [18], [19]. When a normal force is applied on the sensing plate of the capacitive

sensor and generates a corresponding pressure, the deformation of the plate will lead to shrinking of the distance between two or more parallel plates and therefore the capacitance of the parallel plates will increase. On the other hand, if one plate shifts due to a shearing force while the other plate remains fixed, the overlapping area of the two parallel plates will decrease and therefore the capacitance will decrease. Based on the direction of applied forces, the capacitance change can be detected by a custom integrated circuit. Other groups also use capacitive difference to construct IOP sensors. A group developed a capacitive IOP sensor with included antenna and showed a 1.6fF/mmHg sensitivity [20].

Compared to piezoresistive pressure sensors, capacitance pressure sensors provide higher sensitivity, low noise and power consumption [21], and have been widely used for automatic, medically related household appliances and so forth for decades. Several IOP examples have also been demonstrated. Wise *et al.* built intraocular pressure sensors, which converted contact area between the silicon diaphragm and the glass surface into capacitance change [22]. The sensing chamber in the sensor was under zero pressure. This was accomplished in the manufacturing process [23], and therefore "touch mode" was utilized to sense the applied pressure in absolute pressure reading between 550 to 850mmHg [22] at which the applied pressure will lead to stacking of the silicon diaphragm on the electro plate [23]. This embedded IOP sensor consisted of an antenna, a glass chamber with a custom integrated circuit (ASIC), another glass chamber with a solar-powered microbattery, and a silicon sensing portion was designed to be attached to the iris [22], [24]. In sum, this device can automatically wake up, take an IOP measurement, calculate the corresponding IOP value, store the value in its memory, and

transmit to the external receiver. However, the size of the device is limited due to space available on the iris that does not either block the pupil or scratch the cornea [22], and hysteresis as well as low sensitivity were observed on this sensor [22].

Another device proposed by P. Irazoqui *et al.* proposed a flexible IOP measurement device with a parylene-based capacitive IOP sensor, an integrated circuit (IC) and a nitinol antenna [25]. The device is flexible and small enough to be implanted in the anterior chamber of a mouse cadaver eye. Two designs were characterized and showed a 0.75fF/mmHg sensitivity in the dynamic range of 0-50mmHg relative to atmospheric pressure [25], as well as a resolution of less than 1mmHg. Because radio frequency (RF) is used to power the device, an imbedded battery is not required and this minimizes the dimension of the device [26]–[28]. However, both devices occupied the whole anterior chamber of the mouse cadaver eye, and thus light cannot go through the pupil and theoretically the mouse has no vision. Nevertheless, P. Irazoqui *et al.* did not report if the device was suitable for implanting in human cadaver eyes. The liquid crystal polymer substrate has no haptic to mount on the iris, and the device might move around in the anterior chamber of the human cadaver eye. Several similar designs were developed and tested to be implanted in either porcine [26] or the Ansoft Human Body Model [29]. They also implanted the device into mouse eyes and acquired a 1.5mHz/mmHg sensitivity [30].

Piezoresistive pressure sensors are based on materials whose resistivity changes under an applied force because the distance between the conduction band and the valence band changes [31]. The gap, or the energy difference between the two bands, will affect the mobility of electrons, and thus affect the resistivity of the material. Though the

piezoresistive pressure sensor consumes more power compared to capacitive pressure sensors [21], piezoresistive pressure sensors were still chosen by Ziaie *et al.* due to the low needed IOP measurement frequency. Contemporary IOP measurement can only be accomplished while visiting the doctor's office, and any improvement to this, for instance, measuring IOP twice a day, is better than the current technique. Therefore, though the piezoresistive pressure sensor cannot perform IOP measurement every 15 minutes [22] like some of the other proposed sensors, it is still an improvement over the current tonometer-based IOP sensing technique. Ziaie *et al.* reported several intraocular pressure monitoring systems utilizing the piezoresistive change of doped silicon to determine the applied pressure [32]. In these systems, implanted between the sclera and choroid, the sensing membrane registered the piezoresistive change and sent the measured change to an external device which converted the signals into pressure values. They proposed two ways to mount the sensor on the eye. Fixed IOP sensors were mounted on the eye by directly attaching them to a miniature positioning stage, and then sutured on the sclera [32]. These IOP sensors compared the IOP measured values with applied IOP values and generated calibration tables. Though these devices were too big to function *in vivo*, they showed that sensing between the sclera and choroid was feasible and therefore this work will use this approach, as will be discussed later. Another group also developed a piezoresistive IOP sensor, which used parylene as the substrate with a coating membrane and embedded circuits. The complete sensor is rollable for easier implantation. The measured sensitivity was 0.1mbar [33].

Inductor based IOP sensors have also been proposed in which the vibration of two parallel plates will be recorded and calibrated according to applied pressure. An IOP

sensor with the sensing coil embedded in a SU-8 negative photoresist package can achieve a 3770ppm/mmHg in saline solution, with the resolution of less than 1mmHg [34].

Unpowered pressure sensors use purely mechanical systems to monitor IOP change. Since they need no power supply, the volume and complexity of the sensor can be simplified, and the cost per sensor can be decreased dramatically.

When air is injected in a hollow helix tube, it will tend to flatten the tube due to difference in bending moment on the two sides of the tube, and thus the tip of the tube will rotate and the curvature of the tube will increase [35], [36]. This tube is known as Bourdon tube, proposed in the 18th Century.

Tai *et al.* reported three kinds of unpowered parylene-based IOP sensors with different Bourdon tube designs [36]–[40]. A customized 19 gauge needle was used to carry the sensor and penetrate through the cornea. The incision was less than 3mm and therefore suturing after surgery was not required [36], [41]. The sensor was placed on the iris due for both ease of optical readout and appropriate pressure sensing [37]. Mounting tests were performed on the iris of rabbit eyes to demonstrate that secure placement was achieved. Parylene posts were used to secure the device on the iris [37]. IOP reading tests were performed *in vitro* and *ex vitro* with designs developed to amplify the readout and increase the sensitivity. These Bourdon-tube IOP sensors had a sensitivity of 0.67degree/mmHg, 3.43μm/mmHg and 0.38μm/mmHg in different designs. Although this approach has an advantage of simplifying the design, it has the potential to block incoming light through the pupil at night since this device occupied lots of space on the iris. A comparison of different sensors based on sensing mechanism, sensing material,

signal transmission mechanism, signal transmission material and energy source were shown in Table 1.

Table 2 shows a comparison of different sensors in sensitivity, resolution, location of the sensor and dynamic range.

The various capacitive pressure sensors, piezoresistive pressure sensors and Bourdon-tubed IOP sensors that have been proposed all addressed some concerns regarding IOP measurement, but none were ideal or resolved all of the existing concerns with commercially available tonometers. Thus, we propose to continue development in this area and propose an unpowered IOP sensor designed to solve contemporary IOP monitor issues.

The goal of the IOP sensor proposed in this dissertation is to estimate actual IOP value without measuring the cornea deflection, which is a known issue leading to inaccurate IOP estimates.

Nerve Conduits for Peripheral Nerve Regeneration

Introduction to Socioeconomic Effects

Three hundred and sixty thousand people in United States and 300,000 in Europe suffer from upper extremity paralytic syndromes each year [42]. More than 200,000 nerve repair procedures are performed each year in the United States [43]. Many workers miss days due to the loss of motor or sensory functions of extremities [44]. In addition to acute nerve injury, chronic neuropathic pain can affect patients' quality of life and lead to a variety of effects including sleep interruption [45], [46].

Peripheral nerve injuries also affect 2.8% of trauma patients [49] and significantly reduce their quality of life. Most nerve repair surgeries have poor outcomes in motor,

Table 1 Comparison of different sensors in: sensing mechanism, sensing material, signal transmission mechanism, signal transmission material and energy source

Group	**Sensing Mechanism**	**Sensing Material**	**Signal Transmission Mechanism**	**Signal Transmission Material**	**Energy Source**
[22]–[24]	Capacitance [22]–[24]	Boron-doped silicon diaphragm with Cr/Au electrode plates [22]	Radio frequency	Antenna	Solar-powered battery [22], [24]
[25], [27][47]	Capacitance	Two Ti/Au membranes	Radio frequency	Nitinol antenna	RF wireless charging [27], [29], [48]
[26]	Capacitance	Not reported	Radio frequency	Antenna	RF wireless charging [27], [29], [48]

Table 1 (continued)

Group	**Sensing Mechanism**	**Sensing Material**	**Signal Transmission Mechanism**	**Signal Transmission Material**	**Energy Source**
[29]	Capacitance	Not reported	Radio frequency	Antenna	RF wirelessly charges a high dielectric ceramic capacitor [29]
[36]–[40]	Bourdon tube	parylene-C [36]	Not reported	Not reported	Not required
Author's research	Microfluidics	IC-Green or AK-Fluor	Visual or optical coherence tomography	Not required	Not required
[32]	Piezoresistive	Not reported	Wire connection	Wire	External power source
[12]	Strain gauge	Platinum-titanium	Radio frequency	Antenna	Not reported

Table 1 (continued)

Group	**Sensing Mechanism**	**Sensing Material**	**Signal Transmission Mechanism**	**Signal Transmission Material**	**Energy Source**
[13]	Resonance gauge	Not reported	Not reported	Antenna	Not reported
[14], [15]	Two pairs of "sensing-resistive strain gauges with compensation-resistive strain gauges"[15]	170nm Platinum and 25nm titanium [15]	Not reported	Gold antenna [15]; Wire [14]	Wireless powering [15]; Link to an external power source through wires [14]

Table 2 Comparison of different sensors in: sensitivity, resolution, location of the sensor and dynamic range

Group	**Sensitivity**	**Resolution**	**Location of the Sensor**	**Dynamic Range**
[22]–[24]	26fF/mmHg[22]	Not reported	On the iris of a human cadaver eye with the cornea removed [22]	-210~90mmHg (absolute pressure 550~850mmHg) [22]
[25], [27], [47]	0.76fF/mmHg for the initial device with poor resolution [25], [27]. 0.3fF/mmHg for the next device with better IC and with better resolution (<1mmHg) [25]	>1mmHg for the initial device; <1mmHg for the next device [25]	Anterior chamber of a mouse cadaver eye	0-50mmHg [25]; 0-60mmHg [27]
[26]	Not reported	Not reported	Porcine eye	Not reported
[29]	6.64fF/mmHg [29]	0.5mmHg [29]	Anterior chamber of an Ansoft Human Body Model	0-50mmHg [29]
[36]–[40]	8.72μm/mmHg in *ex vivo* sample [36]. 0.67degree/mmHg for spiral design [40]. 3.43μm/mmHg for long-armed design [40]. 0.38μm/mmHg for serpentine-tube design [40]	3.56mmHg for *in vitro* sample [36]	Mount on the iris [36]	29-88mmHg for *ex vivo* sample [36]
Author's research	0.061mm/mmHg for the dynamic range between 0-22mmHg; 0.667mm/mmHg for the dynamic range between 22-50mmHg	Varied between 2-5mmHg	Between the conjunctiva and the sclera of either human, porcine or rabbit eyes.	0-50mmHg
[32]	Not reported	7.35mmHg [32]	Between the sclera and choroid in three human cadaver eyes	10-47mmHg [32]

Table 2 (continued)

Group	**Sensitivity**	**Resolution**	**Location of the Sensor**	**Dynamic Range**
[12]	Not reported	Not reported	Outside of the cornea of live human eye	Not reported
[13]	Not reported	Varied between 2-7mmHg	Outside of the cornea of porcine cadaver eyes	Either 0-25mmHg or 0-78mmHg [13]
[14], [15]	109μV/mmHg [15]	1mmHg [15]	Outside of the cornea of porcine cadaver eyes	20-30mmHg [15]

sensory and pain functions [50] with contemporary treatments [45], spurring research into alternative methods to address this clinical need.

Clinical Rationale

Based on Sunderland Classification [51], nerve damage can be classified into five grades: neuropraxia, axonotmesis, neurotmesis with preservation of the perineurium, neurotmesis with preservation of the epineurium, and complete transaction of the nerve trunk [52]. Most of the Grade 1 (neuropraxia) patients can fully recover without any surgery since only some blockage of electrical and chemical signals in axon transmission occurs in this stage, and no mechanical or physical break of the nerve has occurred. For Grade 2, since only the integrity of the axon is broken, with proper treatment (e.g., providing nerve growth factor), repair will by itself because the endoneurium will guide the axon to grow properly. However, in Grades 3-5, due to the fact that the nerve is actually cut, or even a particular part is missing in the worst case scenario, physical bridging is required to guide the axon to grow to the distal site on the patient.

About 87.4% of upper limb nerve injuries could be repaired by end-to-end approximation, while 1.8% of upper limb nerve injuries require grafts or another form of bridge to connect the two nerve stumps [53]. End-to-end tension-free severed nerve re-approximation is performed for peripheral nerve gaps less than 10mm, while special bridging techniques are required for gaps larger than 1-2cm [52]. For those requiring bridging techniques, nerve autografts are the gold standard, but still have some limitations, such as donor site deficits or morbidity [54], [55], possible disease spread and secondary deformity [56]. Thus, there is significant need for methods of nerve repair that avoid these concerns. Because short distance nerve conduits and autografts can achieve

similar functional outcomes for regeneration [57], research has been conducted using a nerve conduit to repair the peripheral nerve gap due to its more flexible selection [58]. Several options have emerged to improve outcomes in repairing peripheral nerve gaps. These include artificial nerve grafts, cadaver grafts and nerve conduits. Nerve conduits made with either natural or synthetic materials have been used to guide axons and bridge nerve gaps ranging from 5 to 80mm [59]. Design and outcome of various kinds of nerve conduits will be discussed in the following sections.

Various Nerve Conduits and Their Outcome

Autologous grafts (autografts) are the gold standard for repairing peripheral nerve gaps greater than 10mm. Currently, nerves with less important functions are used to serve as autografts, such as superficial nerves, sural nerves and lateral antebrachii cutaneous nerves [60]. However, autografts have the drawbacks of donor site deficits in which not only is a proper donor nerve hard to find for particular clinical application, but a significant risk of forming a neuroma in the donor site is expected [60]. Therefore, various studies have been proposed and conducted in order to build a nerve conduit to replace an autograft in repairing peripheral nerve gaps of more than 10mm. These materials include natural and synthetic materials, which will be discussed in the following paragraphs. The materials to form the nerve conduits can be either collagen, polyaniline (PANI), polyglycolic acid (PGA), poly 2-hydroxyethyl methacrylate methyl methacrylate (PHEMA-MMA), polylactide co-caprolactone (PLCL), polylacticcoglycolic acid (PLGA), poly l-lactic acid (PLLA), polyphosphoeaster (PPE), polypyrrole (PPY) or polyurethane (PU). Table 3 shows a comparison of different nerve conduits in material, drug, result, animal and target.

Table 3 Comparison of different nerve conduits in: material, drugs, results, animals and targets

Reference	Material	Drug	Result	Animal/target
[61]	Collagen	GDNF & NGF	Both GDNF and NGF were bioactive after 30 days of release study	Chick/ dorsal root ganglia explants.
[58]	Collagen	n/a	Both the electrophysiological and histomorphometry showed a similar outcome for the autograft or the collagen repaired groups.	Monkey/ ulnar or median nerve. Gap size of 5 to 15mm. Experimental period: 70day inspection, and a total of 3.5 years.
[62]	PLGA-coated collagen	Collagen	The group bridged with PLGA-coated collagen tubes filled with collagen gel had better outcomes in both electophysiology and morphology compared with another group bridged with collagen-filled vein grafts.	Rabbit/ peroneal nerve. Gap size of 15mm. Experimental period: 12 weeks.
[63]	Collagen	Controlled collagen gel or magnetically aligned collagen gel	The group bridged with the supply of magnetically aligned collagen gel showed superior outcomes in distal axon density after 30 days post surgery compared to the group with either the supply of control collagen gel or without supply in repairing both 4mm and 6mm gaps.	Mouse/ sciatic nerve. Gap size of 4mm or 6mm. Experimental period: 30 or 60 days.
[64]	PGA-collagen	NGF, fibroblast growth factor and laminin-containing gel	Five months after the implantation, presence of myelinated, unmyelinated axons and Schwann cells was confirmed. Electrophysiology also showed a recovery of sensory function 5 months after the implantation.	Cat/ sciatic nerve. Gap size of 25mm. Experimental period: 4-16 months.

Table 3 (continued)

Reference	Material	Drug	Result	Animal/target
[65]	PGA-collagen	Laminin-soaked collagen sponge	Walking track analysis showed a similar result for the group bridged with PGA-collagen tube compared to the normal uninjured group. Histology showed a relatively high quantity of immature axon at the distal nerve stump.	Dog/ peroneal nerve. Gap size of 80mm. Experimental period: 12 months.
[66]	Collagen or silicone	Collagen-glycosaminoglycan matrix	The collagen-glycosaminoglycan-filled collagen tube could achieve a similar result in electrophysiology and histomorphometry compared with autograft, and had a superior result over empty collagen or silicone tubes in axon size and quantity.	Rat/ sciatic nerve. Gap size of 10mm. Experimental period: 60 weeks.
[67]	(solid bar) collagen	n/a	The number of myelinated axons at the distal nerve stump was bigger when bridged with collagen filaments compared to autografts.	Rat/ sciatic nerve. Gap size of 20mm. Experimental period: 8 weeks.
[68]	PHEMA-MMA hydrogel	n/a	Sixty percent of the group repaired with PHEMA-MMA hydrogel conduits showed similar results in electrophysiological response compared with the group treated with autografts.	Rat/ sciatic nerve. Gap size of 10mm. Experiment period: 16 weeks.

Table 3 (continued)

Reference	Material	Drug	Result	Animal/target
[69]	PHEMA-MMA hydrogel	Either collagen matrix, collagen with neurotropin-3, collagen with brain-derived neurotrophic factor, or collagen with acidic fibroblast growth factor	The conduit with higher dosage of acidic fibroblast growth factor could produce the best result in fiber density in the conduit, and this result was similar to the group repaired with autografts.	Rat/ sciatic nerve. Gap size of 10mm. Experiment period: 8 weeks.
[70]	PHEMA-MMA hydrogel	Fibroblast growth factor-1	The coil-reinforced PHEMA-MMA hydrogel conduit with fibroblast growth factor-1 coating showed similar results in both electrophysiology and histomorphometry compared to autograft	Rat/ sciatic nerve. Gap size of 10mm. Experiment period: 16 weeks.
[71]	PHEMA-MMA hydrogel	NGF	NGF-loaded microspheres or NGF-incorporated channel could deliver NGF constantly in the 28-day period compared to the NGF-imbibed channel	No animal model.
[72]	PGA	n/a	The PGA-bridged group showed better functional recovery compared to end-to-end reapproximation (for gaps less than 4mm) or autografts (for gaps greater than 8mm)	Human/ digital nerves. Gap size of either less than 4mm or greater than 8mm. Experiment period: 12 months [59].

Table 3 (continued)

Reference	Material	Drug	Result	Animal/target
[73]	PLCL	n/a	The PLCL-bridged group showed a similar axonal regrowth in length compared to autografts. It also showed a similar sensory recovery compared to the group bridged with autografts.	Human/ digital nerves. Gap size of lesser than 20mm. Experiment period: 12 months.
[74], [75]	PLLA	Schwann cells	PLLA conduits coated with Schwann cells showed better outcomes in both 2-month gastrocnemius muscle loss comparison and 4-month axon density test at distal nerve stumps.	Rat/ sciatic nerve. Gap size: 12mm. Experiment period: 4 months.
[76]	PPE	n/a	PPE conduits with higher molecular weight had better outcome in the reflex test on the repaired sciatic nerve.	Rat/ sciatic nerve. Gap size: 10mm Experiment period: 3 months.
[77]	Silicone conduits filled with NGF-encapsulated PPE microspheres	NGF	The group with NGF-encapsulated PPE microsphere had better ratio for axonal regrowth (4 out of 6 works) compared to the NGF-only group (3 out of 6 works) and empty group (none works).	Rat/ sciatic nerve. Gap size: 10mm Experiment period: 2 weeks.
[78]	PPE conduits filled with NGF-loaded PPE microspheres	NGF	The NGF-loaded PPE microsphere had better outcomes over the control groups in morphological analysis of fiber diameter, fiber population and fiber density	Rat/ sciatic nerve. Gape size: 10mm Experiment period: 3 months.

Table 3 (continued)

Reference	Material	Drug	Result	Animal/target
[79]	PLGA (85/15)	GGF & Schwann cells	GGF-only foam conduit had higher axon numbers compared to the one with both GGF and Schwann cells. The foam conduit with both GGF and Schwann cells had higher myelination index and fastest conduction velocity compared with the GGF-only group.	Rat/ sciatic nerve. Gap size of 10mm. Experiment period: 12 weeks.
[80]	PLGA (85/15)	Schwann cells	The PLGA foam conduit with Schwann cells had a denser axon distribution at the middle of the gap compared to the one bridged with autografts.	Rat/ sciatic nerve. Gap size of 7mm. Experiment period: 6 weeks.
[81]	PLGA (75/25)	Pluronic F127	In histology, the group bridged with Pluronic F127-coated PLGA conduits showed a faster (4 weeks earlier) physical recovery compared to the group bridge with empty PLGA conduits or empty silicone conduits. In electrophysiological testing, the group with Pluronic F127-coated PLGA conduit transmitted the signal faster compared to the other two groups after 24 weeks	Rat/ sciatic nerve. Gap size of 10mm. Experiment period: 24 weeks.
[82]	PLGA (90/10)	n/a	These empty PLGA conduits could promote peripheral nerve regeneration in rats.	Rat/ sciatic nerve. Gap size of 12mm. Experiment period: 9 weeks.

Table 3 (continued)

Reference	Material	Drug	Result	Animal/target
[83]	PU	n/a	At 4-week postoperation, functional recovery was achieved in both walking track analysis and electrical stimulation. Histology data also show that axons are denser at distal nerve stump after 8 weeks of repair compared to the one after 4 weeks.	Rabbit/ femoral nerve. Gap size of 12mm. Experiment period: 6 months.
[84]	Collagen-PU	n/a	The group treated with collagen-PU bilayer conduit had better outcome in histology, walking track analysis and electrophysiological tests compared to the PU-only conduits.	Rat/ peroneal nerve. Gap size of 10mm. Experiment period: 6 weeks.
[85]	PU	ACTH4-9 NGF	The group treated with NGF-loaded PU conduits had a similar result in electrical stimulation test compared with the one treated with autograft. The group with NGF-loaded PU conduits showed denser axon compared to the group with autograft.	Rat/ sciatic nerve. Gap size of 8mm. Experiment period: 16 weeks.

Natural Materials

An environment that more successfully mimics a biologic environment can be generated by natural materials due to the extracellular matrix that will create a cell-adhesive surface to possibly reduce foreign body response and fibrosis [59].

Collagen

Due to the fact that collagen is a key element in the extracellular matrix, collagen is suitable for forming the nerve conduits for repairing peripheral nerve gaps. One study showed that collagen tubes can store and deliver both glial cell line-derived neurotrophic factor (GDNF) and nerve growth factor (NGF) for a 30-day period, and the bioactivity of both GDNF and NGF was verified with chick DRG cells [61]. Another study showed that empty collagen conduits can achieve similar results in both histomorphometry and electrophysiology studies to repair 5 to 15mm gaps on monkey ulnar or median nerves compared to the autograft group [58]. Another study created a 15mm gap on the peroneal nerve of rabbits and showed that PLGA-coated collagen conduits filled with collagen gel can achieve better electrophysiological and morphological outcomes compared to the group bridged with collagen-filled vein grafts [62]. Another study used a different design of collagen tubes to bridge either a 4mm or a 6mm gap on mouse sciatic nerves, and it showed that the group with the supply of magnetically aligned collagen gel has superior outcomes in distal axon density 30 days post surgery compared to the groups with either the supply of control collagen gel or without supply in repairing both 4mm and 6mm gaps[63]. Another study focused on repairing a long gap distance by first repairing a 25mm gap on cat sciatic nerves with a PGA-collagen conduit filled with laminin-containing gel with NGF and fibroblast growth factor for 4 to 16 months. Five months

after the implantation, they confirmed the presence of myelinated, unmyelinated axons and Schwann cells [64]. Electrophysiology also showed a recovery of sensory function at 5 months after the implantation. In a subsequent study, these researchers used a PGA-collagen conduit filled with laminin-soaked collagen sponge to bridge an 80mm gap created on dog peroneal nerve for 12 months. Walking track analysis revealed a similar result to the normal uninjured dog, though histology shows a relatively high quantity of immature axons at the distal nerve stump 12 months post surgery [65]. Another study compared empty collagen tubes, empty silicone tubes, autografts and collagen-glycosaminoglycan-filled collagen tubes to bridge 10mm gaps on rat sciatic nerves for 60 weeks and showed that the group with the supply of collagen-glycosaminoglycan matrix in a collagen tube has the superior outcome in axon size and quantity compared to the other groups bridged with either empty collagen or silicone tubes. The histomorphometric and electrophysiological results of the group bridged with collagen-glycosaminoglycan-filled collagen tubes are similar to the group bridged with autograft [66]. Yet another sutdy used collagen as a solid bridge to repair a 20mm gap created on rat sciatic nerves for 8 weeks. It showed that the number of myelinated axons at the distal nerve stump is greater compared to the group bridged with autografts after 8 weeks [67].

Synthetic Materials

An advantage of synthetic materials is that a custom property (e.g., degradation rate) and structure are relatively easy to acquire compared to natural materials. In addition, a more consistent structure can be achieved compared to natural materials.

Conductive Polymers

A study showed that electric stimulation from conductive polymers such as PPY and PANI could promote local nerve regeneration by stimulating neurite outgrowth [86].

Hydrogel

A 16-week study used PHEMA-MMA to form 12mm long hydrogel conduits for repairing 10mm nerve gaps created on rat sciatic nerves [68]. It showed that 60% of the group repaired with PHEMA-MMA hydrogel conduits had similar results in electrophysiological response compared to the group bridged with autografts. Prior to this study, a preliminary study conducted by the same group showed that the PHEMA-MMA conduit would cause some chronic inflammation when repairing 10mm gaps on rat sciatic nerves [87], and this research group indicated that a further study would be conducted to increase the biocompatibility of the conduit. Another study filled a 12mm long PHEMA-MMA hydrogel conduit with either collagen matrix, collagen with neurotropin-3, collagen with brain-derived neurotrophic factor, or collagen with acidic fibroblast growth factor to bridge 10mm nerve gaps on rat sciatic nerves for 8 weeks [69]. It showed that the conduit with higher dosage of acidic fibroblast growth factor could lead to the best result in fiber density inside the conduit, which was similar to the group repaired with autografts. Another study showed that a coil-reinforced PHEMA-MMA hydrogel conduit with fibroblast growth factor-1 coating could achieve similar results in electrophysiology and histomorphometry compared to autograft when bridging a 10mm gap on rat sciatic nerve for 16 weeks [70]. Another study compared three ways to incorporate NGF into a PHEMA-MMA hydrogel channel and found that NGF-loaded microspheres or NGF-incorporated channels could deliver NGF constantly in the 28-day

period compared to the NGF-imbibed channel [71], but no animal data were available for this study.

Polyglycolic Acid (PGA)

A study used a PGA conduit without a supply of drug to repair human digital nerve gaps (n=120) from less than 4mm or greater than 8mm and showed a better sensory recovery compared to end-to-end re-approximation (for gaps less than 4mm) or autografts (for gaps greater than 8mm) [72].

Polylactide Co-caprolactone (PLCL)

A study showed that a PLCL conduit without the supply of drug was able to achieve similar axonal regrowth and sensory recovery for human hand nerves (n=30) for a 12-month period compared to autografts [73].

Poly L-lactic Acid (PLLA)

A study compared the results for Schwann cell-coated PLLA conduits with empty silicone conduits, isografts and collagen-filled PLLA conduits to bridge a 12mm gap on rat sciatic nerves. For gastrocnemius muscle loss comparison, the PLLA conduits coated with Schwann cells showed a superior result compared to the other groups 2 months after the implantation. It also showed that a higher density of axons was found at the distal nerve stump in the group treated with Schwann cell-coated PLLA conduits 4 months after the implantation [74], [75].

Polylactic Co-glycolic Acid (PLGA)

A study showed that PLGA nerve conduits with the supply of glial growth factor (GGF) and/or Schwann cells implanted in rat for 12 weeks could successfully promote

axonal outgrowth through a 10mm gap, and the GGF-only group had denser axon, while the combination of GGF and Schwann resulted in higher myelination index and faster conduction velocity [79]. Another study showed an 85/15 PLGA foam conduit with diameter from 60 to 550 μm coated with Schwann cell could bridge a 7mm sciatic nerve gap on rat models for 6 weeks, with a higher axon density in the middle of the gap compared to the group treated with autografts [80]. Another study also showed that PLGA pellets could deliver recombinant human NGF (rhNGF) consistently in a 14-day diffusion chamber study [88], and the NGF was released from the PLGA microspheres through hydrolysis of PLGA [89]. Another study using Pluronic F127-coated 75/25 PLGA conduits showed that a faster recovery rate (4 weeks versus 8 weeks in repairing a 10mm gap on rat sciatic nerves) was found compared to empty PLGA conduits. It also showed that a faster electrophysiological signal transmission was found in the group treated with Pluronic F127-coated PLGA conduits compared to the group with empty PLGA conduits at 24 weeks postimplantation [81]. The other study showed even an empty 90/10 PLGA conduit was able to promote peripheral nerve regeneration on a 12mm gap on rat sciatic nerves in a 9-week period [82].

Polyphosphoester (PPE)

PPE shows a better hydrolysis degradability because the phosphoester linkage is easier to cleave compared to the ester linkage in PLGA [59]. A study implanted two groups of empty PPE conduits with different molecular weight (15kDa and 19kDa) in rats (n=12) to bridge a 10mm gap created on sciatic nerves for a period of 3 months. It showed that the conduit with higher molecular weight had better outcomes in reflex test on the repaired sciatic nerve [76]. The same group also compared NGF-encapsulated

PPE microspheres suspended in saline, NGF dissolved in saline and empty silicone conduit to bridge 10mm gaps in rat sciatic nerves for 2 weeks. It shows that the group with NGF-encapsulated PPE microspheres had better chances to promote axonal regrowth to the distal nerve stump (4 out of 6 worked) compared to the NGF-only group (3 out of 6 worked) and empty conduit group (0 worked) [77]. Therefore, they filled PPE conduits with these NGF-loaded PPE microspheres and started another 3 months implantation study to bridge 10mm gaps on rat sciatic nerves. It showed better outcomes in morphological analysis of fiber density, diameter and population compared to the control groups [78].

Polyurethane (PU)

PU has been used to construct nerve conduits because of its flexibility, which can be an advantage in some implantation places that require frequent motion. A study used 20mm nerve conduits made of PU to repair 12mm gaps on rabbit femoral nerve for a period of 6 months [83]. It showed that these drug-free conduits could result in functional recovery in both walking track analysis and electrical stimulation at 4-week postoperation. It also showed that at 8-week postoperation, the axon at the distal nerve stump was denser compared to the one at 4-week postoperation. The same researchers later embedded a collagen tube into the PU nerve conduit in order to allow better nutrient transportation in the nerve conduit. This study used this bilayer PU-collagen nerve conduit to bridge a 10mm gap created on rat sciatic nerve for a period of 6 weeks. The group with bilayer conduit had a better result in histology, walking track analysis and electrophysiological tests compared to the PU-only conduits [84]. Another study also used PU to construct a nerve conduit, but loaded the conduit with ACTH4-9 NGF to

repair an 8mm gap on rat sciatic nerve for a period of 16 weeks. It showed that the PU nerve conduit could achieve a similar result in electrical stimulation test compared with the group treated with autograft. It also showed that axons were denser at the proximal nerve stump in the group treated with these PU nerve conduits compared to the group treated with autografts [85]. The other study used polyester urethane nerve conduit to repair an 8mm gap created on rat sciatic nerve for 24 weeks for a preliminary degradation study and showed that the nerve conduit could degrade four weeks post implantation [90].

Innovation of the Nerve Conduit Proposed in This Study

Due to the fact that empty nerve conduits can achieve comparable results to autografts when the gap size is smaller than 5cm in humans, or 1.5cm in rats [59], nerve conduits will provide a starting point and then be filled with protein or drug to stimulate axonal regrowth. The combination of drug delivery and physical nerve guidance is hypothesized to lead to better nerve regeneration outcomes.

Though some tissue-engineered conduits provide results comparable or superior to autologous grafts [91], [92], it is difficult to switch the neurotrophin or protein in the device to fit different target nerve gaps. In addition, the use of various drug delivery mechanisms, such as microspheres, coatings, collagen sponges or filling with neurotrophin solution in the lumen of singe conduits, suffers from a lack of flexibility in choosing various drugs and drug concentrations when used with different types of peripheral nerve repair surgery. Thus, a device that is easily customizable in both dimensions and drugs (growth factors) of interest is proposed in this paper. NGF was chosen as the drug delivered in the project because not only are there fewer adverse effects observed when using NGF over other proteins or cells as the stimulant for axon

growth [57], but also because denser axon branches are observed in chick DRG cells when treated with NGF over GDNF [93], [94]. Research has shown that locally delivered NGF can accelerate sciatic nerve regeneration [95]–[97].

The work included in this dissertation proposes a new, easily tailored approach to delivering drugs to treat peripheral nerve gaps. The general concept is to create a nerve guidance conduit surrounded by a drug reservoir that delivers drug into the lumen of the conduit, thereby encourage rapid, directed nerve growth. Switching drugs should be straightforward as the kinetics of release can readily be modeled and calculated, in comparison to techniques that require material degradation. This work focuses on a PDMS device that implements the critical functions of the proposed device, followed by a biodegradable PLGA device in a more advanced study with *in vivo* data.

The advantage and biocompatibility of polydimethylsiloxane (PDMS) have been addressed in the previous section of this dissertation to form an IOP sensor. PDMS with the same recipe will be used to form the prototypes of the concentric nerve conduits, with bovine serum albumin (BSA), vascular endothelial growth factor (VEGF), nerve growth factor (NGF) and Dextran used as the drug or test molecule of interest to reveal the release function of the device.

After testing prototypes made of PDMS, PLGA with a 75/25 PLA/PGA copolymer ratio was chosen to form the biodegradable nerve conduit discussed in this dissertation due to its moderate degradation time compared to 50/50 or 85/15 PLGA polymers. 75/25 PLGA has a half life about 20 days, which is longer compared to 65/35 PLGA due to the methyl group in PLA impeding the reaction between water and PLGA [98], reducing the speed of hydrolysis, which is the main mechanism in PLGA degradation.

Combining the advantage of the synthetic nerve conduit's flexible design and NGF's effect on nerve growth, several types of nerve conduits will be designed, fabricated and verified *in vitro, ex vivo* and *in vivo* in this dissertation.

Dissertation Overview

Chapter 2 of this dissertation will discuss a project to design, fabricate, verify and characterize several IOP sensors. Chapter 3 of this dissertation will explain a PDMS nerve conduit loaded with either NGF or Dextran for peripheral nerve regeneration. Chapter 4 of this dissertation will describe a PLGA nerve conduit loaded with NGF for peripheral nerve regeneration with *in vitro* and *ex vivo* verification data. Chapter 5 of this dissertation will provide all supplementary data for both PDMS and PLGA nerve conduits loaded with either VEGF, BSA, Dextran or NGF for *in vitro* release study or *in vivo* animal study. This chapter will also describe the model for predicting local NGF concentration at the proximal nerve stump. Chapter 6 will conclude the whole dissertation by summarizing the contributions of the author and future work.

CHAPTER 2

INTRAOCULAR PRESSURE SENSORS: NEW APPROACHES FOR REAL-TIME INTRAOCULAR PRESSURE MEASUREMENT USING A PURELY MICROFLUIDIC CHIP

Introduction

Glaucoma and Contemporary Intraocular Pressure Measurement

Glaucoma is the second leading cause of blindness in the United States, and its primary symptom is elevated intraocular pressure (IOP) [1]. Normal IOP is near 10mmHg, whereas higher IOP, between 23 to 35mmHg, can cause hypertension inside the eye and result in glaucoma and eventual damage to sensitive eye tissues, leading to blindness.

Due to "white-coat compliance," where patients consume a drug right before visiting an ophthalmologist to ensure their symptoms are minimal [2], [3], detection of lethal-pulse, high IOP is difficult. Current IOP measurement uses a tonometer, which measures cornea deflection caused by an applied air-flow [4], providing the ophthalmologist an easy, relatively cheap way to estimate IOP. However, tonometry lacks accuracy because of assumptions of a "normal" cornea stiffness, while cornea stiffness varies from patient to patient. Tonometry is not readily adaptable to real-time measurements, and is not ideal for capturing transient spikes in IOP [5]–[7]. Different approaches have been proposed and developed to acquire better accuracy in tonometry [8]–[15] but none of them can provide accurate real-time IOP measurement.

Contemporary implantable IOP sensors can be divided into two categories based on the sensing technique: electrical or mechanical. With proper signal processing and antennas or other techniques, these devices can transmit IOP data into storage wirelessly and the ophthalmologist could potentially assess if the patient needs further treatment. As an example on the electrical side, a research group recently showed that a flexible, capacitive IOP sensor occupying the whole anterior chamber of a mouse cadaver eye can simultaneously record IOP and transmit it through a built-in antenna [25], [27], [47]. Porcine eyes and soft human body model [26], [29] were also used to determine the performance of the device in what is proposed to be a better model of the human eye. Though the flexible structure of the IOP sensor minimized the likelihood of scratching tissues in the anterior chamber [25] and RF wireless charging minimized the size of the device by eliminating the battery [26], [27], this device was still too big to be implanted into the human eye without blocking the incoming light through the pupil when dilated. In addition, lack of a securing mechanism can be an issue when transferring these IOP sensors designed to fit in mouse eyes into human eyes since these IOP sensors may move around inside the anterior chamber and cause problems. In another example, a group proposed a capacitive IOP sensor with a solar battery and an antenna that could detect and record the IOP value every 15 minutes and store it in memory [22], [24], [99]. The data could be retrieved by the patient everyday through wireless communication to an external device. Because this IOP sensor had a computing system and a power supply unit, it was claimed as the first “cubic-millimeter computer” in the world [24]. While the system is quite impressive, it is relatively complex and expensive. A third group proposed a capacitive IOP sensor made of parylene-C that could detect the pressure

change and transmit signals through resonant circuitry [100]. Instead of capacitive IOP sensors using the capacitance change due to the deflection or displacement of two parallel plates under pressure, B. Ziaie *et al.* developed and tested piezoresistive IOP sensors that measured the pressure difference between the choroid and the sclera [32]. Testing was performed in three human cadaver eyes under 10 to 47mmHg. However, these devices were too big to be fully implanted into the eye, and the fact that they needed physical connections to external equipment makes animal experiments difficult.

In contrast, unpowered mechanical IOP sensors using parylene-C as Bourdon tubes to sense the pressure change have been demonstrated [36], [37], [39], [40], [101], [102]. Pressure resolution with *in vitro* testing in water was 3.56mmHg, and the sensitivity for *ex vivo* testing in several enucleated porcine eyes was 8.72 μm/mmHg for a the dynamic range of 29 to 88mmHg [36]. Mounting techniques for the sensor on the iris were also discussed and found successful for a 1 month period on the iris of rabbit cadaver eyes [36], [37].

Despite the fact that electrical IOP sensors can monitor and store IOP data on a constant basis, unpowered IOP sensors have shown advantages over other IOP sensors, since they need no energy source, minimize the cost for fabrication, and simplify the design. Because Bourdon-tube IOP sensors have drawbacks such as requiring expensive cleanroom fabrication processes and a relatively large size that can block the optical path via the pupil at night, we propose an approach using a manometer-based microfluidic device designed for periodic monitoring of IOP in glaucoma patients. The principle for our IOP sensor is similar to a manometer and involves a dye solution in a pressure-sensing pad covered with a flexible membrane. An elevation in IOP results in ingress of

the membrane that pushes the dye solution out of the sensing pad. The movement of sensing dye corresponding to a change in pressure can be measured and calibrated to monitor IOP. This sensor can be implanted either in the lens capsular bag (referred to as an intracapsular IOP sensor) or sandwiched between the conjunctiva and the sclera (referred as a subconjunctival IOP sensor).

Materials and Methods

Design of Intracapsular IOP Sensors

The intracapsular IOP sensor was our initial IOP sensor design and was intended to be implanted in the lens capsular bag after cataract surgery. For reference, basic eye anatomy is shown in Figure 1. The intracapsular IOP sensor [103], is based on the design of a capsule drug ring, which is placed around an intraocular lens (IOL) and used to deliver Avastin to the back of the eye for the treatment of age-related macular degeneration. Our initial efforts focused on a semicircular IOP sensor that could be placed into the capsular bag in a manner similar to that of the capsule drug ring. Figure 2a shows the design of the intracapsular IOP sensor, in which dye located in the sensing pad is be squeezed into a channel at a rate dependent on the pressure in the eye. Figure 2b shows a fabricated intracapsular IOP sensor placed on top of a human cornea.

The subconjunctival IOP sensor is designed to be placed between the conjunctiva and the sclera, and a basic design is shown in Figure 3. A sensing pad filled with an IR sensitive fluorescent dye pushes the dye into the channel when pressure is applied on a sensing membrane on top of the sensing pad. Depending on the length of the dye inside the channel as a function of applied pressure, a calibration curve can be generated and, therefore, an ophthalmologist can determine the intraocular pressure based on a dye

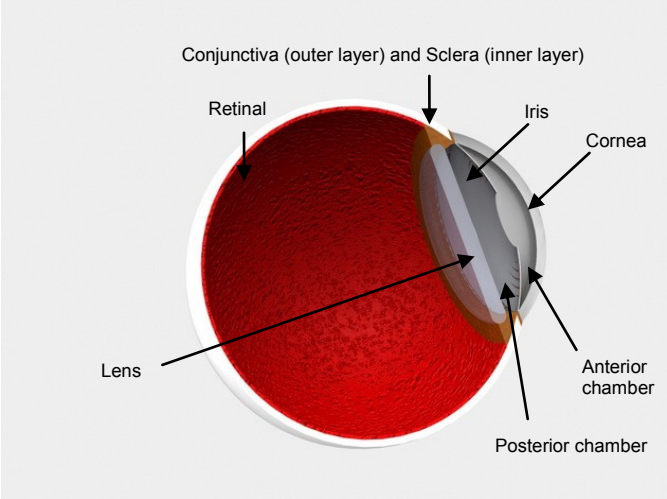

Figure 1 Schematic view of a human eye

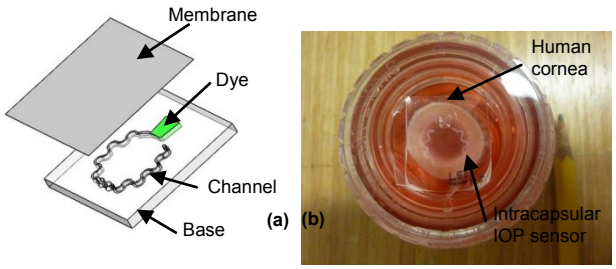

Figure 2 Intracapsular IOP sensors (a) Illustration of an intracapsular IOP sensor; (b) an intracapsular IOP sensor placed on a human cornea to show size

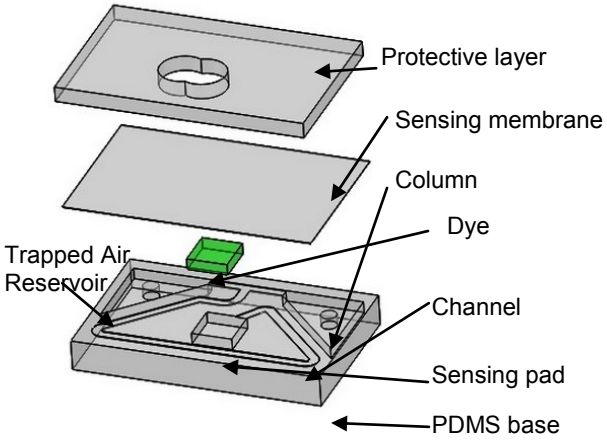

Figure 3 Illustration of a subconjunctival IOP sensor

length measurement.

The subconjunctival IOP sensors are implanted between the conjunctiva and the sclera, where there is not only no risk of blocking the light coming through the pupil, but also the IOP value can be measure accurately. Ziaie *et al.* have shown that IOP sensors mounted between the conjunctiva and the sclera can accurately measure IOP between 10 to 47mmHg [32]. In order to fit in the subconjunctival space, a 8x5x2 mm dimension limit has to be achieved so the patient will not feel discomfort.

When a pressure is applied to the sensing pad, the dye begins to move into the sensing channel and to compress the air that is in the channel. The pressure inside this channel will eventually build up and prevent further movement of the dye. To allow the dye to travel more easily inside the channel, two relatively large triangle-shaped air reservoirs are placed at the end of the channel to store the trapped air from the sensing channel and reduce the pressure build-up in the channel and the two reservoirs themselves. The reservoir dimensions are based on the volume of the channel and sensing pad and the maximum allowable pressure buildup in the channel as calculated using the ideal gas law and a square membrane deflection equation under constant, distributed loads.

Materials

The intracapsular IOP sensor consists of a base made of polymethylmethacrylate (PMMA) or polydimethylsiloxane (PDMS) and a silicone elastomer sensing membrane (HT6135 and HT6210, Bisco). For the subconjunctival IOP sensor, PDMS was chosen as the structural material due to its biocompatibility [104], [105], the ability to form fine structures, and its transparency and flexibility.

For the dye in either the intracapsular or the subconjunctival IOP sensors, either IC-Green [106] (17478-701-02, Akorn) or AK-Fluor 10% (17478-243-10, Akorn) [107] diluted with PBS into 1% AK-Fluor was chosen to be the sensing dye in the sensing pad. Both dyes are known to be biocompatible in the eye and have been used for intraocular staining for decades. An additional layer made of either a glass cover slip or PDMS was added on top of the PDMS membrane in the subconjunctival IOP sensor to prevent the channel and the air reservoirs from being under pressure when testing.

Fabrication

The intracapsular IOP sensor fabrication started by carving the PMMA base using a laser ablation machine (VLS 3.60, Universal Laser Systems) with a desired channel geometry, as shown in Figure 2a, A silane mixture to bond the PMMA base to the silicone elastomer was prepared by mixing aminopropyltriethoxysilane (APTES) and bistrimethoxysilylpropylamine (BTMSPA) in isopropanol at a 1:1:20 ratio and applied on top of the PMMA. Before bonding, the PMMA base was typically roughened with sand paper to help the bonding mixture adhere to the PMMA. The bonding surfaces were activated using a corona plasma treatment (LM4243-05, Enercon) on both the PMMA and the silicone elastomer for 15 minutes after applying the mixture onto the PMMA. Then, the silicone elastomer was placed on top of the PMMA, clamped, and incubated at 65°C for at least 14 hours. The IC-Green dye was then injected into the sensing pad, and this IOP sensor was ready to be tested.

For the subconjunctival IOP sensors, the same silicone-to-PMMA bonding was first tried, but a poor outcome in the device integrity was quickly observed, and the material of the subconjunctival IOP sensors were changed to PDMS due to better bonding results.

The subconjunctival IOP sensors were made of PDMS using soft lithography techniques. The soft lithography mold was made from a layer of double-coated tape (9019, 3M) and two layers of removable film (InstaChange 15 SM4, Gerber Scientific) that were placed on a glass slide (8201, Premiere). Laser ablation was used to carve the desired feature into the tape, and in this case, the double-coated tape, which was 28μm thick, contained the sensing channel and the combination of all three layers contained the sensing pad and air reservoirs, making them ~368μm thick. Low-power laser cutting was used to cut the tape layer by layer, and each layer was peeled after each laser cutting pass. After laser cutting, the glass slide with the tape mold was attached to a Petri dish (25384-302, VWR) by an adhesive (4011, Loctite) to serve as a container for the uncured PDMS. The PDMS was prepared by mixing the PDMS liquid and the PDMS curing agent in a 10:1 ratio and then degassing. The uncured PDMS then was poured into the mold and baked at 65˚C in an oven. A 20μm PDMS membrane was generated by pouring uncured PDMS on the top surface of a Petri dish cover and spinning at 3000rpm for 1 minute. Since bonding an extremely thin PDMS membrane on a PDMS piece is difficult, partially cured PDMS was used [108], in which the PDMS base – as shown in Figure 3 – was baked for 55 to 65 minutes, and the PDMS membrane was baked for 40 minutes. Then, the PDMS base was carefully peeled from the mold and placed upside-down on the PDMS membrane, and baked for another 2 hours in the incubator at 65˚C.

Since only the sensing pad was designed to be exposed to the applied pressure, a protective layer made of a glass cover slip (48366-067, VWR) or a 500μm PDMS layer (10:2 liquid to curing agent ratio) was designed to be placed on top of the PDMS membrane to protect the rest of the area of the sensor from the ambient pressure. For the

design with glass cover slip as the protective layer, a window is cut in the glass cover slip using the laser and a corona air plasma was applied on both the PDMS membrane (already bonded with a PDMS base using a partially-cured technique) and the glass cover slip for 5 minutes. For the design with PDMS as the protective layer, the corona air plasma was used to bond the PDMS protective layer with the PDMS membrane. For both protective layer manufacturing processes, a 1-hour 65°C postbake was performed with the sensor clamped.

Pressure Testing Stations and Pressure Testing Settings

In order to simulate the intraocular pressure change, which typically ranges from 0 to 50mmHg, either compressed air or water was used to pressurize the IOP sensor. For the compressed air pressure station, compressed air passes through a pressure regulator to reach a pressure of less than 100mmHg and then goes into both the pressure gauge and the base for holding an IOP sensor. An IOP sensor was sandwiched in the base of the pressure testing station, and a hole for the outlet of the compressed air directly accessed the sensing pad The pressure gauge read the current pressure, which was controlled by a pressure regulator, and an optical image of the sensing channel was recorded using a camera (MD900E, Amscope). The images were stored on a connected computer for later data analysis. The pressure gauge had a precision of 0.2mmHg pressure difference. All the intracapsular sensors were tested with this compressed air pressure station. The subconjunctival sensors used a different system since this pressure testing station was not particularly flexible and needed to be modified for every design, the pressure distribution was not well controlled, and the natural environment for these sensors is liquid, not gas. The water based pressure generating system consisted of water stored in a square PMMA

column and the IOP sensor was placed at the bottom of the column. The height of the water column was varied to simulate changes in the IOP.

For the subconjunctival IOP sensors, optical coherence tomography (OCT) images were also collected of the fluorescent dyes to verify that these dyes could be used to measure the length of the pressure measurement column. Some of the subconjunctival IOP sensors were covered with a piece of swine conjunctiva in order to verify if the signal is readable through the conjunctiva to verify whether or not the OCT imaging could be used in a real eye to collect the pressure repeatedly and noninvasively.

Results and Discussion

Fabrication Results

Several designs and fabrication processes were tried before finalizing the subconjunctival IOP sensor tested in the hydraulic pressure station. Bonding issues were observed in the preliminary subconjunctival IOP sensors with silicone-to-PMMA bonding. Later subconjunctival IOP sensor design using PDMS achieved a better signal consistency, and even sensors with air bubbles trapped in the sensing pad could produce a readable signal in the hydraulic pressure station. Images of some of the fabricated devices are shown in Figure 4.

Bonding Issues for Subconjunctival IOP Sensors

In the beginning, two kinds of 254μm silicone elastomer sensing membranes (HT6135 and HT6210, Bisco) were chosen and bonded with the PDMS base. The HT6135 silicone elastomer had a smoother surface, which would result in better bonding, since corona plasma bonding of PDMS to silicone requires a flat surface for contacts; its high durometer of 35 led to a high Young's modulus and thus was more difficult to

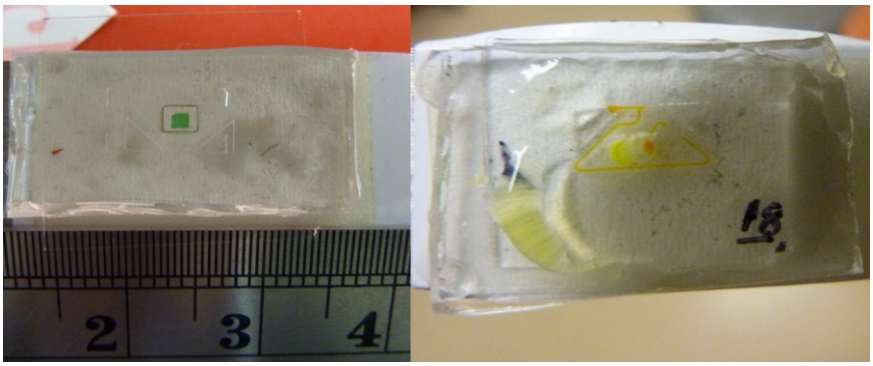

Figure 4 PDMS-based subconjunctival IOP sensors filled with either IC-Green (left) or AK-Fluor (right)

deform when pressure was applied. Since the IOP sensor required a deformable and soft material to serve as its sensing membrane, Bisco HT6210 with 10 durometer was chosen for the device though its surface was rougher than HT6135's. The lower durometer gave a better deformation of the membrane under pressure and led to a greater sensitivity in theory. Experiments showed that the IOP sensor with a HT6210 silicone elastomer could generate a representative dye length under applied pressure, but none of the HT6135 ones could.

Nevertheless, surface roughness resulted in difficulty for bonding when using corona plasma so that bubbles developed between the silicone membrane and the PDMS base, leading to leaks and failure of the device.

In order to get a better bond without losing the deformability of the sensing membrane, a thin PDMS membrane was introduced to take the place of the silicone elastomer. Though its Young's modulus was more than that for silicone elastomers, the thin PDMS membrane saw a reasonable deformation under applied pressure. The air bubble issue was solved by using the partially cured PDMS method, and the repeatability was good, so about 80% of the samples could form a consistent structure, leading to more

repeatable testing results. Figure 4 shows PDMS-based subconjunctival IOP sensors filled with either IC-Green (left) or AK-Fluor (right). The transparency of the PDMS sensing membrane results in a clearer image compared with the PMMA-based intracapsular IOP sensors because the measurement image can be taken from the thinner (membrane) side instead of the thicker (base) side of the sensors.

Air Bubbles for One of the Particular Subconjunctival IOP Sensors

Air bubbles occasionally formed in the sensing pads during loading of the sensing dye. The bubbles were not always problematic. For the subconjunctival IOP sensors, one of the samples that experienced an air bubble in the sensing pad while testing under hydraulic pressure, showed that it could still obtain the same sensitivity when measuring pressure, but it had a larger offset than the others. The bubbles appeared to form when the dye was injected into the acrylic square tube of the hydraulic system and went into the sensing pad through the injection hole for filling the dye into the sensor. This situation could be minimized since there was no air inside the eye and therefore no air bubble would be generated outside of the IOP sensor. Even if this situation happened, the ophthalmologist could still get a pressure readout according to the dye length measurement by just applying the offset value.

Intracapsular IOP Sensor Testing

The corresponding dye length inside the channel based on different applied pressure was recorded in order to compare the different response in intracapsular sensors. Three of the intracapsular IOP sensors achieved a sensitivity of 0.038, 0.044, and 0.085mm/mmHg, respectively. A graph of the dye length in the intracapsular IOP sensor versus the applied pressure shows that a maximum dye length of about 4.5mm was

recorded, as shown in Figure 5.

Subconjunctival IOP Sensor Pressure Reading Result

After acquiring images of the IOP sensor under different applied pressures, Image J (public resource, NIH) was used to calculate the dye length. AutoCAD was also used to help calculate the effective dye length around the corners in the channel. Images of subconjunctival IOP sensors under hydraulic pressure were recorded by either the Amscope or the OCT. The former was performed for most of the samples, and the length of the dye (IC-Green or AK-Fluor) was recorded for data analysis.

Figure 6 shows the average dye length under increasing and decreasing pressure with error bars based on the results of three different devices measured using the Amscope and measurements for an OCT trial (using AK-Fluor). Error bars for individual

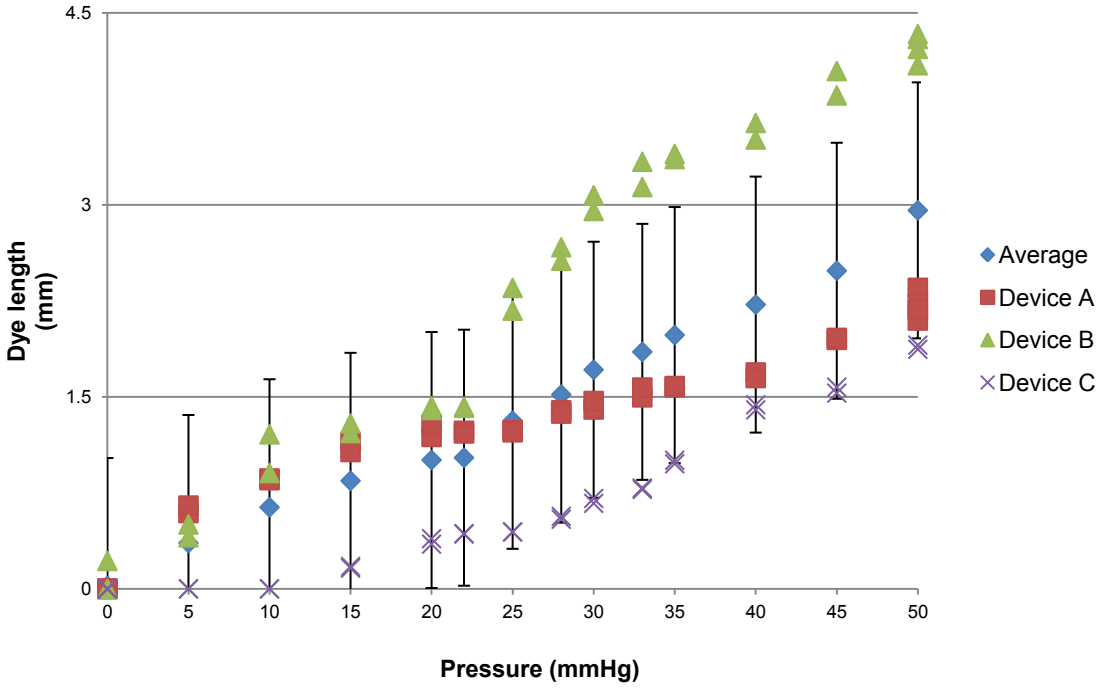

Figure 5 Graph for dye length versus pressure for intracapsular IOP sensors

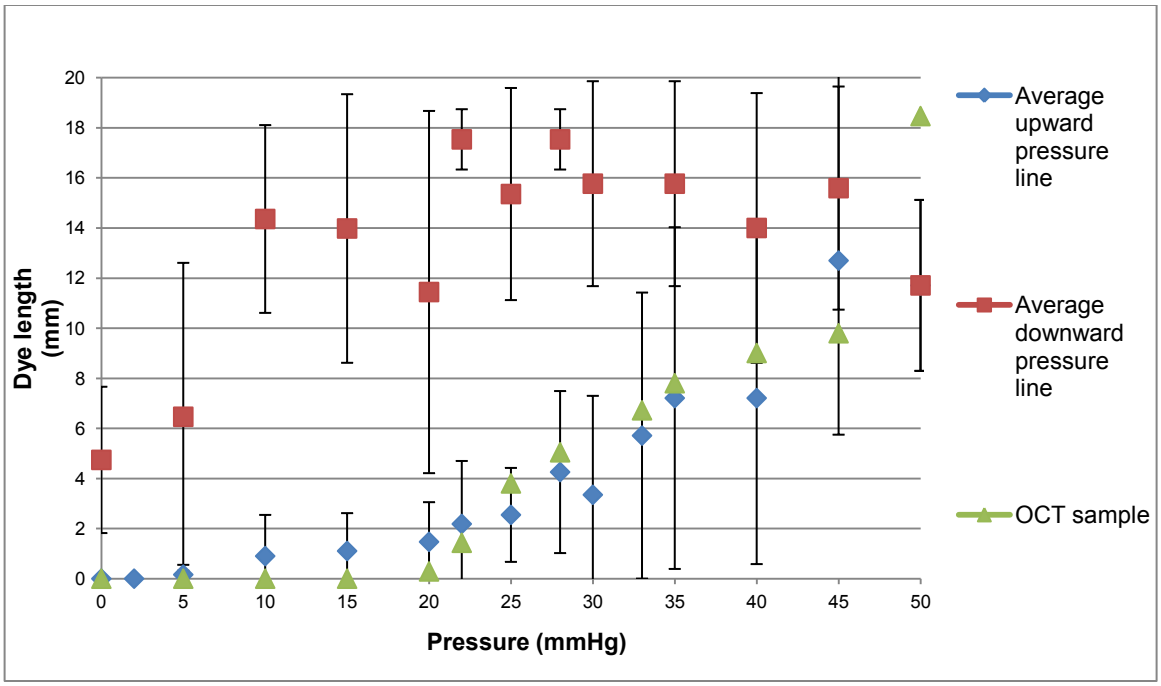

Figure 6 Graph for dye length versus pressure for subconjunctival IOP sensors

devices were much smaller. Except for the OCT sample's 50mmHg reading, most of the OCT's readings fell in the margin of error region for the IC-Green sample measurement,suggesting that the methods are comparable and compatible. For an increasing pressure, the sensitivity of average IC-Green dye length in the normal IOP region was 0.099mm/mmHg and in the glaucoma IOP region the sensitivity increased to 0.34 mm/mmHg. The reason for the difference in sensitivity appears to that the sensing pad is not fully filled, so a pressure must build up and the dye must fill potentially empty space before moving into the sensing channel. Once these initial effects are overcome, the dye can move through the channel readily, providing the higher sensitivity in the pressure range of interest – the one between 22 to 35mmHg. The high sensitivity of the IOP sensor in this pressure region is advantageous for an ophthalmologist to discriminate pressure differences for tracking potential glaucoma, while measurements at the "normal"

range are relatively less important, the range of high sensitivity can likely be expanded by improved dye loading methods.

Figure 7 shows the Amscope image of a subconjunctival IOP sensor under hydraulic pressures of 0 to 45mmHg. The contrast of the dye using the IC-Green and the Amscope was limited, making dye length measurements more difficult. In contrast, the OCT image with AK Fluor-dye, shown in Figure 8, gives a clear dye signal compared to the Amscope one. In the infrared and spectrum mode of the OCT, the 1% AK-Fluor dye was bright and easy to observe. This sensor, shown in Figure 6, had a sensitivity of 0.065mm/mmHg in the normal intraocular pressure region, and a 0.481mm/mmHg sensitivity in the glaucoma intraocular pressure region. The results suggest that either AK-Fluor or IC-Green could serve as the dye for the IOP sensor, but that use of OCT with an IR fluorescent dye might be preferred.

To test the ability to read the sensor through the outer eye tissues, several swine conjunctivas were harvested and placed over these sensors to see if the OCT could image the dye through a typical eye tissue, and it was shown that in fluorescence mode, the OCT could distinguish the dye from the background. Since swine conjunctiva is thicker than human conjunctiva, it is highly likely that the dye could be sensed when implanted in a human eye and observed through the human conjunctiva.

Hysteresis of the Sensors

Both intracapsular and subconjunctival IOP sensors were tested with increasing pressure, but only the subconjunctival IOP sensors were tested with decreasing pressure. Hysteresis in the measured signals, or a difference between the increasing and decreasing pressure measurements, was observed in the subconjunctival IOP sensors, meaning that

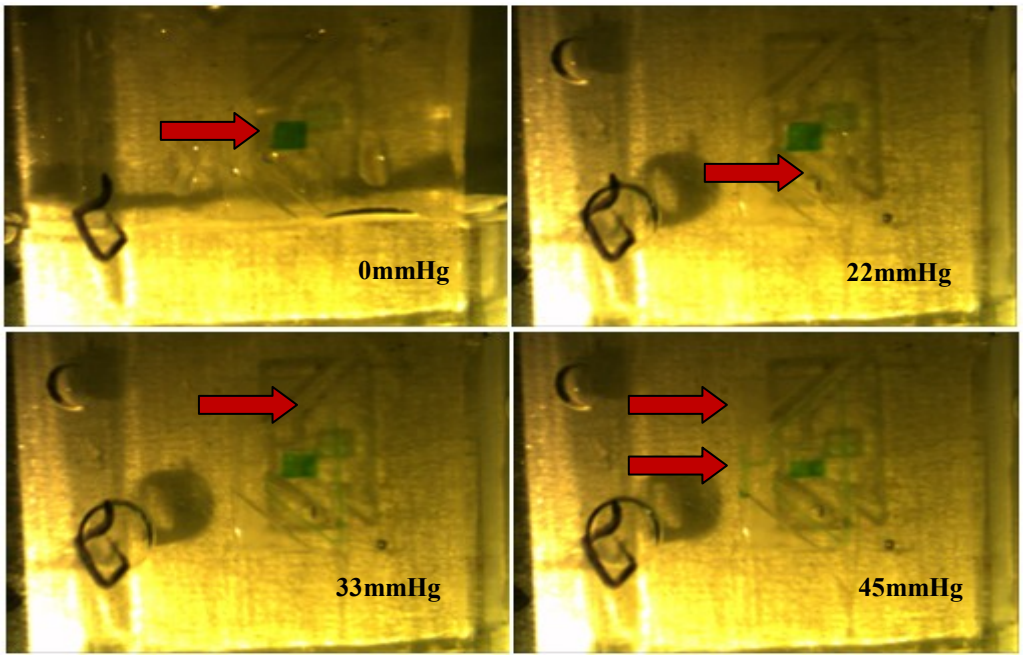

Figure 7 Amscope image of the subconjunctival IOP sensor with IC-Green dye under 0 to 45mmHg hydraulic pressure

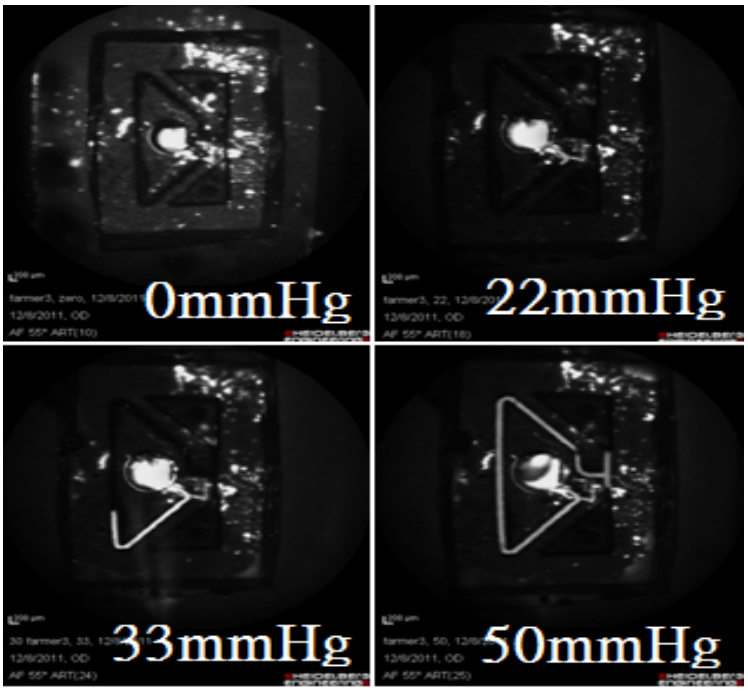

Figure 8 OCT image of the subconjunctival IOP sensor with 1% AK-Fluor dye under 0 to 50mmHg hydraulic pressure

the dye length for a particular pressure was different when the pressure was dropping instead of climbing to a particular value. Hysteresis happened for all the subconjunctival IOP as shown in the difference between two average lines in Figure 6. This hysteresis appears to be mostly associated with bubbles in the sensing chamber, which seem to be due both to the loading of the dye and the gas permeability of PDMS sensing membrane. Some of the bubbles occur when the air originally in the channel and the sensing pad is compressed when filling the sensing pad with the dye, and the air get further compressed when the hydraulic pressure is applied. Some of the compressed gas may be pushed out through the PDMS and so a vacuum does not form when the pressure on the sensing pad is released, so the dye column is not pulled back into the sensing chamber as readily. Overall, for both the increasing and decreasing paths, there seems to be an "inertia" effect, in that once the dye begins to move, it moves more easily. The hysteresis is also not consistent in that some devices possess a lower hysteresis and the dye would go all the way back into the sensing pad at 0mmHg; while in other cases, the dye would leave a 1.5mm length in the channel at 0mmHg, even though all the experiments started from 0mm of dye in the channel. For comparison, hysteresis was not discussed at all in other IOP sensor publications [12]–[14], [23]–[27], [29], [32], [36]–[40], [47] and was only mentioned briefly in the work of Wise *et al.* [22]. Based on the likely causes of the hysteresis, the best solutions to reduce the hysteresis would likely be a channel coating to reduce capillary forces, elimination of dead volumes or trapped bubbles by better dye loading, or use of membranes and materials that do not exhibit high gas permeability.

Conclusion

Two types of IOP sensors have been designed, fabricated and tested. The subconjunctival IOP sensors possess a more broad application compared to the intracapsular IOP sensors because they can be used with any patient and they are easier to to both implant and observe.

Conclusion for Intracapsular IOP Sensors

Over 50 intracapsular IOP sensors were fabricated and tested; three final devices using the design reported in this paper were shown to show repeatable and sensitive results for pressure measurement in the range of pressures relevant to glaucoma patients. The PMMA base itself had some drawbacks, including that the dye would tend to stick on the wall of the channel, resulting in poor sensitivity of the sensor. In addition, the silicone to PMMA bonding challenges led to inconsistent sensor dimensions leading to inconsistent measurement results between sensors. Moreover, the amount of dye filling the sensing pad was difficult to control, which also affected the uniformity of results from sensor to sensor. In addition, the signal can only be observed through the thicker (base) side of the sensor because of the non-transparent sensing membrane, leading to a relatively blurry image.

Conclusions for Subconjunctival IOP Sensors

Nearly 70 subconjunctival IOP sensors were fabricated and tested before a final design was developed using the partially cured PDMS technique to bond two PDMS components together, and seven devices based on the final design worked such that the dye could move forward and/or backward based on the applied pressure. These devices also showed a similar pressure response curve with low sensitivity in the normal

intraocular pressure region (below 22mmHg) and a much higher one in the glaucoma intraocular pressure region (22-35mmHg), which is of particular interest in this work. The devices were shown to work with IC-Green and AK-Fluor dyes. In addition, the AK-Fluor signal was readable when covering the subconjunctival IOP sensor with a piece of swine conjunctiva. Moreover, though hysteresis did happen, another calibration curve for decreasing pressure can be generated with an offset from the calibration curve under increasing pressure. Since these sensors were tested in a water-based hydraulic system, these sensors were shown to be waterproof and could function inside the eye. In order to achieve better signal consistency, additional tests with identical devices should be performed to acquire more data for the average dye length calibration curves in order to get a more precise prediction of intraocular pressure based on the dye length measurement.

CHAPTER 3

PDMS DRUG DELIVERY DEVICES: POTENTIAL APPLICATION IN NERVE REGENERATION

Introduction

Peripheral nerve injuries affect 2.8% of trauma patients [49], significantly reducing their quality of life due to the loss of function and sensory for extremities.. Most nerve repair surgeries have poor outcomes with contemporary treatments [45], spurring research into alternative methods to address this clinical need.

Currently, end-to-end tension-free nerve re-approximation is performed for peripheral nerve gaps less than 1cm, while special bridging techniques are required for gaps larger than 1-2cm [52]. The preferred clinical bridging technique uses autologous nerve grafts (autografts), which not only require additional surgery, but also lead to donor site deficits in function or sensation [55]. Thus, there is significant need for methods of nerve repair that avoid these concerns.

Following a peripheral nerve injury, axons will tend to regrow or regenerate and cross short gaps, though they need guidance in order to find their target [109]. Both natural and synthetic materials have been used to repair nerve gaps ranging from 5 to 80mm [59], including nerve grafts and artificial tubes made from collagen, PLGA, silicone or polyurethane [52], [110]. Additionally, several drugs have been shown to be effective in promoting axonal outgrowth across the nerve gap [56]. A 3-month study of nerve growth factor (NGF) loaded in polymeric microspheres has demonstrated potential

in repairing peripheral nerve gaps [78]. Collagen tubes loaded with NGF alone, or in combination with glial cell line-driven neurotrophic factor (GDNF), have been shown to enhance axon growth [111], [112]. In cell culture studies, NGF or GDNF with a concentration of 0.01 to 100ng/mL have resulted in significant axon growth in chick dorsal root ganglion cells. Several review papers suggest that better peripheral nerve regeneration can be expected by either the presence of physical bridge or the supply of neurotrophins or growth factors [52], [56], [57], [59], [93], [109], [110], [113]–[115]. Though some tissue-engineered conduits provide results comparable with autologous grafts [91], it is difficult to change either the growth factor or the dimension of the device based on different target nerve gaps. Thus, a device that is easily customizable in both dimension and drugs (growth factors) of interest is proposed in this paper.

The work included in this paper proposes a new, easily tailored approach to delivering drugs to treat peripheral nerve gaps. The general concept is to create a nerve guidance conduit surrounded by a drug reservoir that delivers drug into the lumen of the conduit, thereby encouraging rapid, directed nerve growth. Switching drugs should be straightforward as the kinetics of release can readily be modeled and calculated, in comparison to techniques that require material degradation. The general concept for the device is shown in Figure 9. This work focuses on a polydimethylsiloxane (PDMS) device with the comparison between using either filter membranes or diffusion holes as diffusion windows, with several different sets of nerve conduits (devices) used to demonstrate different molecule release from drug reservoirs into the environment (a receiver chamber). Prior to this work, a PDMS device without a nerve conduit was first developed to deliver human vascular endothelial growth factor (VEGF) for 5 days,

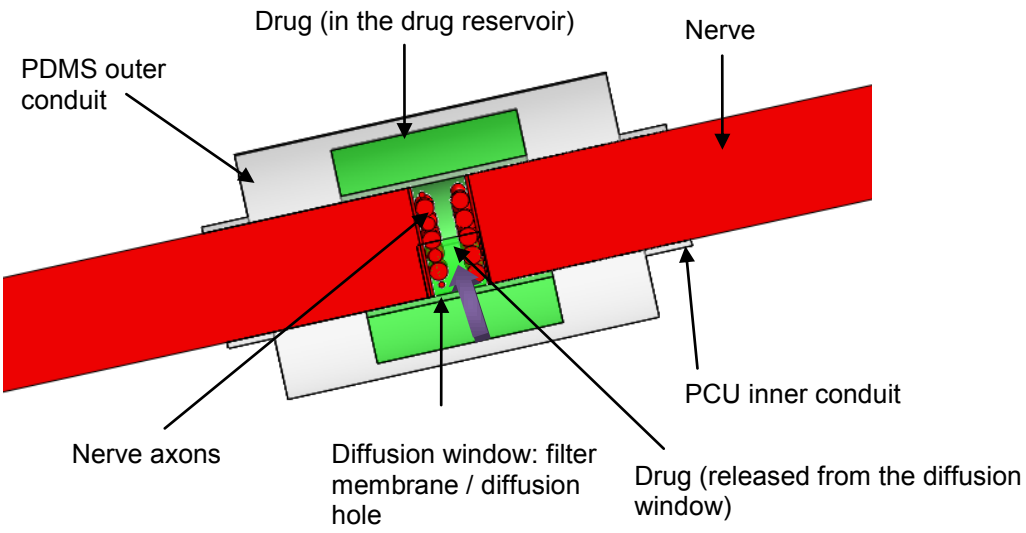

Figure 9 The schematic diagram of the device showing membrane placement and the assembly of the device on the nerve. Purple arrow indicates the release route of the drug

suggesting that the concept of drug release through a membrane on a nerve conduit could work (data unpublished). Then, a PDMS device with a nerve conduit, schematically shown in Figure 9, was developed and showed the ability to deliver bovine serum albumin (BSA) for 6 days. In this 6-day study, 100mg/mL BSA solution was filled into PDMS devices (n=3) with a PES filter membrane as the diffusion window. All three fabricated devices released the drug, and two out of three PDMS devices released BSA at a rate that would be of interest for drug delivery and with reasonable release kinetics over the 6-day period. The best devices had a higher release rate in the first 61 hours and a slower one for the remaining period. The low release device likely had a blockage caused by either an air bubble or adhesive on the membrane [55]. This paper expands on this preliminary work by first studying the same PDMS device design when delivering NGF and then explores a potentially improved design of the PDMS device using diffusion holes to replace the filter membrane as the diffusion window. This second device will be used to deliver Dextran as a drug stimulant for 31 days. The Dextran

model was chosen for its low cost, ease of use, stability, and similar size to the drugs of interest.

Materials and Methods

In this work, a 21-day NGF diffusion study was first conducted using PDMS devices with a PES filter membrane as the diffusion window. The results of the initial NGF study suggested some changes should be made, so modified PDMS devices using diffusion through holes as the diffusion windows were tested with Dextran and compared to the release kinetics of PDMS devices using PES filter membranes in a 10-day study.

A 21-day NGF Diffusion Release Study

Devices made of PDMS with a membrane for release were designed, manufactured, and tested using NGF in a 21 day experiment. The amount of NGF released was measured and used to improve the design and construction of the device.

Design

The concept behind this work is that bridging nerve gaps requires a physical structure to guide axon growth in addition to drug release to encourage rapid growth. Therefore, we designed a modified PDMS device capable of delivering a drug into the lumen of a nerve conduit that was designed to bridge a nerve gap [55]. The space between two concentric tubes served as a reservoir for storing the desired drug. When released, the drug will diffuse through a filter membrane and a window to enter the nerve conduit (inner tube), and contact the proximal nerve stump to promote axon growth. Figure 10 shows the designed storage reservoir of the drug, and the release route to the regenerating nerve. The PDMS device was designed to serve as a proof of concept of the

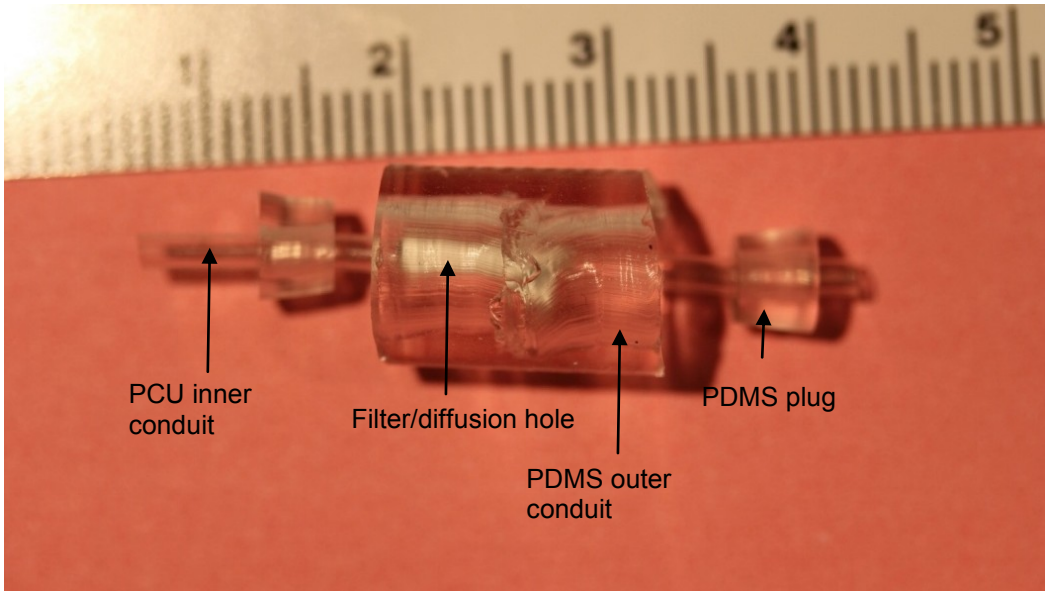

Figure 10 Photograph of the PDMS device for NGF release test

device.

To form the nerve regeneration device, two tubes with different dimensions were aligned to form a set of concentric tubes, with the lumen between the inner tube (nerve conduit) and the outer tube serving as the drug reservoir, as shown in Figure 9. A polycarbonate-urethane (PCU) [103] tube was chosen to serve as the inner tube. The encircling drug reservoir made of PDMS was formed by the space between the inner conduit and the PDMS outer conduit. The PDMS outer conduits were cut into 8.6mm outer diameter and 5mm inner diameter tubes. A 12-mm-long PDMS outer conduit and a 15-mm-long PCU inner conduit were assembled together with two ring-shaped PDMS plugs at each end of the drug chamber, which resulted in a drug reservoir volume ranging from 50 to 100μL, depending on the sealing ring location.

Fabrication

The fabrication process of these PDMS devices for NGF delivery can be divided into the manufacturing of each part, assembly of the device, and drug filling. Before

assembly of the device, the PDMS outer conduit and plugs, the filter membrane and PCU inner conduit were prepared.

For making the parts, The PDMS components were made by pouring 10:1 ratio PDMS solution into 1.5mL Eppendorf vials and polystyrene Petri dishes and then baking them for 2 hours in a 65ºC incubator. PDMS outer conduits were obtained by carefully peeling the rigid PDMS column from the Eppendorf vial and punching a hole through the cylinder with a 5mm biopunch. PDMS plugs were formed by punching concentric circles on the PDMS slab in the Petri dish mold with 5mm and 1.5mm biopunches.

For the PCU inner conduit, pellets of thermoplastic PCU (BioNate II, DSM Biomedical, Berkeley, CA) were heat extruded into tubes with a 1.5mm outer diameter and a 1.3mm inner diameter. It was further cut into 15mm long pieces, with an approximately 1mm x 2.5mm window drilled by a Dremel tool. A piece of PES filter membrane was cut into a rectangular shape to cover the window. Loctite 4011 adhesive (18680, Loctite, Westlake, OH) was applied along the edge of the window to attach the filter membrane without blocking the pores on the membrane [55].

Figure 10 shows the device before assembly. When assembling, one side of the PDMS plug was squeezed into the PDMS outer conduit followed by the application of uncured PDMS and RTV silicone sealant (RTV 734, 2307774-1008, Dow Corning, Midland, MI) to seal the end. The device was then baked for 1 hour at 65ºC to ensure proper sealing of the device. The other end of the PDMS outer conduit remained open until NGF was injected into the drug reservoir.

When filling the reservoir with NGF, the maximum amount of NGF solution was injected in order to minimize bubbles that tended to block the filter and impede the drug's

diffusion into the nerve conduit. Therefore, around 50 to 100μL of the desired drug was injected into the drug reservoir. After filling, the uncapped end of the PDMS outer conduit was sealed with a PDMS plug and RTV silicone sealant, followed by curing at room temperature for 15 minutes. Unlike uncured PDMS, RTV silicone sealant requires no elevated temperature to cure and will preserve the bioactivity of the desired drug.

Test setup for NGF Diffusion Experiments

The NGF release experiments were similar to the BSA diffusion experiments performed using a related device [116]; instruments, controls, and sampling occurred in a similar manner. The differences will be highlighted.

The 21-day NGF diffusion study started with the preparation of the base NGF solution. Because previous studies had shown that the combination of a PES filter membrane and polyvinyl alcohol (PVA) with a 50mg/mL concentration can help generate a controlled release rate [41], PVA was mixed with NGF. The NGF solution was prepared by dissolving 0.1mg of NGF powder (N2513, Sigma-Aldrich, St. Louis, MO) in 1mL of PBS solution containing 0.1% BSA. The NGF solution was diluted with 50mg/mL PVA to either 0.7μg/mL or 1.4ng/mL NGF final concentrations for devices or a reference sample, respectively, as shown in Table 4. NGF solution was filled into the drug reservoir in such a way as to minimize the volume of air in the drug reservoir, which would potentially block the release across the filter membrane.

The NGF solution was loaded into devices according to the dosage shown in Table 4. The positive NGF control without any drug delivery device was designed so that a maximum concentration of NGF could be established and measured in the ELISA assay to follow. A separate reference sample without a device was prepared to approximate the

Table 4 List of samples corresponding to drug and receiver chamber for NGF diffusion experiments

Sample Name	**Drug in the reservoir**	**Maximum possible concentration in the receiver chamber**
Positive control	105µL 0.7µg/mL NGF	9800pg/mL
Reference sample	105µL 1.4ng/mL NGF	19.6pg/mL
Negative control	70µL 1x PBS with 0.1% BSA	0
Device A	82µL 0.7µg/mL NGF	7653.3pg/mL
Device B	105µL 0.7µg/mL NGF	9800pg/mL
Device C	80µL 0.7µg/mL NGF	7466.7pg/mL

NGF signal in ELISA when only a small concentration of NGF is present. The concentration was chose to be the same as if 1/500 of the NGF is released from the drug reservoir into the receiver chamber. A negative control consisting of a PBS filled device was prepared in order to identify the noise. Glass amber vials (27002-U, Sigma-Aldrich, St. Louis, MO) filled with 7.5mL PBS solution were used as receiver chambers for all the groups.

The experiment was performed at room temperature and set on an rotary shaker for 3 weeks while samples were taken after 1, 37, 161, 335 and 504 hours from setup. Samples of 500µL were taken from each vial at each time period and stored at -20°C, while 500µL PBS solution with 0.1% BSA were refilled into each vial in order to maintain the receiver chamber volume and minimize air bubbles. All samples were

transferred onto a 96-welled plate for ELISA (ab100757, Abcam, Cambridge, MA) at the same time after the last set of samples was collected. For the ELISA plate, standards were prepared at 20.58, 61.73, 185.2, 555.6, 1666, 5000 and 15000 pg/mL in order to cover both extremely low release (e.g., 19.6pg/mL) and extremely high release (e.g., 9800pg/mL) scenarios. The instructions with the ELISA kit were followed and the results were read at 450nm with the plate reader.

A 31-day Dextran Diffusion Study

As a possible improvement for the PDMS devices with PES filter membranes, PDMS devices using through holes (diffusion holes) were proposed in order to possibly achieve more consistent release kinetics and also allow for lower release rates. The design of these PDMS devices with diffusion holes is introduced, followed by the fabrication process of these PDMS devices with either PES filter membrane or diffusion holes. A 31-day release study was conducted to verify and compare the release kinetics of PDMS devices with diffusion holes and PDMS devices with PES filter membranes for delivering Dextran.

Design and Modeling

Because the adhesive applied on the PES filter membrane can block the filter window and reduce its release capabilities, while also making the release inconsistent from device to device [55], [117], as was found in some of the devices releasing both BSA previously and NGF in this work, an alternative design using through holes (diffusion holes) on the inner conduit (PCU conduit) was proposed to replace the filter membrane. The holes were expected to be more robust while still providing a fairly

controlled, consistent release rate. Thus, an experiment to compare the usefulness of diffusion holes rather than a membrane was developed.

As the stability of the NGF had also come into question in some of the experiments, labeled 10kDa Dextran was used to simulate the NGF release in the tests of this device. In addition to being stable over the length of these experiments, Dextran is also much lower in cost, which made it a good candidate for these early device tests.

To determine the appropriate size of the release holes and the optimal concentrations of drug in the release reservoir, a model based on Fick's First Law of Diffusion was developed. Fick's First Law of Diffusion is given by

$$J = -D\frac{C_0 - C_1}{\Delta x}, \qquad \text{Equation 1}$$

where J is the diffusion flux $(\frac{\text{ng}}{\text{m}^2\text{s}})$; D is the diffusion coefficient $(\frac{\text{m}^2}{\text{s}})$; C is the concentration $(\frac{\text{ng}}{\text{m}^3})$; and Δx is the distance between two stages. Using Equation 1, a model was built to predict the final drug or polysaccharide concentration in the receiver chamber. The model was used to optimize hole sizes and drug concentrations to ensure the concentrations of drug released were both within the detectable range of the measurement methods (between 30ng/mL to 250µg/mL) and consistent with dosage levels likely to increase growth of nerve tissues.

The model was designed to represent the physical processes and geometry through which drug will leave the drug reservoir and reach either the nerve stump or the end of the drug delivery conduit. The model can then be used to predict the Dextran concentration in the receiver chamber when the sink method is used. The sink method is a method in which all the media in the receiver chamber will be replaced with the same

amount of fresh media each time a sample is collected [61], [71], [118], [119]. If the model is applied correctly, a proper starting donor chamber Dextran concentration and a diffusion hole dimension can be calculated to produce a detectable Dextran concentration in the receiver chamber. Preliminary work showed that a Dextran concentration between 30ng/mL and 250µg/mL is detectable in the plate reader. Figure 11 shows the concept of this model, in which a drug reservoir (stage 0) filled with the desired drug releases the drug through diffusion holes into the inner conduit (stage 1). The drug then diffuses from the inner conduit to the receiver chamber (stage 2).

Two equations specific to this model and based on Equation 1 are:

$$J_{0-1} = -D\frac{C_0 - C_1}{\Delta x_{0-1}} \qquad \text{Equation 2}$$

$$J_{1-2} = -D\frac{C_1 - C_2}{\Delta x_{1-2}} \qquad \text{Equation 3}$$

in which the diffusion flux between stages 0-1 and 1-2 are $J_{0\text{-}1}$ and $J_{1\text{-}2}$, respectively; the area for the diffusion filter or holes and inner conduit transverse cross-sectional area are $A_{0\text{-}1}$ and $A_{1\text{-}2}$, respectively; the concentration at stages 0, 1 and 2 are C_0, C_1 and C_2,

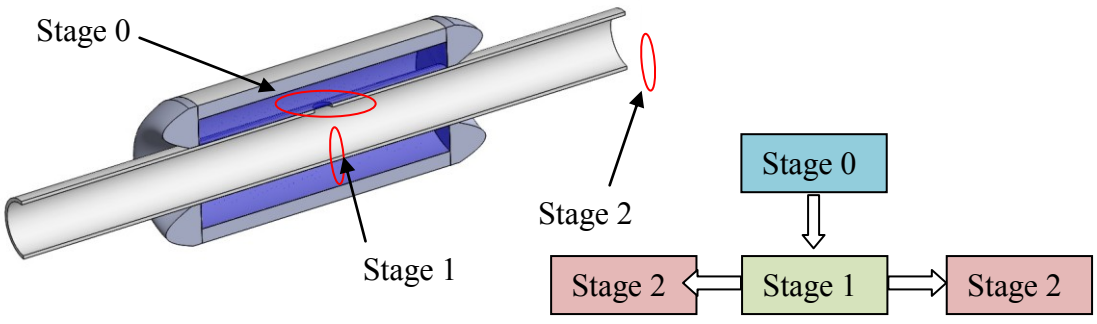

Figure 11 Illustration of the model to predict the protein concentration in the receiver chamber

respectively; and the distance between stages 0-1 and 1-2 are $\Delta x_{0\text{-}1}$ and $\Delta x_{1\text{-}2}$, respectively.

Because the diffusion in the inner conduit to the receiver chamber can go in two directions, the diffusion mass flow at steady-state is:

$$J_{0-1}A_{0-1} = J_{1-2} \times 2 \times A_{1-2} \qquad \text{Equation 4}$$

Also, the net drug increase (in mass) in the receiver chamber equals the net mass flux across the inner conduit in a given time; thus,

$$dC_2 = \frac{-J_{1-2} \times 2A_{1-2} \times dt}{V} \qquad \text{Equation 5}$$

where t is the time (s) allowed for diffusion, and V is the volume (m^3) in the receiver chamber.

From these equations, we can derive the concentration of the inner conduit just outside of the release holes (C_1) as:

$$C_1 = \frac{-2D^2 \times A_{0-1} \times A_{1-2} \times t \times C_0 - D \times A_{0-1} \times \Delta x_{1-2} \times V \times C_0}{-2D^2 \times A_{0-1} \times A_{1-2} \times t - D \times A_{0-1} \times \Delta x_{1-2} \times V - 2D \times V \times A_{1-2} \times \Delta x_{0-1}} \qquad \text{Equation 6}$$

Then, the concentration in the receiver chamber (C_2) is:

$$C_2 = C_1 + \frac{\Delta x_{1-2} \times J_{1-2}}{D} \qquad \text{Equation 7}$$

In this model, the diffusion coefficient for the 10kDa Dextran (0.00000130 cm^2/s) is considered to be similar to the 0.00000126cm^2/s diffusion coefficient for NGF [120].

All calculations were conducted in Microsoft Excel, and after entering the parameters shown in Table 5, the concentrations in the receiver chamber after day 1, 5, 10, 15, 20,and 31 using the sink method are shown in Table 6.

Table 5 Fixed parameters for the model

Description	**Notation**	**Value**	**Unit**
Cross-sectional area in the inner conduit	$A_{1\text{-}2}$	1.33×10^{-6}	m^2
Wall thickness of the inner conduit	$\Delta x_{0\text{-}1}$	100	μm
Distance between the diffusion hole to the receiver chamber	$\Delta x_{1\text{-}2}$	10	mm
Diffusion coefficient	D	0.00000126	$\frac{cm^2}{s}$
Receiver chamber volume	V	14	mL

Table 6 Design and expected Dextran delivery (in ng/mL) in a 31-day period

Device Name	**Design and Dextran dosage**	**0 hour**	**Day 1**	**Day 5**	**Day 10**	**Day 15**	**Day 20**	**Day 31**
Devices A-D	With four 40μm holes and 125μL 40mg/mL	0	1311	5090	6445	6379	6108	13159
Devices E-H	With PES filter membrane and 112.5μL 40mg/mL	0	8051	29407	33316	29066	24560	43518
Device I-L	Sealed device and 125μL 12.5mg/mL	0	0	0	0	0	0	0

Two sets (n=4) of PDMS devices, one with holes and one with membranes, and three sets of controls (n=4) were used in order to verify both the integrity of the device and the consistent release in the same design. Table 6 shows the modeling results for the Dextran concentration in the receiver chamber at different time points using the sink method for all three sets of the PDMS devices.

PDMS devices using either the filter or diffusion holes as the diffusion window were proposed, with the latter expected to achieve a more consistent result in biomolecule release over a 31-day period, because they reduce the manufacturing defects associated with adhesive that can completely or partially block the diffusion window, making the release inconsistent across devices. The primary control consisted of the PDMS device with neither the filter membrane nor the diffusion hole to verify the sealing of the device and detect any Dextran release through any other mechanisms. The other controls consisted of reference samples with either high or low concentrations of Dextran. These reference samples enabled both calibration and comparison of Dextran stability. Because samples were collected on the 0, 1st, 5th, 10th, 15th, 20th, and 31st day, these two sets of reference samples (n=4) were able to identify the Dextran signal fluctuation for a similar concentration of a net 5-day Dextran release in the 31-day period. In these reference samples, the receiver chambers were filled with a Dextran concentration of either 6400 or 32800ng/mL in 14mL PBS to simulate the Dextran signal of the 10th day collection from the PDMS devices with either the diffusion holes or PES filter membranes, respectively. Table 7 shows the volume and design for each device and control used in this 31-day Dextran release study. Reference samples M, N, O, P were prepared at a Dextran concentration of 6400ng/mL, while reference samples Q, R, S, T were prepared at a

Table 7 PDMS devices and reference samples used in the 31-day Dextran release study

Device number	**Design of the PDMS device**	**Volume of Dextran (µL)**
Device A	Four 40µm diffusion holes	125
Device B		140
Device C		125
Device D		125
Device E	With filter	100
Device F		125
Device G		100
Device H		125
Device I	Without filters or holes	100
Device J		125
Device K		125
Device L		125

Dextran concentration of 32800ng/mL. In addition to these reference samples, 14mLPBS was filled into 15mL centrifuge vials and served as the medium of the receiver chamber.

Fabrication

A fabrication process similar to the NGF devices was used to fabricate the PDMS devices used in the Dextran release study. One change in this study is that the length of the PCU conduit increased from 15mm to 20mm so that better sealing at the ends could be achieved. In addition, a 6mm biopunch instead of a 5mm biopunch was used so that a greater volume of the drug reservoir could be accessed.

For the PDMS device with four 40µm holes, laser machining was used to create the through holes on the PCU inner conduit, as shown in Figure 12.

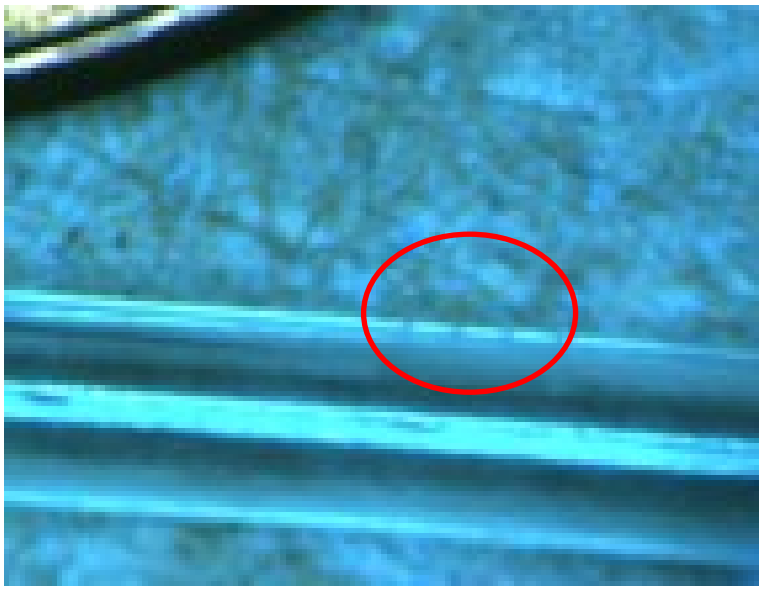

Figure 12 Four 40µm hole drilled by laser on the PCU inner conduit of the PDMS device compared to a United States penny. The holes look like lines on the conduit in the circle.

Test setup for Dextran Diffusion Experiments

Table 6 shows the design and expected Dextran concentration in the receiver chamber in a 31-day period, and Table 7 shows the approximate volume of Dextran loaded into each device. Forty mg/mL Dextran was prepared by dissolving 25mg Dextran with PBS. Undissolved Dextran was removed by centrifuge at 5000rpm for 5 minutes, as suggested by the receiver chambers, with the lid sealed by parafilm. The vial was wrapped in aluminum the manufacturer. To lower both the adhesion on the glass walls and any evaporation through the lids, sterilized 15mL centrifuge vials were used as foil in order to both reduce evaporation and reduce signal degradation due to light exposure. The vials (receiver chamber) were then placed on a rack and stored in a drawer without shaking to minimize the possibility of introducing air bubbles into the inner conduit, which will partially stop or lower the diffusion. In addition, the sink method was

used in which the entire receiver chamber media was replaced with a fresh 14mL PBS every time after collection. Each inner conduit was flushed 20 times with 400μL of the media in the receiver chamber to remove any trapped air bubbles. Reference samples M-T did not contain any PDMS devices, but rather were filled with known concentrations of Dextran. Unlike the device groups where the entire volume of receiver chamber fluid was removed, only three aliquots of 400μL samples were collected from the reference samples each time, with no fresh PBS placed into the receiver chambers. Samples collected from both the devices and reference samples were stored at -20^{o}C and analyzed at the same time. The plate reader was used with an excitation wavelength of 494nm and an emission wavelength of 521nm as appropriate for the Fluorescein dye on the Dextran.

Results and Discussion

Initial fabrication results suggested that the devices would be ready and able to release drugs as designed, which led to the 21-day NGF diffusion study where the results were comprised of the NGF release amount (in ng). The results of the NGF study led us to complete the 31-day Dextran diffusion study. The release data for both NGF and Dextran diffusion studies provided some interesting results which will be discussed. As noted, some of the results led to suggestions for a possible improvement of the design and fabrication process, and the results of these changes are addressed.

A 21-day NGF Diffusion Study

The scope of this 21-day NGF diffusion study was to reveal the diffusion kinetics of NGF in terms of NGF amount delivered in the given period. Discussions for the release kinetics results were then given, followed by possible improvements of the design

and setting of both the device and the experiment.

The fluid in the receiver chambers were collected over a period of 21 days as noted in the Methods section. The NGF concentration in each sample was calculated from the enzyme-linked immunosorbent assay (ELISA) plate reading values according to an NGF calibration curve prepared with each measurement and consisting of NGF concentrations from 20 to 5000pg/mL. After acquiring the NGF concentration in each sample, the concentration was converted into the NGF mass (in ng), and the data were summed to show the cumulative NGF release amount in the 21-day period, as shown in Figure 13.

Because the NGF concentration of the high reference sample or positive control was 9800pg/mL, which exceeded the detectable range of the NGF calibration curve, it could not be plotted in Figure 13. The negative control shown in Figure 13 set the noise level for the reading, and it showed that there was no statistical difference between the negative control, the low reference sample, and device A. NGF release kinetics simulated by the proposed model showed that 30.8ng NGF was expected to be delivered into the receiver chamber at the end of 21 days, with a steadily decreasing delivery rate from day 1 to day 21.

In Figure 13, the cumulative NGF amount released from device A stayed near zero, indicating that the PES filter in this device was likely blocked. For device B, the large NGF release between the 1st hour and the 37th hour (1.5 days) suggested that this device was not sealed completely. Twenty-three ng of NGF in device B was released during this period. The decrease of the cumulative NGF amount after 37 hours (1.5 days) was likely due to either the degradation of the NGF over time, reducing its signal in the ELISA, or possibly adhesion to the walls or absorption by the PDMS making up the delivery device.

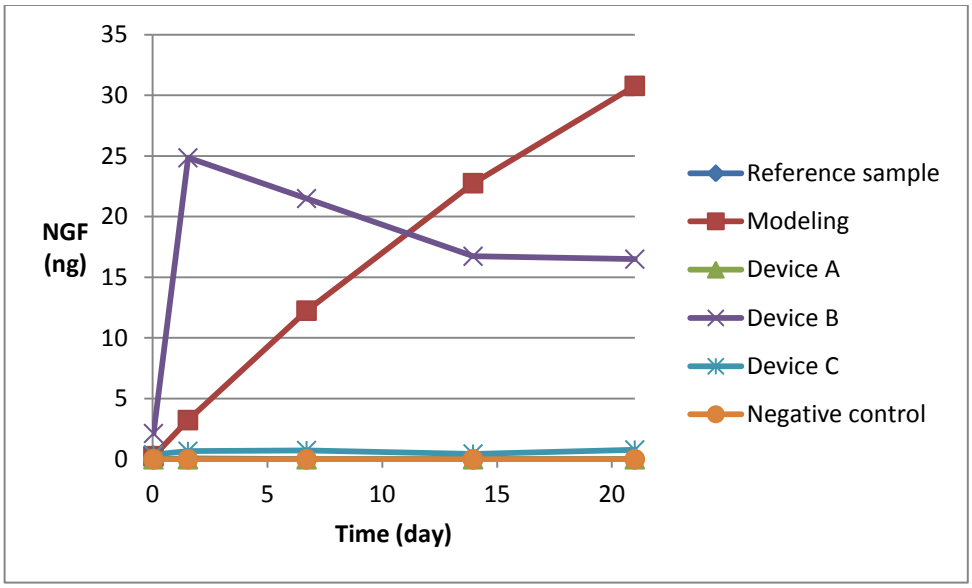

Figure 13 Cumulative NGF amount released into the receiver chamber in a 21-day period. Though device B showed a higher release compared with devices A and C, it still showed a lower release compared with the modeling result

Device B also showed a lower cumulative NGF release in the 21-day period, though possessed a higher release at the 37th hour (1.5day). Because only 0.5mL out of 7.5mL of the receiver chamber media was collected, and no mixing was performed before collecting the sample, the NGF that was released early in the study remained in the receiver chamber for a long period of time, likely degrading and possibly swamping out any later release of NGF from the device. For device C, the increase of the cumulative NGF amount from 211 to 561.4pg in the 21-day period indicated that the diffusion rate of NGF was greater than the degradation rate of NGF or the protein adhesion rate of NGF to the glass wall.

Overall, this study suggested that some modifications to the experiments needed to be made. First, the NGF "loss" over time could not be explained well and certainly a reduction in cumulative release over time is impossible, so the sinking method was developed to measure only any new drug release and avoid issues with degradation of

molecules resident in the receiver chamber for a long period of time. Second, it was not clear if the NGF was stable, so Dextran was chosen due to its improved stability. Use of Dextran also allowed us to use a plate reader rather than an ELISA, which should reduce noise at these lower concentrations. Third, the devices fabricated were quite inconsistent in their release, suggesting that modifications would need to be made to the manufacturing process. The prime culprit in the inconsistency seemed to be the membrane and possibly the adhesive that was used to attach the membrane. Thus, devices using holes were developed to release the drug rather than an adhered membrane. The cause of the high release was not clear, and could be associated with either leakage or possibly drug on the outside of the device walls. In either case, improved manufacturing methods were needed. The results did suggest that there was potential for the devices to work, but an improved design was needed, leading to the 31-day Dextran study.

A 31-day Dextran Diffusion Study

As it was possible from our work with NGF that the NGF was degrading, we chose to use Dextran with an attached fluorophore to model NGF release and hopefully avoid this problem. To assure that the Dextran and fluorophore were stable, during the 31-day experiment, a separate sample of Dextran at different concentrations was kept in the same environment to serve as a reference sample. The plate reader measurements from the low reference samples M-P and the high reference samples Q-T are shown in Figure 14. Note that the M-P reference sample is expected to be in the range of the release from the devices with holes and the Q-T samples are expected to be closer to the release from devices with membranes. The results suggest that the Dextran signal is fairly stable with

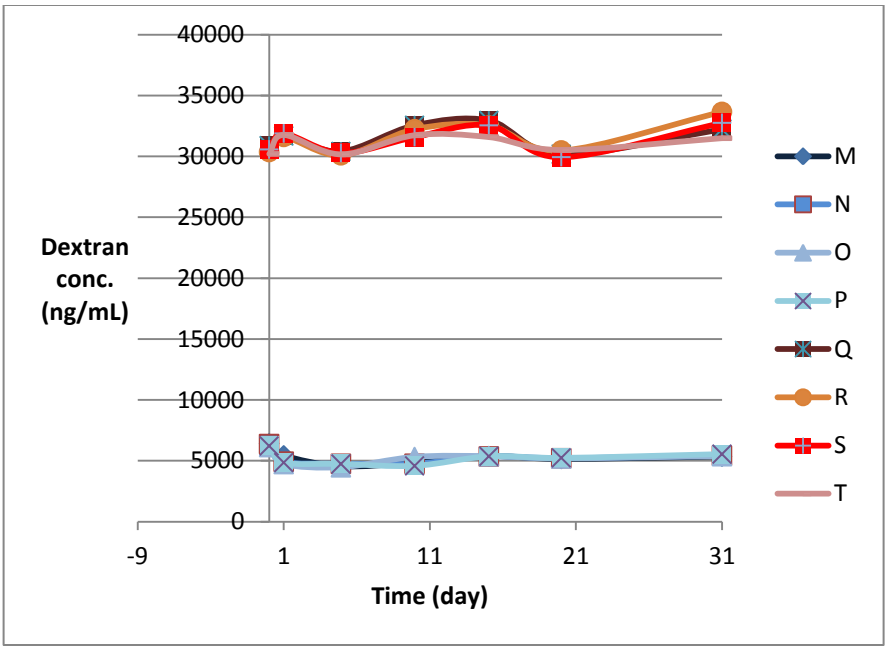

Figure 14 Dextran concentration of reference samples M-P and Q-T in a 31-day period. The former represents the Dextran signal in net 5-day release from PDMS devices with filter membrane; the latter represents the one from PDMS devices with four 40μm holes

a 7% standard deviation over the 31 days for the Dextran concentration of 32800ng/mL, and a 3% standard deviation for the Dextran concentration of 6400ng/mL. Both controls indicated that the Dextran signal was consistent in the 31-day period with reasonable signal fluctuation.

The sealed devices (I-L) served as negative controls to both verify the sealing of the devices and provide a background signal for the devices designed to release drug. One device showed a slow release reaching 0.2% of the total Dextran loaded on the device. The other three devices showed no release, indicating that the sealing for all four devices was reasonable and that the devices could be expected to perform without major leakage issues. Therefore, it is reasonable to assume all the Dextran detected in the receiver chamber for the device experiments is released from either the filter or the diffusion holes, instead of leaking from the device.

Devices A-D with four 40µm holes demonstrated a cumulative 3.8-9.0% Dextran release in the 31-day period, compared to modeling results showing a 10.2% Dextran release, as shown in Figure 15. The coefficient of variation for the four devices was 0.41 at day 31, suggesting there is still some manufacturing variability or possibly random interference from air bubbles. Nevertheless, continuous release was observed for all devices with holes (A-D) in the 31-day period.

The release profile shows a bit of a burst effect, meaning the delivery was relatively high the first day, followed by a fairly steady, nearly zero order, release over the last 4 weeks. Much of the variation associated with device C can be entirely attributed to the be related to small amounts of Dextran being absorbed to the outside of the devices during filling, as in many cases the Dextran leaks out of the device when being filled. The outside of the devices are washed thoroughly, but there may still be some material on the surface. Another possibility is the drug is essentially released somewhat in advance into

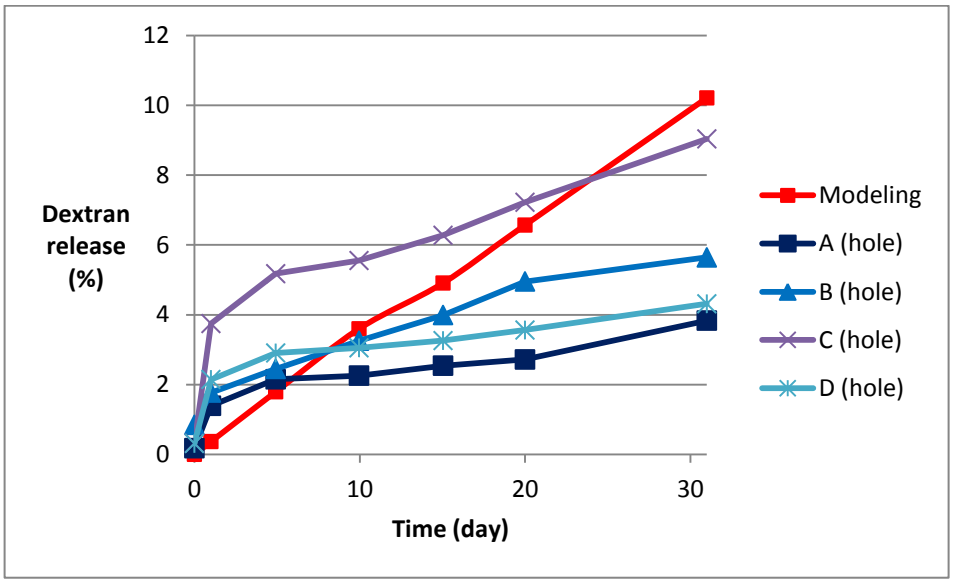

Figure 15 Cumulative Dextran release percentage for the devices with four 40µm holes

the inner lumen through the drug delivery holes, as the devices are loaded and then stored briefly. Some drug may be pushed through the drug delivery holes or membranes during loading, or variation in burst release the first day. The cause of the burst release is not clear, but it may allowed to release through the holes or membranes during storage, and then released quickly once placed in the receiver chambers. In any case, a small burst effect is not necessarily a problem and can be advantageous in helping to rapidly start the growth of axons in the conduit.

Some of the variation in the release may be associated with the laser drilling process, as the laser drilling process is somewhat challenging to control for these small, rounded devices. A 5μm measurement error was expected and images of the holes indicates that they have some taper as they cross the wall of the inner conduit, leading to some reduction in diffusion area. Removal of undissolved Dextran might also contribute to the relatively low release profile, when compared to the model predictions, so that less Dextran was filled in the device than designed.

Devices E-F with PES filter membrane showed a wide variety of release rates, just as found for earlier work with NGF, as shown in Figure 16. Device E showed no release in the 31-day period suggesting that the filter was blocked by the adhesive. Devices F and H showed a rapid release in the first 10 days followed by a steady release in the next 21 days. The rapid release could be associated with leaking around the membrane or in other locations on the device. The slowing release over time in these two devices might due to the lack of Dextran stored in the device for later release and is expected for high release devices. Device G showed a burst release and then a release rate lower than the modeling predictions after 5 days, suggesting that either the filter was partially blocked,

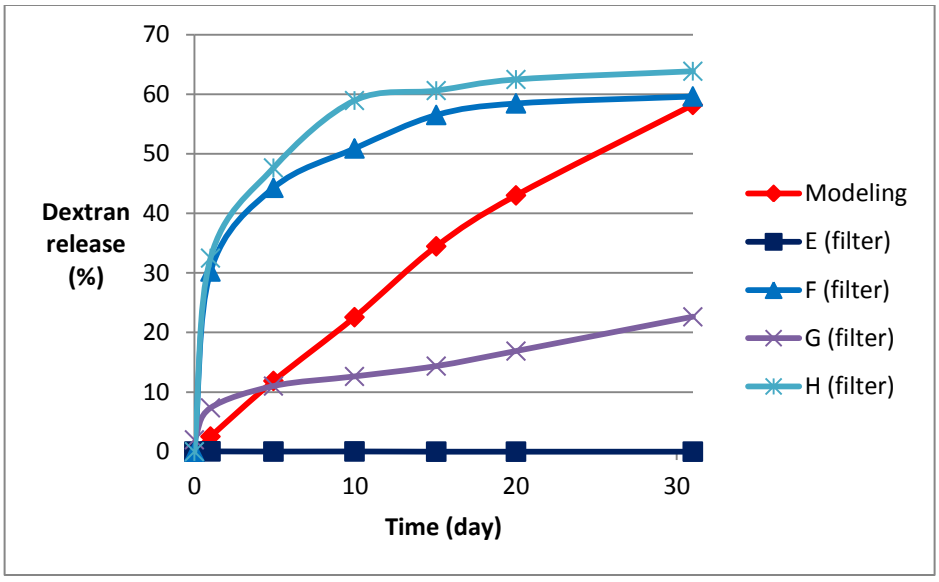

Figure 16 Cumulative Dextran release percentage for the devices with filter membrane

or the porosity of the filter is less than anticipated in the model. The drug delivery devices are designed to generate a steady release over at least 1 month. Figure 17 shows the relative release rate for each device over time. For the sealed devices (I-L), the release rate is near zero, as expected. For the devices with four 40µm holes, all four devices (A-D) showed a higher rate between the 1st and the 5th day, and then the rate dropped to a level fairly consistent with model predictions. The membrane (Devices E-H) generally showed a higher release rate, except for the devices that were completely or partially blocked. Overall, the membrane devices showed the most variation both within a single device and between devices.

Figure 18 shows a picture of devices A and F, respectively, after the 31 day experiment. The darker color of device A confirmed that a relatively high amount of Dextran is still available in this device (potentially 96% of the Dextran remained). Thus, both types of systems the PDMS device with diffusion holes should be able to deliver Dextran for more than 31 days, if needed.

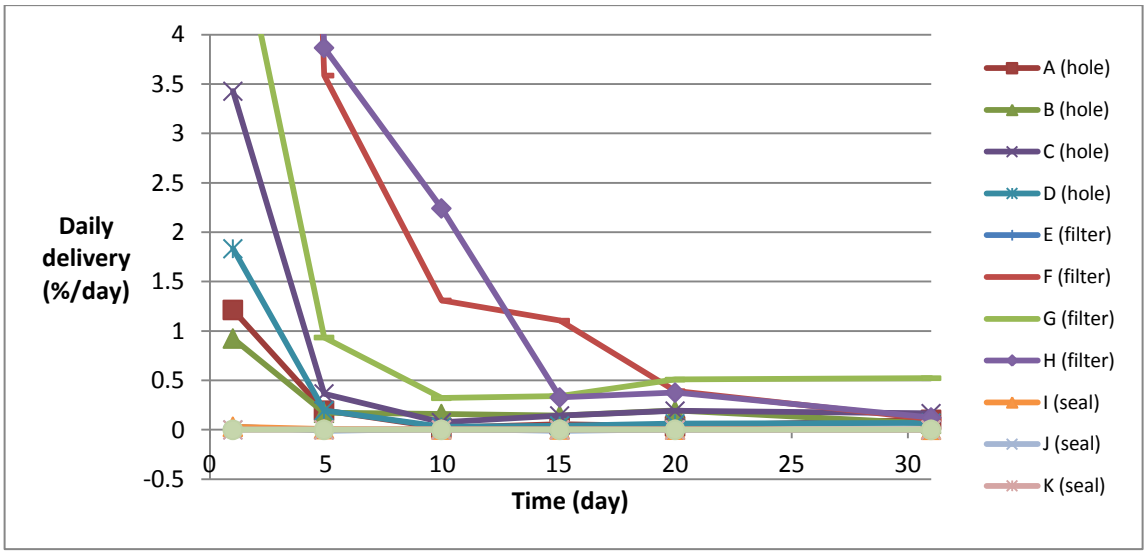

Figure 17 Average daily Dextran delivery (in percentage) over the 31-day period

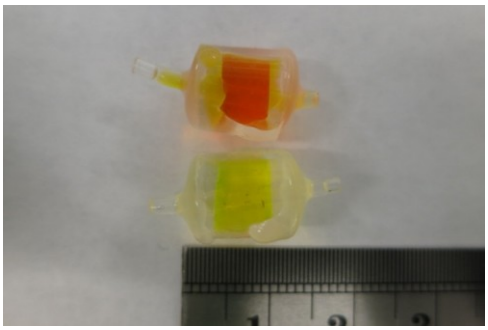

Figure 18 Image of devices A (top) and F (bottom) after 31-day release. This image shows the relative difference in Dextran remaining, with 96% of the Dextran still available in device A, and about 40% of the Dextran available in device F. The lighter color of device F than device A confirmed that more Dextran was released from device F

Overall, PDMS drug devices with diffusion holes shows a higher degree of consistency compared to PDMS devices with filters, because the coefficient of variation for the former is 0.41, which is half of the one for the latter of 0.84 over the 31-day period. These results indicate that the PDMS devices with diffusion holes achieved more showed that they could release drug over time and at a steady rate once initial burst effects are allowed to finish.

Conclusions

Several prototype drug delivery devices for use in nerve regeneration were designed, fabricated, tested and characterized to deliver drugs of interest over time. The inconsistent release data for the filter-based PDMS devices used in both NGF and Dextran release studies as well as the consistent release of the diffusion hole-based PDMS device in the Dextran release study suggested that using diffusion holes rather than an adhered membrane would be a better approach. In the 31-day Dextran release study, all of the controls acted as expected, showing that the release occurs by the desired route – either through the PES filter membrane or four 40μm diffusion holes and the inner conduit, validating the general drug delivery approach. A model based on Fick's First Law of Diffusion was used to predict the release from the various devices and diffusion hole-based PDMS devices (devices A-D) in the Dextran study. The model results were generally in the same range as the experimentally measured values, but there was significant variation both in rate and overall release for the experimental devices, so the appropriateness of the model is only generally confirmed. Nevertheless, the model is likely valuable for designing future diffusion hole sizes and drug dosages to fit various applications. In future work, a biodegradable conduit will be developed and designed based on the model and methods introduced in this paper. Biodegradable materials should better suit the desired *in situ* application.

CHAPTER 4

BRIDGING PERIPHERAL NERVE GAPS USING NGF-LOADED PLGA NERVE CONDUITS FOR NERVE REGENERATION

Introduction

Traumatic injury to peripheral nerves often leads to loss of motor control or sensation in the extremities if the severed axons on the proximal nerve stump do not regenerate and cross the nerve gap quickly [121]. For peripheral nerve gaps greater than 10mm, special bridging techniques are required to encourage nerve regrowth in the proper direction, and currently either autografts or nerve conduits are used. About 87.4% of upper limb nerve injuries can be repaired by end-to-end approximation, while 1.8% of upper limb nerve injuries require grafts or other forms of bridge to connect the two nerve stumps [53]. For those requiring bridging techniques, nerve autografts are the gold standard, but have some limitations, such as donor site deficits in muscle control and sensation [54]. Because short nerve conduits and autografts can achieve similar functional outcomes and regeneration results [57], use of nerve conduits to repair peripheral nerve gaps in a variety of anatomical locations is preferred when feasible [58].

A variety of nerve conduits have been fabricated using a range of materials, coatings, and impregnated drugs. Biodegradable materials have the advantage over non-biodegradable materials of being eliminated naturally once their function is no longer needed. Some nerve bridges provide not only guidance for axonal regrowth but also provide growth-supporting cues such as growth factors to promote optimal nerve

regeneration [52]. Nerve conduits loaded with either transplanted cells such as Schwann cells [80], stem cells [91], [122] or axon-growth promoting proteins, such as vascular endothelial growth factor (VEGF) [123] or nerve growth factor (NGF) [78], [93], [95], [124], typically show better axon growth. NGF has been found to be particularly helpful because not only are fewer adverse effects observed when using NGF compared to other nerve stimulating proteins or cells [57], but also because denser axon branches are observed in chick dorsal root ganglia (DRG) cells when treated with NGF compared to glial cell line-derived neurotrophic factor (GDNF) [93], [94]. Research has also shown that locally delivered NGF can accelerate sciatic nerve regeneration [95]–[97].

Combining the ability of a synthetic nerve conduit to direct nerve growth and NGF's ability to encourage axon growth while exhibiting a reduced adverse response [57], is a known way to improve nerve regeneration. Building upon this success, in this paper, we propose a novel biodegradable nerve conduit with a surrounding drug delivery reservoir for treatment of significant peripheral nerve injuries. The proposed device is made of biodegradable PLGA and the drug reservoir is filled with NGF that can access the lumen of the nerve conduit through a diffusion membrane, as shown in Figure 19. The expected benefit of the drug reservoir is that a single device design can be used to deliver a variety of drugs to the lumen of the nerve conduit (the space between the inner and outer tubes in Figure 20) without needing to reengineer the entire system for each drug of interest. The delivery rate of the device should be predictable for any drug, as drug diffusion through membranes is well understood, unlike microsphere-based PLGA applications [88], [89], [118], [125], [126] which depend on PLGA degradation rates.

Thus, the objective of this paper is to demonstrate a PLGA device that delivers drug

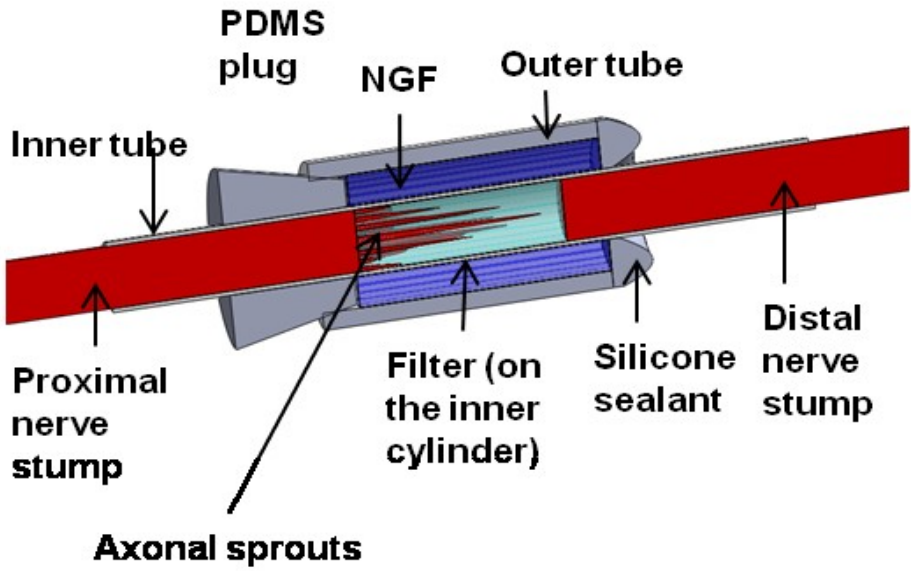

Figure 19 Schematic diagram of a PLGA nerve conduit. Drug (NGF) loaded in the space between the outer and inner tubes will diffuse through the filter and enter the lumen of the inner tube, contacting nerve stumps and stimulating axon growth on the proximal nerve stump. The inner tube can hold the two nerve stumps and guide the new-grown axon to meet the distal nerve stump. Silicone sealant and a PDMS plug are used to seal and connect the two tubes

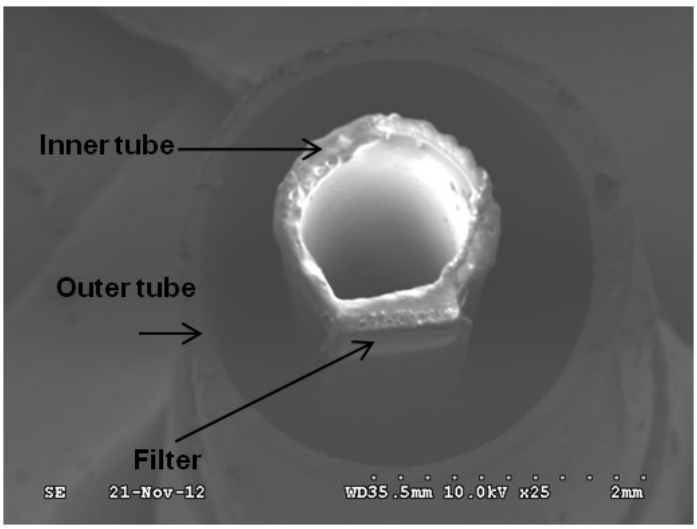

Figure 20 A scanning electron microscope image of the transverse cross-sectional view of the PLGA nerve conduit. The filter is attached on a window on the inner tube to allow the drug (not shown) stored between the inner tube and the outer tube to release into the lumen of the inner tube and promote local axonal outgrowth on the proximal nerve stumps

at a steady rate to a nerve conduit.

Materials and Methods

Drug delivery devices made of PLGA were fabricated and the drug release filters attached to the inner tube. Several tests were proposed to verify the function (drug delivery rate, bioactivity of the drug, and biocompatibility of the device) of the proposed device. A diffusion chamber study was conducted to see if NGF can be released from the device. Different combinations of NGF in polyvinyl alcohol (PVA) were also tested as PVA can help control the drug release [103] by partially blocking the pores on the filter and slowing NGF diffusion. The experiments lasted 25 days, as that should be sufficient for the nerve to grow the length of the 10mm nerve gap, as previous studies have shown that the ulnar and median nerve regrow an average of 1mm/day in monkeys [58]. The bioactivity of the drug (NGF) was tested using chick dorsal root ganglion (DRG) cells [127] treated with media released from the proposed device at different time points. Mouse models were also used to test the biocompatibility of the device, as the dimension of mouse sciatic nerve is similar to human digital nerve. The details of these experiments follow.

Design

The overall concept of the nerve regeneration device is to use a physical bridging technique with the aid of NGF to stimulate rapid repair of peripheral nerve gaps. A previous study by our group has reported the release of bovine serum albumin (BSA) across a polyethersulfone (PES) filter into the lumen of a nerve conduit with the BSA stored in the space between concentric tubes [55]. Another preliminary study showed that a similar PLGA device could deliver BSA for a period of 1 week [117].

In this paper, a similar PLGA device is used to deliver NGF. The device is fabricated using 75:25 polylactic acid (PLA) to poly-co-glycolic-acid (PGA) copolymer ratio instead of 65:35 PLGA to increase the half-life of the PLGA degradation slightly. The PLGA was used to form the outer and inner tubes of the PLGA nerve conduit. A PES filter membrane, a PDMS plug and some silicone sealant were also used to fabricate the nerve conduit. Figure 19 illustrates the design of the nerve conduit in which the drug (NGF) stored in the space between two concentric tubes is released into the lumen of the inner tube through the filter, as shown in Figure 20, and thus is available to the proximal nerve stump. Axon growth is expected to be constrained by the inner tube to meet the distal nerve stump, and the NGF should accelerate the nerve regeneration process.

Device Fabrication

Both the PLGA inner and outer tubes for the device shown in Figure 19 were fabricated from a PLGA emulsion in acetone and ethanol by solvent diffusion [128] and precipitation polymerization [129], respectively. First, the PLGA emulsion was prepared by completely dissolving 10g PLGA (7525 DLG 7E, Evonik) in 20mL acetone with constant stirring at 44ºC on a hot plate. Then, 6mL of ethanol was added into the PLGA emulsion at the same stirring rate and temperature until the emulsion turned transparent.

To fabricate the inner tube, 200µL glass calibrated micropipets (2-000-200, Drummond Scientific) were used with the aid of a plastic bulb to suck the PLGA emulsion into the micropipets, coating the walls. The micropipets with PLGA emulsion inside were then frozen overnight, and placed horizontally in a chemical hood for 10 days in order to remove the residual acetone and ethanol, leaving only a thin PLGA wall covering the micropipets. The micropipets were than immersed in distilled water for 1

additional day to harden the PLGA. The PLGA inner tubes were then obtained by breaking these micropipets and removing the glass. A carbon dioxide laser machining tool (VLS3.60, Universal Laser Systems) was used to generate a 0.8mm X 0.2mm window and trim the inner conduit into 15mm long pieces. A 2.5mm X 0.8mm PES filter membrane (PES0032005, SterliTech) was attached to the window of the inner conduit by instant adhesive (4011, Loctite).

For the outer tube, 1/8" Teflon rods were dipped in the PLGA emulsion, and immediately immersed in distilled water to form a thin layer of PLGA covering the outside of the Teflon rod. The outer tube was then peeled from the Teflon rods by hand, and a blade was used to cut the outer tube into 7mm long pieces.

For assembly, the outer tubes were placed around the inner tubes and the gaps filled by a PDMS plug that both secured and aligned the inner tube to the outer tube. The PDMS plugs were made of a 10:1 ratio of PDMS to curing agent [55] and a biopsy punch was used to trim the PDMS pieces into plugs. RTV silicone sealant (734 flowable sealant, Dow Corning) was used to seal the ends of the conduit around the PDMS plug.

After the nerve conduit was made, a radio frequency glow discharge (RFGD, commercially known as STERRAD, University of Utah Healthcare) was used to sterilize the device [130] before starting the release or biocompatibility tests.

Release Test Protocol

Samples and Controls

An average drug delivery rate of at least 2ng/day release is desired as determined by a review of the NGF literature. While different values of optimal NGF concentration or optimal daily dosage have been reported, a NGF concentration of 10ng/mL for chick

DRG cells was shown to be optimal [93] while a 80ng/day NGF daily delivery rate for adult male Lewis rats [96] was shown to generate optimal nerve recovery. In addition, the literature showed that optimal dosage may vary according to different goals (concentration or delivery rate) or verification methods (*ex vivo* or *in vivo*) used. To meet these general goals, NGF in a concentration of either 0.05 or 0.1mg/mL with PVA at either 25 or 12.5mg/mL [41] was filled in the PLGA nerve conduits for the release tests. The hypothesis is that the device with the highest concentration of NGF and the lowest concentration of PVA will result in the highest NGF release, and vice versa. A relatively low NGF release is also expected for the device without PES filter (the diffusion window) compared to all other groups.

To minimize contamination, the sterilized PLGA conduits were filled with a selected combination of PVA and NGF right before starting the release test. The drug was prepared by dissolving 0.1 mg lyophilized NGF (N2513, Sigma-Aldrich) in 0.5mL PBS with 0.1% BSA to form a 0.2mg/mL stock NGF solution. A 50mg/mL PVA solution was prepared by dissolving PVA powder (363103, Sigma-Aldrich) in distilled water, and the solution was filtered through a 0.22μm filter. The serial dilution of stock NGF solution with 50mg/mL PVA solution and PBS formed the desired combination and was filled into either the devices or the controls. Device experiments were performed in triplicate, and the combination of NGF with either 0.1mg/mL or 0.05mg/mL and PVA at either 25mg/mL or 12.5mg/mL was filled into each PLGA nerve conduit (device), as shown in Table 8. For the controls, a no PVA test filled with only 0.05mg/mL NGF without PVA was performed to determine the impact of PVA on NGF release in the device. A leakage control test was also performed by using a PLGA conduit without

Table 8 NGF and PVA dosage in the devices and controls for NGF release test

Device name	**NGF conc. (mg/mL)**	**PVA conc. (mg/mL)**	**Drug volume (μL)**	**Max. NGF amount (ng)**
Device 1	0.1	25	26	2600
Device 2	0.1	25	32	3200
Device 3	0.1	25	25	2500
Device 4	0.1	12.5	26	3600
Device 5	0.1	12.5	18	1800
Device 6	0.1	12.5	28	2800
Device 7	0.05	25	25	1250
Device 8	0.05	25	22	1100
Device 9	0.05	25	27	1350
Device 10	0.05	12.5	27	1350
Device 11	0.05	12.5	20	1000
Device 12	0.05	12.5	30	1500
No PVA test	0.05	n/a	16	800
Leakage test	0.1	25	25	2500

either the window on the inner tube or the PES filter membrane, so that no NGF release is expected. The positive controls consisted of 40 μL of 0.1mg/mL NGF in a 25mg/mL PVA solution in a 4mL receiver chamber filled with media. The negative controls were 4mL receiver chambers filled with media only.

Receiver Chamber

For both devices and controls, Dulbecco's modified Eagle's medium (DMEM, SH3026101, Thermo Scientific) with 10% fetal bovine serum (FBS, SH3091003, Thermo Scientific) was used as the medium for the receiver chamber. This solution was used so that the media from the receiver chamber could be directly used to treat DRG cells in order to verify the bioactivity of the NGF used in the experiment. Fifty mm polypropylene Petri dishes were used as the chamber for the release test.

Test Setup

Each PLGA nerve conduit was filled with the desired drug, as shown in Table 8, and sealed using the PDMS plug with silicone sealant. The device was dried for 1 hour and then mounted individually onto the bottom of the Petri dish using silicone sealant. Thirty minutes was added to ensure the silicone sealant was dry before the application of the media to the receiver chamber. After applying 3mL DMEM with 10% FBS into each dish, the Petri dishes were transferred into a 37ºC incubator. Media samples in the receiver chambers for both devices and controls were collected after 1, 4, 14, 25, 117, 254, 351, 480 and 600 hours. For the experiments listed in Table 8, all the media in the receiver chamber was replaced with fresh DMEM with 10% FBS (sink method) so that data on all the NGF released into the receiver chamber in each period could be obtained. In addition, 500µL of sample were collected each time from the positive control without replacing the media. An NGF ELISA kit (ab100757, ABCam) was used to analyze the NGF concentration at each time point for both devices and controls.

NGF Bioactivity Test with DRG cells

In order to verify the bioactivity of NGF released from the conduits over an extended period of time, especially the last period of the release study, a bioactivity test was performed in which the media from the receiver chambers of the release test with the highest cumulative percentage of NGF released in the 20-day period would be used to treat DRG cells for 72 hours. The 1st, 25th, 117th and 480th hour collections from the release test were used to verify and compare the bioactivity of NGF during the first 20-day period of the 25-day release test. In addition to the devices, a 0-5ng/mL NGF dosage curve on DRG cells was also tested in order to compare DRG axonal outgrowth when

treating DRG with freshly prepared NGF solution with the released NGF media. Both the standards (dosage curve) and media from the devices were plated on laminin-coated microplates (BioCoat, 35488, BD Medical) and incubated for 72 hours in a 37ºC incubator. A methanol fixation process was applied on the plate to stop further growth of axons after the 72 hour incubation. Rabbit beta-Tubulin (ab6046, ABCam) was used as the primary antibody, and Alexa Fluor 568 donkey anti-rabbit IgG antibody (A10042, Life Technologies) as the secondary antibody. After the primary antibody binds to the axon and the secondary antibody stains the axon, 4',6-diamidino-2-phenylindole (DAPI, D1306, Life Technologies) was used to stain the cell body of the DRG cells in order for us to distinguish the axons from the cell bodies in the image. Manual measurement was performed using Image J to calculate the axon growth in DRG cells outside of the cell body after the image was taken through a fluorescence microscope. Axonal outgrowth length shorter than twice the cell body's length was neglected because we assumed the axon was wrapped together in this case.

Pilot Biocompatibility Animal Study

A 3 week biocompatibility study in mice was performed. Before implantation, the PLGA inner tubes were first trimmed to 5mm in length and sterilized by STERRAD [130], [131]. Then, these tubes were used to bridge 5mm gaps created on the right sciatic nerve of 3-month-old Sprague Dawley male mice (n=3). A 140μm suture was used to suture the device to the sciatic nerve at both ends, and a polypropylene suture was used to suture the muscles, followed by a silk suture to suture the skin. Animals were sacrificed after 3 weeks and images were taken to evaluate the biocompatibility of the device.

Results and Discussion

The PLGA devices were successfully fabricated and tested. Details on the results of several of the experiments follow.

Device Fabrication

More than 30 devices were fabricated and tested in various ways. No obvious leakage of the device was noticed when filling the reservoir chambers of the nerve conduit with NGF. However, the drug reservoir volume was observed to be less than designed when filling the device with a calibrated syringe. An average of 24.8μL drug reservoir volume was found in the devices and controls used in the release test compared to the designed 34.2μL drug reservoir volume. The loss of volume in the reservoir chamber is likely due to the sterilization process as shrinkage has been shown to occur for PLGA devices [130]. Even with the reduction in reservoir volumes, these devices have enough space to store the desired volumes and concentrations of drug.

NGF Release Results

Figure 21 shows the cumulative NGF amount released from each PLGA device into the receiver chamber (Petri dish) at a series of time points according to the ELISA readings. Many of the devices demonstrated a "burst effect" where a large amount of drug was released in the first day before settling into a steady release rate, which will be explored more later. As can been seen in Figure 21, some of the experiments had to be stopped early due to fungal contamination developing in the receiver chamber (the Petri dish) as early as the day 10 collection, and the ones with contamination were discarded without measurement. Therefore, the number of data points for the device samples and controls varied, and only two devices had data for the 25th day collection. None of the

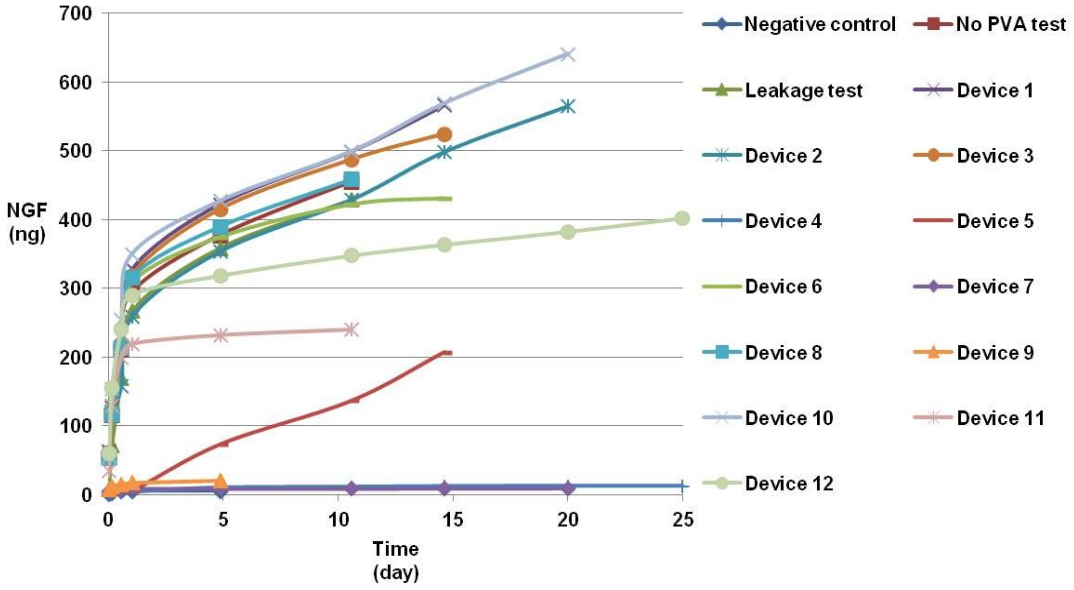

Figure 21 Cumulative NGF amount released into the receiver chamber. In each collection, all the media in the receiver chamber was replaced with fresh media. Thus, the sum of NGF concentration detected in each collection was shown in this figure to present the cumulative amount of NGF released from the PLGA device at each time point. Concentration of NGF and PVA filled in each devices: devices 1-3: 0.1mg/mL NGF in 25mg/mL PVA; devices 4-6: 0.1mg/mL NGF in 12.5mg/mL PVA; devices 7-9: 0.05mg/mL NGF in 25mg/mL PVA; devices 10-12: 0.05mg/mL NGF in 12.5mg/mL PVA

controls had data for the 25th day collection.

Since all the media in the receiver chamber was replaced with fresh media during each collection, concentration data measured using the NGF ELISA were converted into NGF mass (ng) and the results were summed over time.

The release data can be also represented in the cumulative percentage of NGF released into the receiver chamber at each time point. The cumulative percentage of NGF release was obtained by dividing the cumulative NGF weight by initial NGF weight in the release chamber. The results show that most devices still had more than 50% of the NGF left at the end of the study, and a constant positive release for all the devices indicates

that the PLGA device can continuously supply NGF even after the 25-day period. Thus, the device as currently designed has the potential to fit clinical applications where a 2 to 3 month consistent release is preferred. The slopes for the data in Figure 22 are different than the ones in Figure 21 because different volumes and concentrations of NGF – shown in Table 8 – were filled into the devices and controls. Figure 23 shows NGF daily delivery for the four designs (four combinations of NGF and PVA concentrations) in which cumulative NGF amount released between each collection time points were divided by the time period. Devices 4, 7 and 9 were excluded from this figure due to their extremely low NGF release. In Figure 23, devices prepared with the same conditions were averaged.

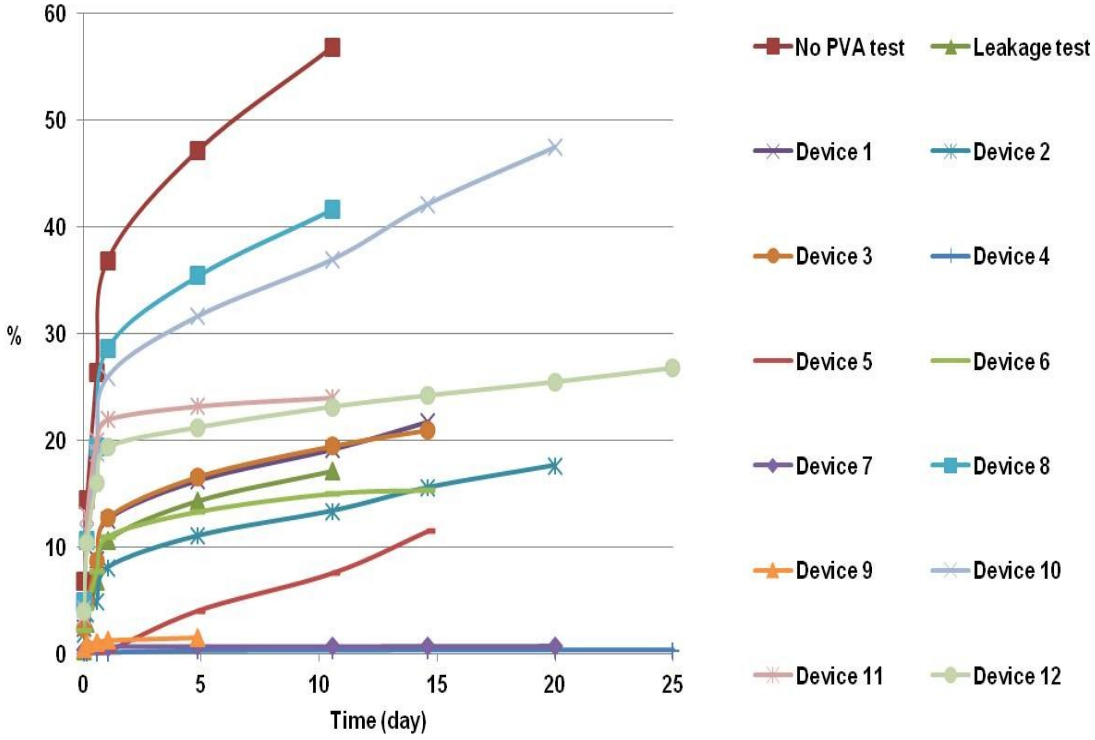

Figure 22 Cumulative percentage of NGF released into the receiver chamber in 25 days

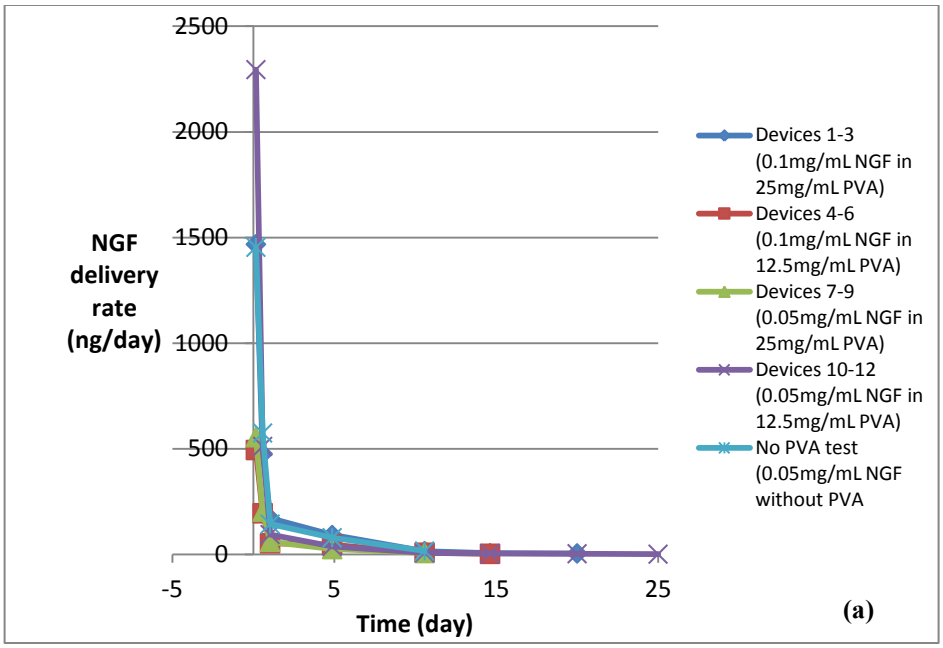

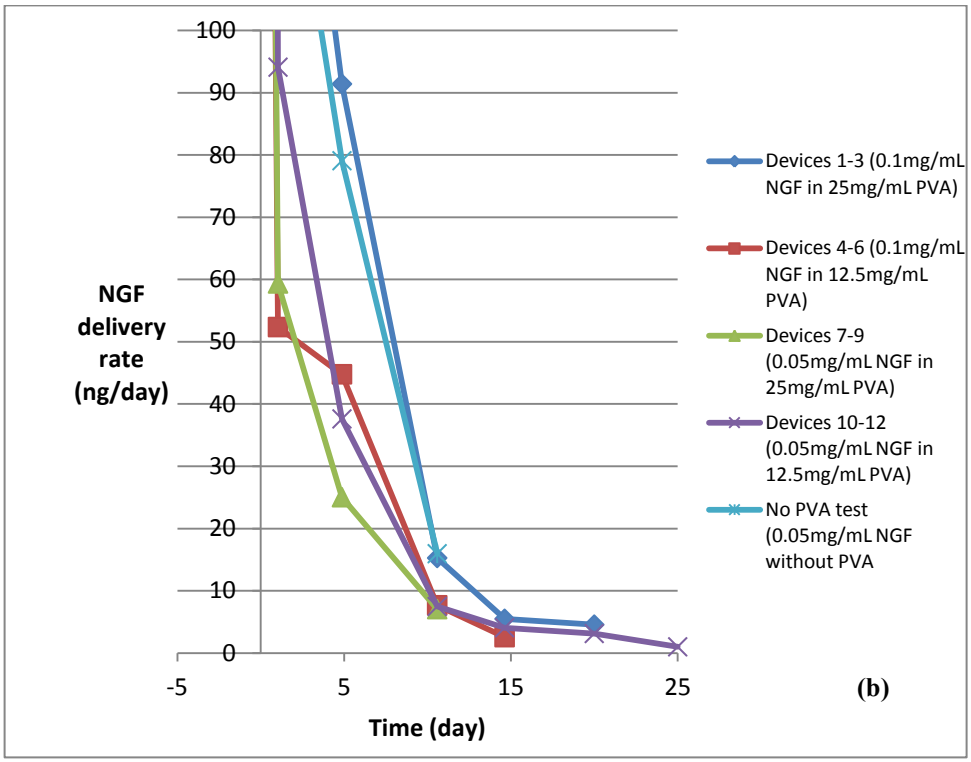

Figure 23 NGF release rate comparison. Plotted data are for the average of results for the same design (same concentrations of NGF and PVA). Devices 4, 7 and 9 were excluded from these results due to their extremely low NGF release levels. (a) All data. (b) Zoomed view showing only data below 100 ng/day.

Devices 1-3, with 0.1mg/mL NGF in 25mg/mL PVA, showed a similar NGF release in the 15-day period with a cumulative NGF release ranging from 500 to 566ng, as shown in Figure 21. The figure also shows that a cumulative NGF release percentage of 16 to 22 for the 15-day period. They possessed a much higher (1468ng/day) release in the beginning, as shown in Figure 23, then the NGF release rate dropped to 4.5ng/day in the period between the 15^{th} and the 20^{th} day. Though a higher initial release rate was observed, which is not necessarily detrimental, they showed a release rate higher than the 2ng/day in the later stages of the release test, which was the minimum release rate desired.

Devices 4-6, with 0.1mg/mL NGF and 12.5mg/mL PVA, showed a wide range of NGF release percentage and release rate. Device 4 showed almost no release with only 13ng cumulative NGF released from this device in a 25-day period, while device 5 and device 6 show a 207ng and 431ng cumulative NGF release in the first 15 days, respectively. Due to the low release of device 4, the average daily NGF delivery rate of devices 4-6 is lower than one of the devices 1-3, though devices 4-6 have less PVA and tend to release faster than higher-PVA-concentrated devices 1-3 by design. The most likely cause of the variation among devices 4-6 is the amount and location of the adhesive applied on the filter, which was difficult to control, and the size of diffusion window varied between devices.

Devices 7-9, with 0.05mg/mL NGF and 25mg/mL PVA, also showed a different NGF amount, release percentage and release rate. Only device 8 continued to release a reasonable amount of NGF in the given period, and ended with a 458ng cumulative NGF release in the first 10 days. Devices 7 and 9 have a small release, and thus the average of release rate of devices 7-9 is expected to be lower. The reason for the low release of

devices 7 and 9 is likely to be the same as device 4, *i.e.*, the filter of devices 7 and 9 were blocked by the adhesive and these devices only deliver less than 21ng NGF cumulatively in the release test. The lower release rate of devices 7-9 (started with 0.05mg/mL NGF in 25mg/mL PVA) compared to devices 1-3 (started with 0.1mg/mL NGF in 25mg/mL PVA) meets the hypothesis that lower given NGF concentration will lead to slower NGF release, although the release rate for the same design (devices 7-9) varied due to diffusion window size difference, which will be improved in the future.

Devices 10-12, with 0.05mg/mL NGF and 12.5mg/mL PVA, showed relatively consistent release kinetics. Devices 10-12 possessed the highest NGF delivery rate in the first 4 hours with the rate of 2295ng/day. The NGF delivery rate dropped to a 3.1ng/day for the period between the 15^{th} and the 20^{th} day, and a delivery rate of 1ng/day in the period between the 20^{th} day and the 25^{th} day, indicating that this combination of NGF and PVA can achieve the desired NGF delivery rate of more than 2ng/day in the first 20-days, while still releasing drug, but at a lower rate, in the following 5-day period.

Other than devices 4, 5, 7 and 9, all devices exhibited a two-step release in which a burst release (average of 286.8ng/day NGF release) was observed in the first day (25 hours), while a slower release was observed for the remaining period. This burst effect might be due to excess NGF that was left on the device when filling, though the devices were washed several times. There is also the potential that during filling, or between the fill time and the beginning of the experiment, that drug was released or flowed into the inner conduit only to then be released when placed in the receiver chamber. This excess NGF was then washed away after replacing the media of the receiver chamber several times.

For the controls, the negative control performed as expected with a very low measure of NGF. For the leakage test, 17.1% of NGF was released from its PLGA device, showing that the device was not totally sealed. Although the release percentage from this leakage test is smaller than half of the devices, it still possesses a "release," and thus a more careful fabrication process needs to be employed to ensure the sealing of the device. The no PVA test showed the highest NGF release with a 455ng cumulative NGF released into the receiver chamber in a 10-day period. When converting to percentage release, 56.9% of NGF was released into the receiver chamber in the 10-day period, confirming that the absence of PVA would allow for more rapid NGF release.

The hypotheses of different PVA and NGF concentration filled in the device are that high PVA will result in low NGF release, and high NGF will result in high NGF release. Within the same given PVA concentration, devices 1-3 (with 0.1mg/mL NGF) have a higher NGF release rate compared to devices 7-9 (with 0.05mg/mL NGF), which fits the expectation. Devices 4-6 (with 0.1mg/mL NGF) also have a higher NGF release rate compared to devices 10-12 (with 0.05mg/mL NGF), which also fits the expectation. On the other hand, within the same given NGF concentration, devices 1-3 (with 25mg/mL PVA) have higher NGF release rate compared to devices 4-6 (with 12.5mg/mL PVA), which does not fit the expectation. The extremely low release of devices 4 and 6 affect the average release rate in devices 4-6. For the devices and control filled with the same 0.05mg/mL NGF, no PVA test (with 0mg/mL PVA) has the highest NGF release rate compared to devices 7-9 (with 25mg/mL PVA) and devices 10-12 (with 12.5mg/mL PVA). Devices 10-12 also show a higher NGF release rate compared to devices 7-9. Both of these results match the assumption that PVA will impede and control the NGF

release.

Both the positive control and the negative control met expectations and set a 103ng and 6ng cumulative NGF release boundary for the devices; all measurements for devices and controls fell between these values. Though the leakage test did indicate some leakage for that device, some devices (such as devices 4, 7 and 9) showed nearly zero release (but still greater than negative control) and indicate the devices can be sealed effectively – even if that was not the goal for these particular devices. Overall, the results suggest that both the device and the drug concentrations with PVA can be used to release drug in a useful range.

Bioactivity Test in DRG cells

Since it was now known that NGF could be released at a desired rate, the next question revolved around the activity of the NGF after being stored in the device and then being released after an extended period of time. The media collected on day 20 from the release tests was delivered to DRG cells to determine if the NGF would still encourage DRG neurite growth.

To provide a reference for these tests, a NGF dosage curve with 0-5ng/mL of NGF on DRG cells, as shown in Figure 24, showed that a maximum average axonal outgrowth of 92μm was reached for these DRG cells when the NGF concentration in the treatment was no less than 1.25ng/mL. The NGF released from device 2 and device 10 was chosen for these experiments, as the average 20-day NGF release was more than 2ng/day. The results for device 2 are shown in Figure 25. Overall, the results showed that the NGF still retained some bioactivity. Surprisingly, all the DRG cells died when treated with the 1st-hour collection which represented a 20.7ng/mL NGF concentration. The color of the

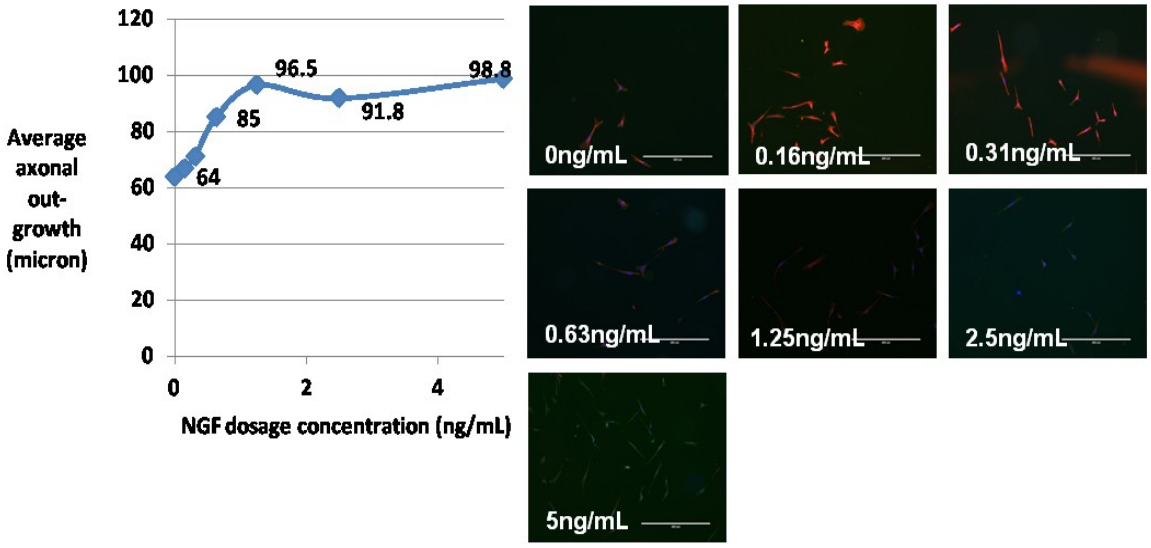

Figure 24 NGF dosage curve on DRG cells. Treatments of 0-5ng/mL NGF were applied to suspended chick DRG cells for 72 hours to obtain the axonal outgrowth length generated by different NGF concentration. This figure shows that at a 1.25ng/mL NGF concentration, axonal outgrowth reaches a maximum of 96.5µm. In the fluorescence pictures, the color purple represents the cell body of the DRG cells, and the color red represents the axonal outgrowth. The white line is a 400µm scale bar.

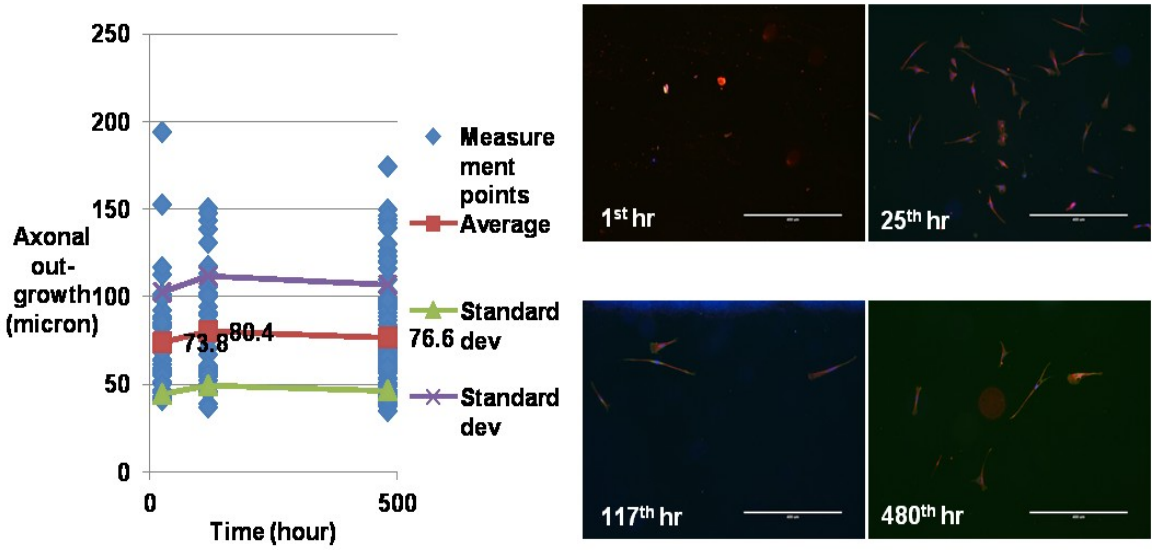

Figure 25 Bioactivity data of treatments collected from device 2. The 1st, 25th, 117th and 480th hour medium from the receiver chamber of device 2 were applied to chick DRG cells for 72 hours in order to verify the bioactivity of NGF in these treatments. This figure shows that no signal (DRG) could be observed in the 1st hour treatment and some signals for the latter treatments, indicating that the NGF in the latter treatments was bioactive to promote axonal outgrowth. The white bar represents 400µm.

treatment was yellow, unlike the treatment's usual color (pink) suggesting that the media for this particular experiment had gone bad for some unknown reason. Later investigation found that the cells were killed due to the presence of uncured silicone sealant releasing acids. As the silicone had cured or the acids removed before the later experiments, the results for them were significantly better. The 25th-hour collection showed a 73.8µm axonal outgrowth for a measured 33.6ng/mL NGF concentration. The 117th- and 480th-hour collections of device 2 showed an 80.4µm and a 76.6µm axonal outgrowth with respect to a 32.3ng/mL and a 23ng/mL NGF concentration, respectively. All of these concentrations were well above those used for our reference experiments, so direct comparison is not possible, but it is known that there is an optimal NGF concentration, as can be seen in Figure 24, and that excess NGF can lead to slightly reduced outgrowth, as appears to be the case here. In any case, the growth associated with the NGF released from device 2 is repeatably above the no NGF growth, indicating that the released NGF still has some bioactivity.

Device 10 also showed positive results for NGF bioactivity, as shown in Figure 26. In contrast to the results for device 2, the treatment from the 1st-hour collection in device 10, resulted in a 41.1µm axonal outgrowth with respect to a 19ng/mL NGF concentration, which, while still being lower than the no NGF control, did not kill the cells. Nevertheless, it is likely that the silicone sealant contamination likely stunted the growth of the axons on these DRG cells, as later tests showed much better results. The treatments from the 25th-, 117th-and 480th-hour collections showed a 75.8µm, a 95.7µm and a 89.1µm axonal outgrowth with respect to a31.9ng/mL, a 26.3ng/mL and a 24.8ng/mL NGF concentration. These results again suggest that the NGF released from

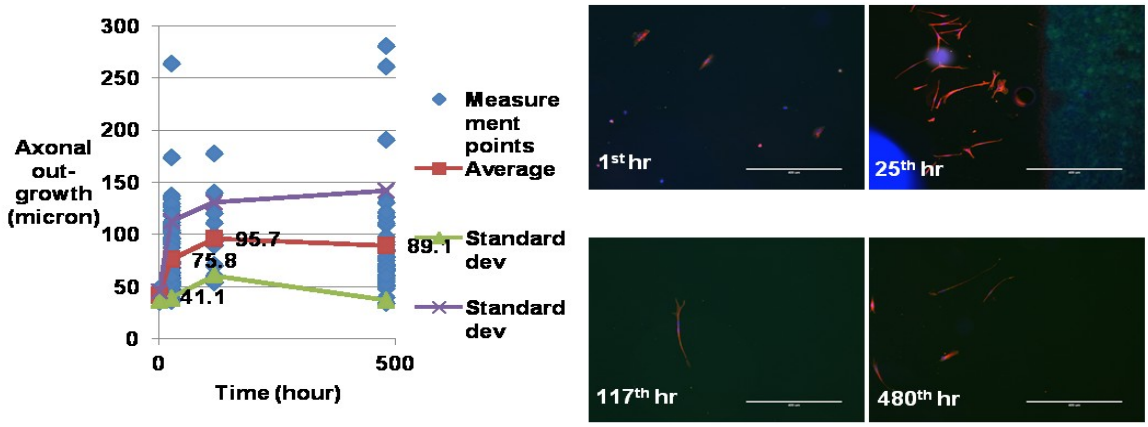

Figure 26 Bioactivity data of treatments collected from device 10. The 1st, 25th, 117th and 480th hour media from the receiver chamber of device 2 were applied to chick DRG cells for 72 hours in order to verify the bioactivity of NGF in these treatments. This figure shows a relatively low bioactivity of NGF in the 1st hour medium with only 41.1μm axonal outgrowth length. Then the bioactivity of NGF climbed in the 25th and 117th hour media, followed by a drop at the 480th hour medium. At the 117th hour medium, axonal outgrowth reaches its maximum level. The white bar in the fluorescence pictures represents 400μm.

the device in this period can promote the maximum axon growth in chick DRG cells, and the results from this device are closer to the optimal results obtained from our reference experiments. For the NGF released between the 351st and the 480th hour, it could still result in an average of 89.1μm axonal outgrowth, which demonstrates that the nerve regeneration device is capable of delivering bioactive NGF for the 20-day period.

Pilot Animal Study Biocompatibility Test

A demonstration PLGA device was implanted in 3 mice for a period of 3 weeks. After the 3 weeks, the observed inflammatory response was similar to that for areas where no device was placed as shown in Figure 27. These results give a preliminary indication that the device would not cause any significant inflammatory or biocompatibility issues over the relevant time frame for nerve regrowth through the

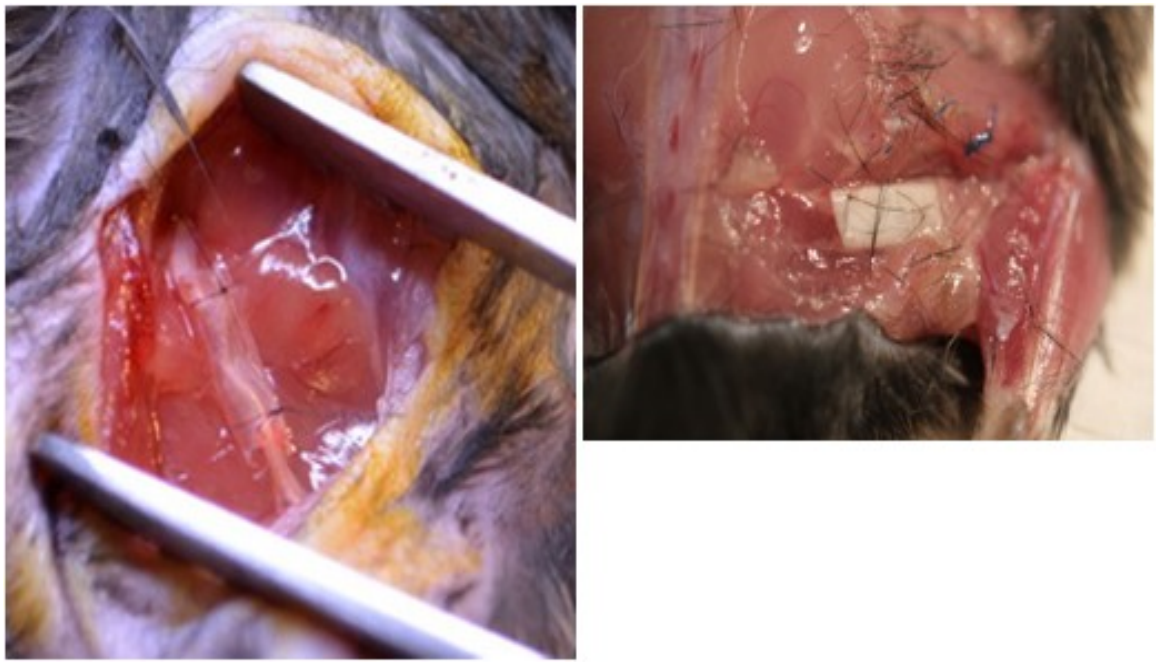

Figure 27 Three week biocompatibility study of inner tube in mice: after the surgery (left) and after 3 weeks (right). No excessive inflammatory response was observed.

conduit. The results also suggest that the sterilization technique was effective.

Conclusion

The proposed PLGA nerve conduit with either 0.1mg/mL NGF in 25mg/mL PVA or 0.05mg/mL NGF in 12.5mg/mL PVA stored in a drug reservoir can constantly deliver bioactive NGF for a 25-day period to the nerve regeneration conduit. The released NGF promoted nearly maximal axonal outgrowth when applied to chick DRG cells. Preliminary implant results suggested that the device would be biocompatible over the at least the first 3 weeks of implantation. Nine out of 12 tested devices possessed an average NGF delivery rate of more than the goal of 2ng/day. It also showed that every combination of NGF and PVA tested can result in a daily NGF delivery rate of more than 2ng/day for most of the 25-day period tested. Most of the average NGF release rate results from different PVA and NGF combination fit the assumption of higher NGF and

lower PVA will lead to a faster NGF release. Several lessons were also learned about the fabrication and testing of the devices. For example, it was learned that the adhesive application process to attached the filters to the inner conduits needs to be improved, as some devices delivered almost no NGF due to membrane clogging. In the future, a complete biodegradable device that eliminates the use of the PES filter membrane will be tested in order to avoid any blockage of the diffusion window by adhesive. Also, a more careful filling process will be conducted to eliminate the presence of any air bubbles in the device. A longer animal study will also be conducted to see if injured peripheral nerves can recover and innervate distal muscles. More thorough verification protocols will be used to analyze the animal test result, including histology and walking track analysis.

CHAPTER 5

NERVE CONDUIT SUPPLEMENTARY DATA

Several designs and experiments of nerve conduits have been proposed and conducted for peripheral nerve regeneration. In this chapter, release studies using either PDMS or PLGA nerve conduits with different proteins will be discussed, followed by modeling to design future complete PLGA devices.

A 5-day Basic VEGF Release Study from PDMS Nerve Conduit

Design and Materials

Prototypes of nerve conduits made of PDMS were first used to demonstrate possible drug release from a drug reservoir through a semipermeable membrane into a receiver chamber without any nerve conduit. These PDMS devices were made thin and designed to occupy the smallest space possible, simulating the size anticipated for future *in vivo* experiments. VEGF was chosen and loaded into this prototype due to its ability to promote axonal outgrowth [114].

PDMS was chosen to form the main structural layer of the drug reservoir due to its biocompatibility [105], [132]–[134], ease of use, and its ability to form nanoscaled structures. Since a semiflexible structure was preferred, a ratio of 10:1 PDMS to curing agent (Sylgard 184 silicone elastomer base and curing agent, Dow Corning, Midland, MI) was used to prepare the PDMS layer, followed by a standard PDMS soft lithography process [135]–[137]. Polyethersulfone (PES) membranes (PES0032005, SterliTech, Kent, WA) with a 0.3μm pore size served as filter membranes for controlled drug release.

Two PDMS devices, as shown in Figure 28, were designed and fabricated in the same way in order to test the ability to deliver VEGF. The dimensions of these PDMS prototypes measured 33mm by 11.5mm by 1 to 1.3mm. Despite the difference in size of these prototypes, the volume of the drug reservoirs was fixed at 14.5μL with the same 4mm by 3mm by 30μm filter membrane and 1.3mm diameter window.

Fabrication

The fabrication process of these PDMS devices can be divided into the fabrication of PDMS layers, preparation of the filter membrane and assembly of the whole device.

Three layers of 160μm tape (Gerber 15 SM4 InstaChange tape, Regional Supply, Salt Lake City, UT) were cut into 12mm by 2mm pieces and attached to a Petri dish to serve as a mold for forming the reservoir part in the PDMS layer. A 10:1 PDMS solution was prepared by mixing silicone elastomer base with its curing agent thoroughly and degassing to remove trapped air in the solution.

This PDMS solution was then poured onto the Petri dish mold and cured at 67.5˚C

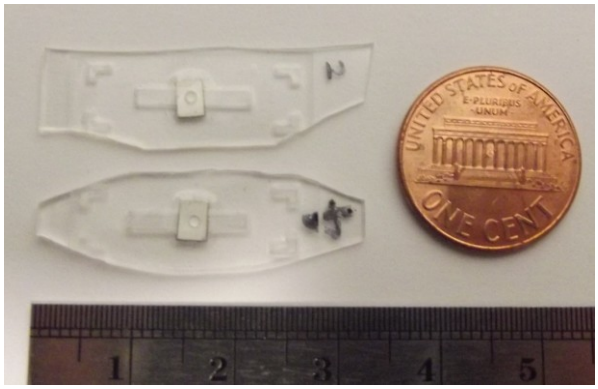

Figure 28 Photograph of the PDMS devices. Two PDMS devices serving as prototypes for demonstrating the ability to store and release drugs were designed and tested with VEGF for a 5-day period

for 4 hours. A PDMS cover layer with a 1mm diameter hole, as shown in Figure 28 was cut to serve as the window for drug release. The cured PDMS layers were then peeled out from the mold. A PES filter membrane cut by a CO_2 laser (VLS 3.60, Universal Laser Systems, Scottsdale, AZ) was sandwiched between the two PDMS layers, and air plasma was used to bond these two PDMS layers together [108].

Test Setup

Earlier experiments showed that these PDMS devices could deliver BSA for 1- and 5-day periods. Since the molecular weights of 56kDa BSA [138] and human 45kDa VEGF [139] are similar, the size of the BSA and human VEGF are likewise similar. The devices designed for running the BSA diffusion test were therefore tested with human VEGF to discover and confirm the result of human VEGF storage and diffusion across the device.

Ten microgram10 μg of human VEGF lyophilized powder (8065SF, Cell Signaling, Danvers, MA) was first reconstituted to form the drug solution with 100μL 5% w/l polyvinyl alcohol (PVA, 363103, Sigma-Aldrich, St. Louis, MO) in phosphate buffered saline (PBS). About 14.5μL of this VEGF solution was filled into the reservoir through a calibrated syringe, and then the PDMS device was placed into a 7mL glass amber vial filled with 4mL PBS, as shown in Figure 29. Two sets of glass amber vials were used, *i.e*., two unknown samples were tested for their diffusion and release rate across the filter membrane to the receiver chamber. These two vials were placed on an orbital shaker at room temperature, and samples were collected at 0.17, 7, 25, 47 and 109 hours after placing the PDMS devices into the glass amber vials. The maximum VEGF concentration in the receiver chamber, if all the VEGF in the reservoir came out would be

Figure 29 Test setup for 5-day VEGF diffusion test. A PDMS device filled with 14.5uL 10ug/mL VEGF was placed in the glass amber vial with 1mL PBS as the receiver chamber medium

362.5µg/mL. ELISA was designed to measure VEGF concentrations in the receiver chamber, and45 of the 96 wells of a human VEGF-A platinum ELISA kit (BMS277/2CE, eBioscience, San Diego, CA) were used for this experiment. Samples were collected in triplicate, with duplicate positive calibration standards ranging from 0.078 to 5 pg/mL and duplicate negative standards.

Results and Discussions

Readings from the VEGF ELISA assay were plotted to generate VEGF release curves, as shown in Figure 30. There was no calibrated VEGF concentration for this experiment due to the design error of the VEGF standards. VEGF standards were prepared 100,000 less than the expected VEGF release region from the devices, thus the reading of the VEGF release cannot be converted into VEGF concentration.

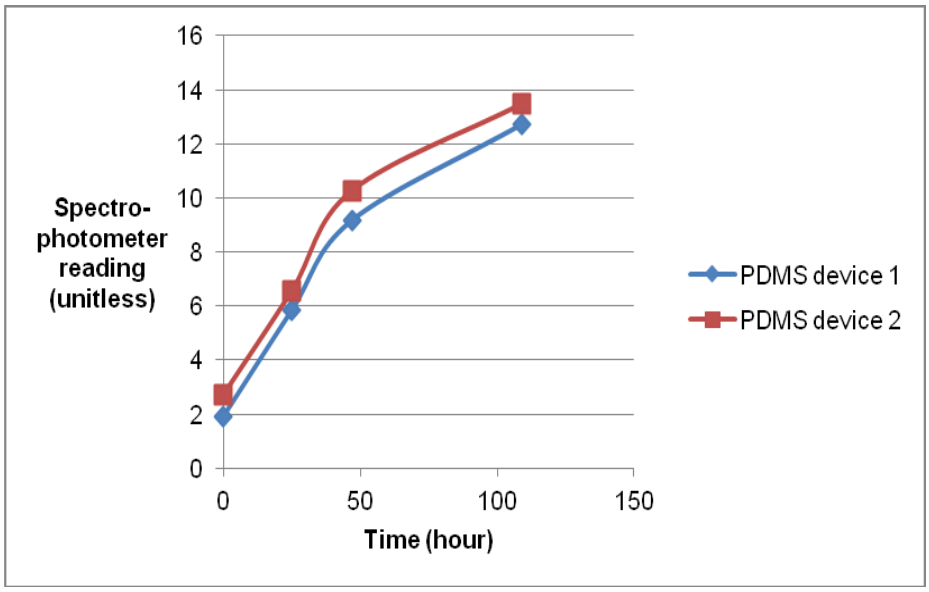

Figure 30 Cumulative 5-day VEGF reading. Though unitless, both devices show near zero-order release over a 5-day period after a small initial burst

Though no calibrated VEGF concentration was obtained from the reading due to the lower range of the VEGF standards, the cumulative reading for 5-day VEGF diffusion teststill had a positive slope and indicates the cumulative release of VEGF among the 109-hour experiment time. This indicates that these two PDMS devices, as shown in Figure 28, could consistently deliver VEGF from the drug reservoir into the receiver chamber, since the slope of the curve in Figure 30 is constant. It also indicates that the PDMS device has the ability to store the drug, and constantly diffuse the drug into the environment. Therefore, further experiments were performed in order to test the device's ability to deliver the desired drug into the nerve conduit, which was used to bridge a nerve gap.

A 6-day BSA Release Study from PDMS Nerve Conduit

Introduction

Almost 3% of trauma patients suffer from peripheral nerve injuries causing lifelong disturbances [49] in function and adverse socioeconomic consequences [46] due to the fact that these injuries are difficult to treat and have poor outcomes with contemporary treatments [45]. Peripheral nerve injuries caused by accidents or battlefield incidents with nerve gaps greater than 1-2cm require special bridging techniques [52]. Autologous nerve grafts are typically used to bridge the nerve gap; however, this requires additional surgery and can result in donor site deficits in function or sensation. Despite successful tension-free re-approximation of severed nerve ends, outcomes are dismal primarily due to poor healing, scar formation and the slow rate of nerve regeneration.

Several options have emerged to improve outcomes in peripheral nerve repair. These include artificial nerve grafts, cadaver grafts and nerve conduits. Nerve conduits made with either synthetic or natural materials have been used to guide axons and bridge the nerve gaps ranging from 5 to 80mm [59]. For example, biodegradable polymer conduits embedded with Schwann cells showed a better result for nerve regeneration compared to autografts over a 6-week period *in vivo* [80]. Additionally, biodegradable polymer nerve conduits with NGF were tested for 3 months *in vivo*, showing significant NGF release in a 10-mm nerve gap in a rat sciatic nerve model [78]. In brief, VEGF [114], [140], NGF [124] and GDNF [112] can all stimulate nerve growth and enhance axon propagation.

Design and Fabrication of the Nerve Conduit

Design and Materials

Prototypes of the nerve conduit were designed, fabricated, and tested to explore the possibility of drug delivery using concentric conduits with a semipermeable membrane. PDMS was chosen to form the main structural layer of the drug reservoir, *i.e.*, the outer concentric tube, due to its biocompatibility [105], [132]–[134] and its ability to form nanoscaled structures. Ten to one PDMS to its curing agent (Sylgard 184 silicone elastomer base and curing agent, Dow Corning, Midland, MI) was used to acquire a relatively flexible PDMS structure. Pellets of thermoplastic PCU, purchased from DSM Biomedical, referred to as Bionate II, were heat extruded into tubes with outer and inner diameters of 1.5 and 1.3mm, respectively. Bionate II tubes show good biocompatibility and can be suitable for *in vivo* drug delivery. Biocompatible polyethersulfone membranes (PES0032005, SterliTech, Kent, WA) with 0.03μm pore size were attached to a window created in Bionate II tube in order to control drug diffusion. Figure 19 shows the sagittal cross-sectional illustration of the nerve conduit. These conduits would be interposed between the cut ends of a nerve. Once the drug diffuses from the reservoir via the filter, it will contact the axon growth cone and enhance axon number, diameter and density within the conduit and across the gap.

A 12-mm-long PDMS outer conduit reservoir with a thinner 15-mm-long Bionate II tube was the prototype used to demonstrate diffusion across the polyethersulfone filter. The drug reservoir volume ranged between 50 to 100μL among the various prototypes. Drug release was controlled by selection of polyethersulfone membranes with different pore size or the window size on the Bionate II tube. The pore size was fixed at 0.03μm,

while the window size slightly varied from one device to another due to the flexible nature of Bionate II tubes.

Fabrication

Ten to one PDMS was prepared using standard methods of PDMS soft lithography [135], [136]. The PDMS solution was then poured into 1.5mL Eppendorf vials and baked at 65°C for 2 hours to form cylinders. A 5mm biopunch was used to create a hollow structure – the drug reservoir – in the PDMS outer conduits and the same tool with a 1.5mm biopunch was used to form the outer PDMS plugs to seal and secure the Bionate II tube in the device, as shown in Figure 10.

The Bionate II tubes prepared with a 1.4mm outer diameter and a 1.0mm inner diameter were used as the nerve conduit for *in vitro* drug release experiments. The tube was cut into 15mm sections and one hole with approximate 1-by-2.5-square millimeter dimension was punched at the center to serve as windows for the drug to diffuse into the tube. A polyethersulfone filter membrane was prepared in squares to cover the window and designed for the control of drug release. Loctite 4011 adhesive (18680, Loctite, Westlake, OH) was applied along the edge of the window to attach the polyethersulfone filter membrane without blocking the pores on the membrane.

The Bionate II tube with the filter membrane secured was then placed in the lumen of the PDMS outer conduit. Small PDMS concentric plugs were prepared by punching a 3mm-thick PDMS layer with 5mm and 1.5mm biopunches. They were then plugged into the Bionate II tube at both ends in order to form a drug reservoir in the lumen of the PDMS outer conduit. One end of the PDMS tube was sealed with this 3mm-thick PDMS plug and some uncured PDMS and baked for 1 hour at 65°C. The drug was then injected

into the reservoir through the other end of the PDMS outer conduit. In order to minimize bubbles, which lead to loss of diffusion area on the filter, the drug reservoir was filled completely. Therefore, the volume of drug ranged between 50 to 100μL. Next, the other side of the PDMS outer conduit was sealed with another PDMS plug, while RTV 734 silicone sealant (2307774-1008, Dow Corning, Midland, MI) was applied instead of uncured PDMS, since it required no heating, which could have damage the drug. After the device was placed at room temperature for 15 minutes to cure the sealant, it was ready to use.

Test and Results

Test Setup

The prototype test experiments utilized bovine serum albumin (BSA, A8022-500G, Sigma Life Science, St. Louis, MO) to demonstrate the diffusion across the device and the receiver chamber, which was a 7mL amber glass vial filled with 7mL of 1x phosphate buffered saline (PBS). The initial concentration of the BSA solution (serving as a drug simulant) was 100mg/mL and was prepared by vortexing 100mg of BSA powder into 1mL PBS at room temperature for 3 minutes. Three unknown samples were tested along with three positive controls and two negative controls, as shown in Table 1. BSA standards (23209 and 23225, Thermo Scientific, Rockford, IL) were used to both prepare the positive standards between 2mg/mL to 10μg/mL and analyze the concentration on three microplates.

For negative control 1 and samples 1, 2 and 3, the 6-day diffusion test started with filling the Bionate II tube (nerve conduit) with the desired drug, as shown in Table 9, then the whole device was immersed into the 7mL of PBS in the 7mL glass amber vial. For all

Table 9 Samples corresponding to drugs and receiver chambers

Sample name	Drug in the reservoir	Maximum possible concentration in the receiver chamber
Positive control 1	120μL BSA	1714.3μg/mL
Positive control 2	80μL BSA	1142.9μg/mL
Positive control 3	2μL BSA	28.6μg/mL
Negative control 1	80μL PBS	0
Negative control 2	n/a (no reservoir)	0
Sample 1	50-80μL BSA	1142.9μg/mL
Sample 2	80-100μL BSA	1428.6μg/mL
Sample 3	75-80μL BSA	1142.9μg/mL

the positive controls, on the other hand, the desired volume of BSA was filled directly into the 7mL of PBS inside the vial. For negative control 2, since no PDMS device was used, 80μL PBS was directly injected into the 7mL PBS in the vial. Multiple positive controls were used to not only serve as controls for different samples with different volumes of BSA, but also to provide readings in extremely small concentration value to better describe the situation when the diffusion rate was limited for some devices. Positive control 1, with 120μL BSA, could serve as the control for all three unknown samples, while positive control 2, with 80μL BSA, could serve as the control for sample 2 and 3.

All vials were placed on a vial holder that sat on an orbital shaker which smoothly mixed the medium in the vials. The purpose for filling the Bionate II tube with PBS before putting the device into the vial was to eliminate air bubbles which would impede the drug from diffusing out since the Polyethersulfone filter membrane was designed to deliver drugs from a solution into another and bubbles in contact with the filter membrane on the receiver chamber side would lead to no diffusion. The same reason also applied to the receiver chamber in which the PBS level was almost full in order to

minimize bubbles in the receiver chamber, and therefore minimize the possibility of bubbles appearing in the Bionate II tube.

Samples were collected after 0.5, 17, 46, 61, 91 and 112.5 hours in triplicate in three 96-well microplates. Standards, on the other hand, were prepared in duplicate in each microplate and thus six copies of one standard were acquired. Before collecting samples from vials, a 30 second vortex step was performed in order to mix the solution well. The same volume of PBS was added into the receiver chamber every time after the same collection in order to maintain the same volume of the receiver chamber. After collecting the last series of samples, 200μL of working reagent was then added in each well and we then followed the standard operation procedure provided by the assay maker for the BSA standard to perform plate reading at 562nm wavelength on a spectrophotometer.

A follow up experiment was designed to determine the magnitude of the diffusion when incorporating a nerve conduit on the device. The similarity in molecular weight between 56kDa BSA [138] and human 45kDa VEGF [139] suggested that they could be used interchangeably for proof of concept, and both were much smaller than the 0.03μm pores on the filter membrane. Therefore, BSA was chosen due to its bigger size and slower diffusion, making it a worst case scenario.

Results

Readings from the spectrophotometer plate reader were analyzed and calibrated using Microsoft Excel. The BSA concentration in the receiver chamber over the 6-day period is shown in Figure 31, and Figure 32 shows the percentage of BSA released into the receiver chamber in the 6-day period. Since the volume of BSA in the three samples

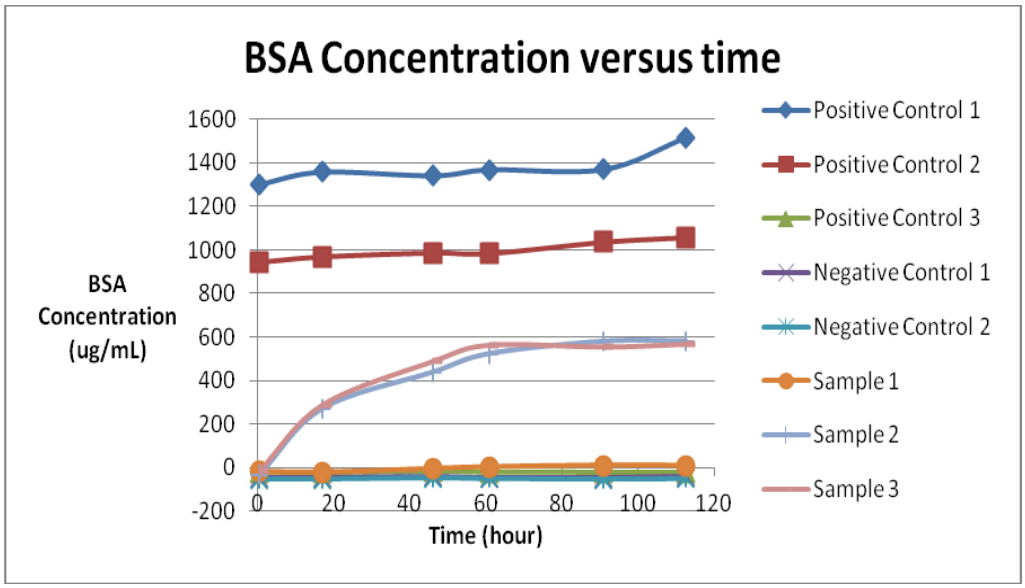

Figure 31 Six-day BSA release concentration (µg/mL) into the receiver chamber. Three positive controls and two negative controls were given along with three unknown samples

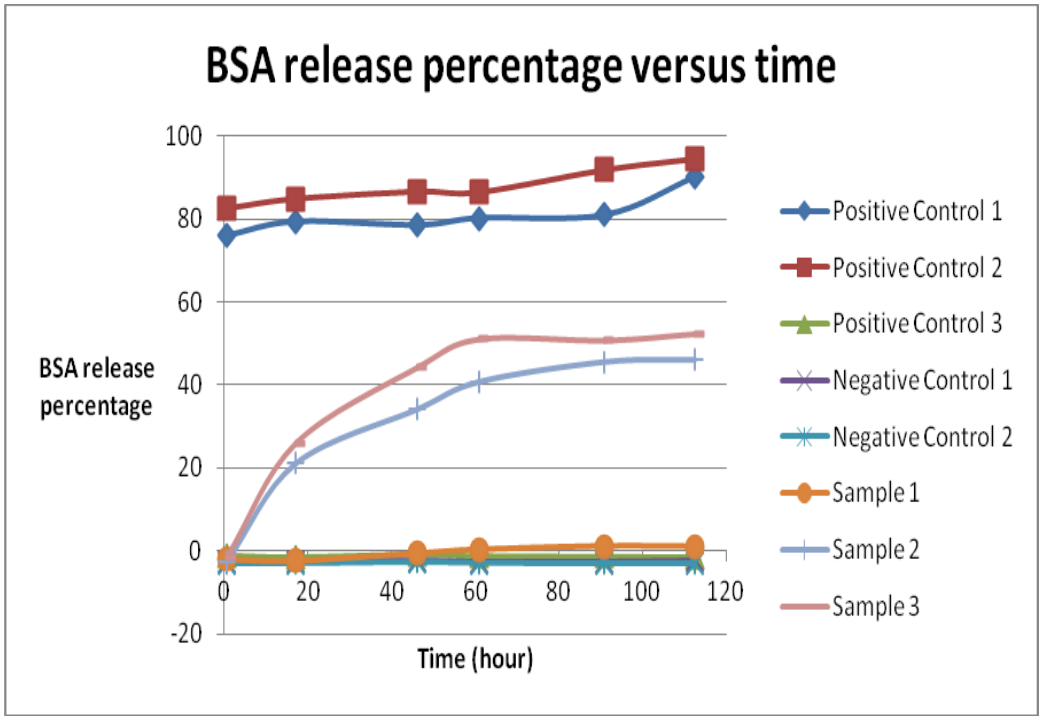

Figure 32 Six-day BSA release percentage into the receiver chamber. Three positive controls and two negative controls were given along with three unknown samples

were within specific ranges, the maximum possible BSA volume was used as the denominator, that is, 80μL for sample 1, 100μL for sample 2 and 80μL for sample 3.

Though the BSA release percentage of positive control 1 in Figure 32 increased from 76 to 101% and that of positive control 2 increased from 82 to 106%, they were relatively flat compared to samples 1 and 2. The BSA release percentage of sample 2 increased 23.6% between the 0.5 and 17^{th} hour, while the release from sample 3 increased from 27.6%. All the samples fall between positive control 1 and negative controls 1 and 2.

Discussion

In the BSA testing, after 61 hours of diffusion, the diffusion rates (the slope in Figure 32) of both sample 2 and 3 slowed down because the BSA concentration in the receiver chamber was higher and thus the diffusion gradient became lower. The diffusion rates for the first 61 hours were 0.68 and 0.85%/hr for sample 2 and sample 3, respectively. In comparison, the diffusion rates for the proceeding 51.5 hours were 0.19 and 0.13%/hr for sample 2 and sample 3, respectively.

Negative values of the BSA release percentage were generated from the negative concentration based on the calibration curve in which the standards were prepared between 0 to 2000μg/mL. Since the calibration equation was a linear function that fits most of the curve to achieve minimum standard deviation, the equation could not interpret the concentration in the region of lower concentration precisely and therefore lower concentrations than were possible were acquired for the same plate reading. If only the reading values of small concentration standards were used to generate the concentration calibration equation, the reading values of both negative controls 1 and 2 were below the reading for 0 concentration standard, while that of samples 1, 2 and 3

were above the reading for 0 concentration standard.

Last but not least, the BSA concentration increment of sample 1's receiver chamber was about 27μg/mL during the 112.5 hours of diffusion based on the readings from lower concentration standards. Its diffusion rate was relatively low compared with samples 2 and 3 probably because the filter was blocked. Either the Loctite 4011 adhesive from the fabrication process, or air bubbles in the drug reservoir blocked the filter; therefore, the drug could not diffuse out and release into the nerve conduit, diffusing into the receiver chamber. Though the filter was blocked in sample 1, it suggests that no or minor leakage was shown on this device since the drug would not leak into the receiver chamber.

Conclusion and Future Work

This work suggests that the prototypes for demonstrating the possibility of drug delivery across the filter membrane and release into the nerve conduit using BSA were successful and could be used for drug delivery at a reasonable release rate. VEGF and NGF will be used to explore the capability of the device followed by *in vivo* drug delivery test on rats.

A 25-day Dextran Diffusion Study

Design

Similar to the 31-day Dextran diffusion study, this 25-day Dextran diffusion study was a pilot study to use Dextran to mimic the NGF release kinetics.

Modeling

The same model as the one shown in Chapter 3 was used to predict Dextran concentration in the receiver chamber. All calculation was conducted in Microsoft Excel,

and after entering the parameters shown in Table 10, the concentrations in the receiver chamber in the 1st-day, 5th-day, 10th-day, 15th-day, 20th-day and 25th-day collection with sink method used are shown in Table 11.

Three sets (n=4) of PDMS devices were proposed in order to verify both the integrity of the device and the consistent release in the same design. Table 11 shows the modeling results for the Dextran concentration in the receiver chamber at different time point, with sink methods used for all three sets of the PDMS devices. Similar to the 31-day Dextran diffusion study in Chapter 3, PDMS devices with diffusion holes were expected to have consistent release kinetics compared to PDMS devices with PES filter

Table 10 Known parameter for the model

Description	**Notation**	**Value**	**Unit**
Cross-sectional area in the inner conduit	$A_{1\text{-}2}$	1.33×10^{-6}	m^2
Wall thickness of the inner conduit	$\Delta x_{0\text{-}1}$	100	μm
Distance between the diffusion hole to the receiver chamber	$\Delta x_{1\text{-}2}$	10	mm
Diffusion coefficient	D	0.00000126	$\frac{cm^2}{s}$
Receiver chamber volume	V	7	mL

Table 11 Design and expected Dextran delivery (in ng/mL) in a 25-day period

Design	**Dextran dosage**	**1st hour**	**Day 1**	**Day 5**	**Day 10**	**Day 15**	**Day 20**	**Day 25**
With two 50μm holes	125μL 12.5 mg/mL	27.7	525.5	2745.6	3169.4	3044.2	3236.6	3007.5
With PES filter membrane	125μL 12.5 mg/mL	213	4000.4	19901.7	21001.2	18321.0	17667.1	14867.8
Sealed device without holes or membrane	125μL 12.5 mg/mL	0	0	0	0	0	0	0

membrane. No release was expected for the sealed device.

In addition to these three sets of PDMS devices, two reference samples (n=1) with known concentrations of 2551ng/mL and 17847ng/mL Dextran in PBS were added into this study to compare the Dextran signal change for the expected 5-day net concentration from the modeling results of PDMS devices with diffusion holes and PDMS devices with filters, respectively. Table 12 shows the volume and design for each device and reference samples used in this 25-day Dextran release study. Seven mL PBS was filled into amber glass vials as the media for the receiver chamber.

Fabrication

The fabrication process of the PDMS devices is similar to the PDMS devices used in the 31-day Dextran diffusion study in Chapter 3. Only the size of the through diffusion holes changed.

Table 12 PDMS devices and reference samples used in the 25-day Dextran release study

Device number	**Design of the PDMS device**	**Volume of Dextran (μL) (approximately)**
Device A	With two 50μm diffusion holes	125
Device B	With two 50μm diffusion holes	100
Device C	With two 50μm diffusion holes	125
Device D	With two 50μm diffusion holes	125
Device E	With filter	125
Device F	With filter	125
Device G	With filter	125
Device H	With filter	100
Device I	Without filters or holes	175
Device J	Without filters or holes	125
Device K	Without filters or holes	125
Device L	Without filters or holes	125

Test Setup for Dextran Diffusion Experiments

Table 11 shows the design and expected Dextran concentration in the receiver chamber in a 25-day period, and Table 12 shows the approximate volume of Dextran loaded into each device. Twelve and a half mg/mL Dextran was prepared by dissolving 25mg Dextran with PBS. The setup of the diffusion chamber is the same as the ones in BSA and NGF release study, besides that the sink method would be used in which the entire receiver chamber media will be replaced with fresh 7mL PBS every time during

collection. Reference samples M and N have no PDMS devices, and Dextran of 10µL 1.79mg/mL and 10µL 12.5mg/mL was directly added into 7mL PBS in the receiver chambers. Unlike the device groups using the sink method, only two aliquots of 400µL samples will be collected from reference samples M and N each time, with no fresh PBS filled into the receiver chambers. Samples were stored as the same manner shown in Chapter 3, and the plate would also be read with the same excitation and emission wavelengths shown in Chapter 3.

Results and Discussion

The reference samples M and N show a varying Dextran concentration in the 25-day period, as shown in Figure 33. For reference sample M, the concentration varies from1873ng/mL to 2537ng/mL, with a 14.1% standard deviation. For reference sample N, the concentration increases from 18566ng/mL to 27051ng/mL, with a 16% standard deviation. Due to the fact that the glass vials used in this 25-day Dextran release study was not new, though possible autoclave sterilization might be conducted before the use, it may contain some residual protein that can interact with Dextran. Also, evaporation of PBS can contribute to the increasing concentration of the reference sample N. For the reference sample M, the varying concentration may result from the liner of the amber vial

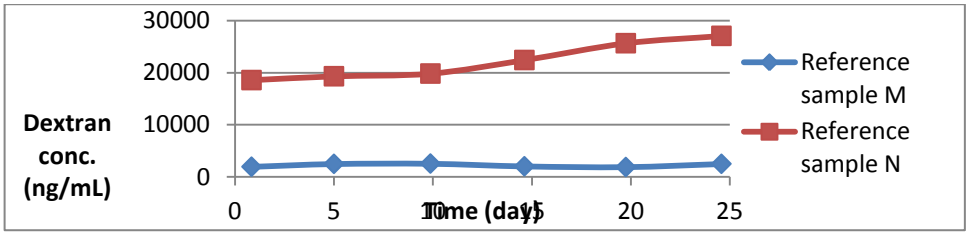

Figure 33 Dextran concentration of reference samples M and N in a 25-day period

trapping some Dextran, since a thorough Vortex process was not taken in order to remain the same collection method as the sample groups. For the device with two 50μm diffusion holes (devices A-D), a relatively consistent results were acquired when comparing to the modeling data, as shown in Figure 34. Experimental data of devices B, C and D mostly fit the model. Device A has an initial release, followed by a zero release. It is due to either air bubbles got introduced into the PCU conduit when replacing the media after collections, or the air bubble in the drug reservoir impedes the drug from diffusing through the 50μm holes.

For PDMS device with filters, Figure 35 shows the experimental data comparing to the modeling result. As observed in the previous 3-week NGF diffusion study, designs with filter as the diffusion window have inconsistent results due to the application of adhesive may partially or totally block the filter window and reduce its porosity. For device F, though relatively similar results in the experimental and modeling data, it suggests that the filter is not securely attached to the PCU conduit because a porosity of 1 was used in the modeling (which assumes that the filter is physically not in appearance).

For PDMS device without filters or diffusion holes, Figure 36 shows the experimental data compared to the modeling result. Only a minor signal of Dextran detected for devices I and L, and no further release of Dextran was detected for any devices with this design. The minor signal of Dextran in devices I and L might result from initial Dextran filling process in which extra Dextran flowed out from the reservoir before the sealing process.

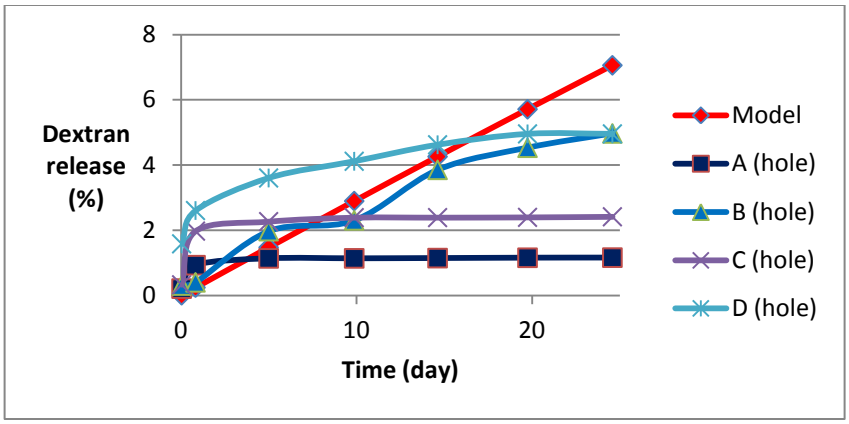

Figure 34 Cumulative Dextran release percentage from the devices with diffusion holes. Two of the devices have a similar release kinetics with the model

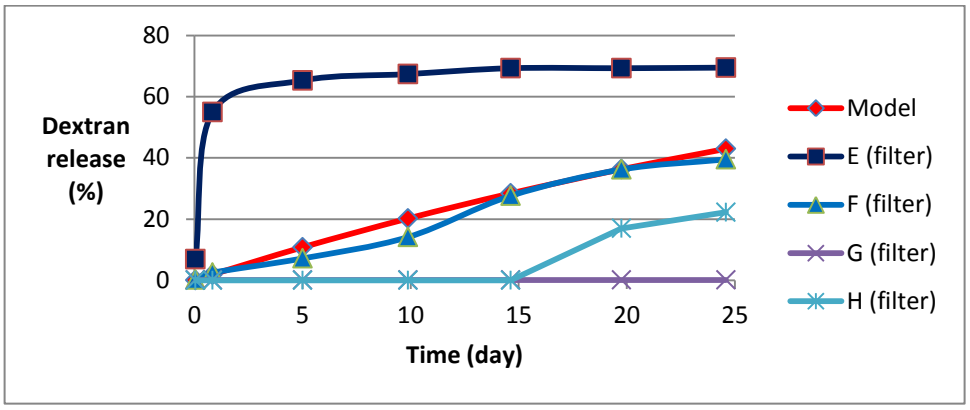

Figure 35 Cumulative Dextran release percentage from the devices with PES filter compared to the modeling result

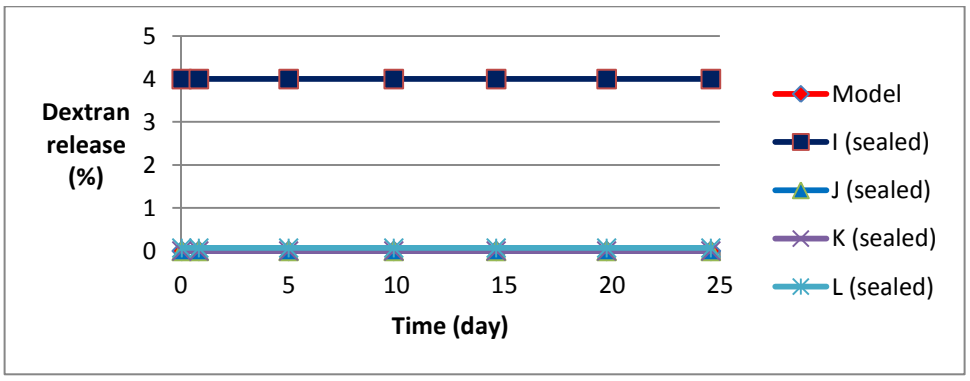

Figure 36 Cumulative Dextran release percentage from the sealed device compared to the modeling result

A 5-day Dextran Control Evaporation Study

This 5-day Dextran control evaporation study shows that only a 5-day period can result in a huge Dextran concentration change under the current experimental setup. Table 13 shows the Dextran concentration variation in this 5-day study. Two out of four controls have a more than 10% concentration change. Table 14 also shows that a 2-7% mass loss was observed in this 5-day study. Because the control with the higher mass loss did not result in a higher concentration change, this indicates that either the glass vial is not clean or the spacer in the cap of the glass vial traps some Dextran.

A Dextran control evaporation study is also proposed in order to identify the effect of the evaporation of PBS in the receiver chamber resulting in a Dextran concentration change. Two groups (n=2) of controls were used in this study in order to explain the Dextran concentration difference in the reference samples M and N in the 25-day Dextran diffusion study. Controls MA and MB have the same content as the reference sample M shown in Table 12, and controls NA and NB have the same content as the reference sample N shown in Table 12. Prior each collection, the whole receiver chamber (the amber glass vial) would be weighted in order to track the PBS loss due to evaporation.

Table 13 Concentration (ng/mL) variation in the 5-day Dextran control evaporation study

Control number	**Day 0 conc.**	**Day 5 conc.**	**Original conc. given**	**average**	**Standard deviation**	**Standard deviation percentage**	**Conc. change percentage**
MA	1757.6	1990.8	2551.0	1874.2	164.9	8.8	13.3
MB	1897.5	1889.7	2551.0	1893.6	5.5	0.3	-0.4
NA	14476.4	14204.3	17857.1	14340.3	192.4	1.3	-1.9
NB	16179.0	14375.3	17857.1	15277.1	1275.4	8.3	-11.1

Table 14 Mass (gram) loss of the receiver chamber (glass vial) in the 5-day Dextran control evaporation study

Control number	**Day 0 mass**	**Day 5 mass**	**Mass change percentage**
MA	16.2	15.9	1.8
MB	16.1	15.6	3.0
NA	16.6	15.4	7.1
NB	16.4	15.7	4.3

A 7-day BSA Release Study from PLGA Nerve Conduit

Introduction

Peripheral nerve injuries affect about 3% of trauma patients and result in significant disturbances in their lives due to lost motor function and sensation. For peripheral nerve injuries with gaps greater than 1-2cm, special bridging techniques are required for nerve repair [52]. Nerve autografts are the gold standard for repairing nerve gaps but these results in donor harvest site deficits. Here, a synthetic nerve conduit with the potential for controlled and sustained drug delivery to improve nerve regeneration has been investigated. Concentric nerve conduits made of PDMS was reported to deliver protein (BSA) for 6 days [55]. As an improvement, a biodegradable material was chosen in this work in order to minimize long-term incompatibility and need for subsequent device removal. BSA was used for proof of principle for assessing the ability of the device to deliver growth factor protein for later applications.

Materials and Methods

Inner (1.6mm diameter, 7mm long) and outer (3.2mm diameter, 17mm long) cylinders were fabricated from PLGA (LP-381, SurModics Pharmaceuticals) using glass capillary tubes and Teflon rods. A PES filter membrane (30nm pore size) (PES0032005, SterliTech, Kent, WA) was inserted into the inner tube wall to serve as the protein release point. The small conduit was placed inside the larger conduit with the space between the two serving as the drug reservoir for BSA (A8022-500G, Sigma Life Science, St. Louis, MO). The space between the tubes at the end was sealed with silicone sealant (RTV 734, 2307774-1008, Dow Corning, Midland, MI) such that protein could only cross the filter membrane for release. A 7-day (171-hour) release and leakage test was performed in order to explore the capacity of this PLGA device to deliver protein. Samples included: 30 µL of 300mg/mL (9 mg) BSA in PBS (n=2), negative controls (PBS alone) (n=2), a reference sample (to show the result if only 1.5% drug released) (n=1) and positive control with 42µL 300mg/mL BSA directly injected into the receiver chamber (n=1). A conduit that had no filter in place in the inner lumen was sealed at the ends to test the sealing of the device (leakage test) (n=2). The devices were placed in glass vials filled with 7.5mL PBS as the release medium for the receiver chambers.

Results and Discussion

In the 171-hour period, 8.8 or 4.3mg BSA (~98% and 48%, respectively, of the total loaded dose) was released from the two test nerve conduits, as shown in Figure 37. The leakage test sample had near-zero BSA release in the 171 hour period supporting the idea that any BSA release observed from the test conduits were through the filter. Positive and negative controls and the reference sample were all in their expected ranges.

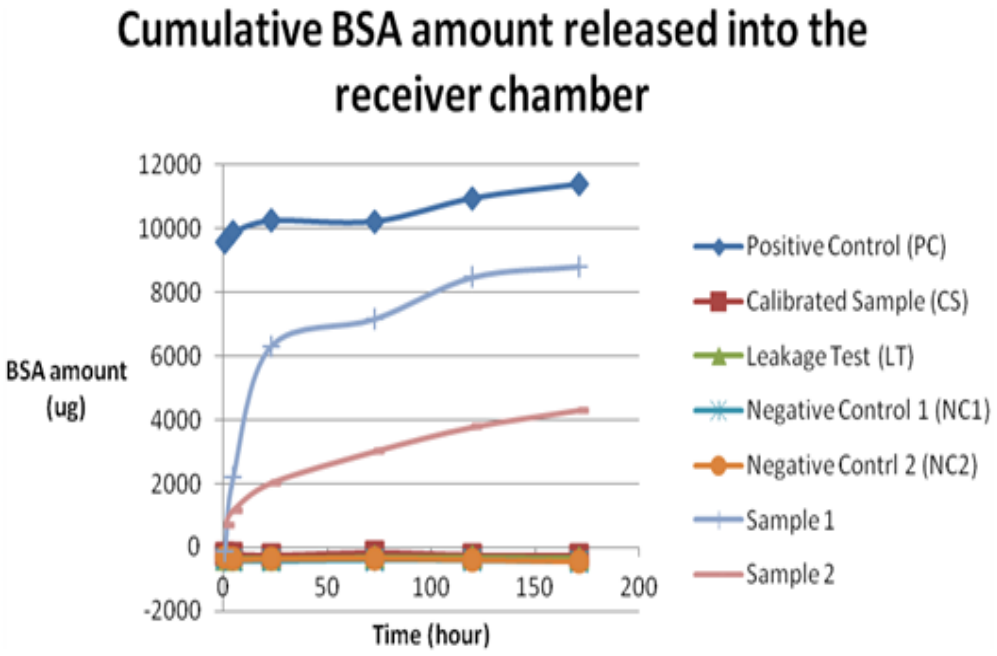

Figure 37 Seven-day (171-hour) BSA release and leakage test of PLGA devices

Conclusions

This device has the ability to deliver protein in a sustained, controlled fashion. Thus, this device will be loaded with drugs such as nerve growth factor which can stimulate axon growth and assessed for efficacy for nerve regeneration in *in vivo* models.

A 26-day NGF Study from PLGA Nerve Conduit

Introduction

Because the model was not available at the time when running this study, the purpose for this pilot 26-day NGF release study with PLGA nerve conduit is to determine the optimal combination of PVA and NGF for a later 26-day NGF study from PLGA nerve conduit.

Materials and Methods

In order to verify the bioactivity of the NGF delivered from the PLGA nerve conduit in a 26-day period, DMEM with 10% FBS was chosen to be served as the media in the receiver chamber instead of PBS to allow future cell culture on chick DRG cells. The fabrication process and the test setup are the same as the ones shown in Chapter 3 previously; only the dosage of NGF and PVA loaded into the device is different. NGF was first dissolved in distilled water to form a drug initial of 0.1mg/mL NGF stock solution, as shown in Table 15. Table 16 shows the dosage of drug filled into each control and device. Drug 1 solution was prepared by mixing 200µL drug initial with 200µL 50mg/mL PVA to form a final 0.05mg/mL NGF in 25mg/mL PVA solution. Drug 2 solution was prepared by mixing 50µL drug 1 solution with 200µL 25mg/mL PVA to form a final 0.01mg/mL NGF in 25mg/mL PVA solution. Drug 3 was prepared by mixing 100µL drug 2 solution with 100µL 25mg/mL PVA to form a final 0.005mg/mL NGF in 25mg/mL PVA solution.

Table 15 Drugs used in the 26-day NGF study

Drug name	**NGF concentration**	**Prepare from**	**Dilute with**	**Volume usage**	**For device**	**PVA conc.**
Drug initial	0.1mg/mL	Initial	Initial	700µL	n/a	n/a
Drug 1	0.05mg/mL	200µL drug initial	200µL 50mg/mL PVA	400µL -50-30-30-30=160µL	PC. LT. D1	25mg/mL
Drug 2	0.01mg/mL	50µL drug 1	200µL 25mg/mL PVA	250µL-30-100=120µL	D2	25mg/mL
Drug 3	0.005mg/mL	100µL drug 2	100µL 25mg/mL PVA	200µL-30=170µL	D3	25mg/mL
Unblocked drug	0.05mg/mL	100µL drug initial	100µL DI water	200µL-30=170µL	BT	0

Table 16 Dosage of drug filled in each control and device

Device name	**Device**	**Drug**	**Receiver chamber**	**Purpose**
Positive Control (PC)	n/a	100µL drug 1 (0.05mg/mL)	10mL DMEM & 10% FBS	To set the maximum boundary
Leakage Test (LT)	w/o window	22µL drug 1 (0.05mg/mL)	3mL DMEM & 10% FBS	To see the device's ability to store NGF without leakage
Device 1 (D1)	w/ window	18µL drug 1 (0.05mg/mL)	3mL DMEM & 10% FBS	Sample: highest conc. Dosage:
Device 2 (D2)	w/ window	24µL drug 2 (0.01mg/mL)	3mL DMEM & 10% FBS	Sample: medium conc.
Device 3 (D3)	w/ window	28µL drug 3 (0.005mg/mL)	3mL DMEM & 10% FBS	Sample: low conc.
Blocking Test (BT)	w/ window	12µL Unblocked drug (0.05mg/mL)	3mL DMEM & 10% FBS	To see the ability of 50mg/mL PVA impedes diffusion
Negative Control (NC)	w/ window	30µL 25mg/mL PVA solution	3mL DMEM & 10% FBS	To determine the background noise

An "unblocked drug" was introduced into this study in order to compare the absence of PVA in the release kinetics, and this unblocked drug was prepared from mixing 100µL of drug initial with 100µL of distilled water to form a final 0.05mg/mL NGF solution.

The positive control (n=2) is to set the maximum boundary for the NGF signal, and the negative control is to determine the background noise. For the leakage test, the device with no diffusion window was used in order to verify the sealing of the PLGA device. Three devices were used to compare the NGF delivery rate for different given NGF dosage (n=1). A blocking test was added in order to verify if the absence of PVA will increase the NGF release.

Fifty μL of 0.05mg/mL NGF in 5mL DMEM with 10% FBS was used as the receiver chamber media for the positive controls, and 500μL solution was taken from each positive control without refilling fresh DMEM with 10% FBS solution back. Contrarily, 3mL DMEM with 10% FBS was used for all the device groups, leakage test and negative control. Sink method was used in these groups in which all the media in the receiver chamber will be replaced each time during collection. All media collected will be stored at -20ºC, and the ELISA will be taken at the same time after collecting all the data points.

Results and Discussion

Due to the space limitation on the NGF ELISA kit, only the first collection of the positive control was measured and a 25558pg/mL NGF concentration was measured. Because it already exceed the NGF ELISA's detection range of 0.049ng/mL to 15ng/mL, these data are meaningless for this study. In addition, the positive control is only to give the idea that the scenario if all NGF released into the receiver chamber between two collections, which is not the goal for the device. In contrast, calibrated samples were proposed and tested in the release studies discussed in Chapters 3. Signals of these calibrated samples fell into the ELISA region due to the better design of experiment. Release results are shown in Figure 38 and Figure 39.

Figure 38 shows the cumulative NGF mass release into the receiver chamber. Device 1 filled with the highest dosage of NGF has the highest release, with an average of 3.4ng/day daily NGF delivery. Due to some blockage of the filter on the device 2, a near-zero release was found in a 26-day period. Device 3 has a moderate release due to no blockage of the filter by the adhesive. Blocking test has a blockage on the filter so

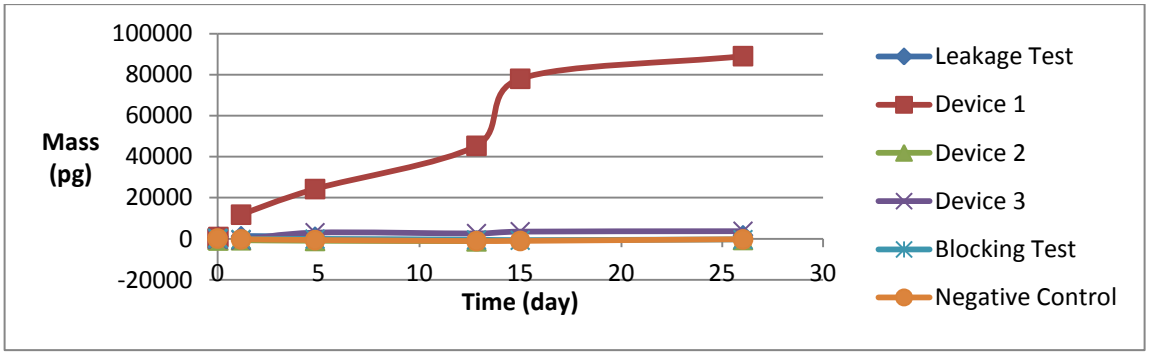

Figure 38 Cumulative NGF (in pg) release into the receiver chamber in a 25-day NGF release study with PLGA devices

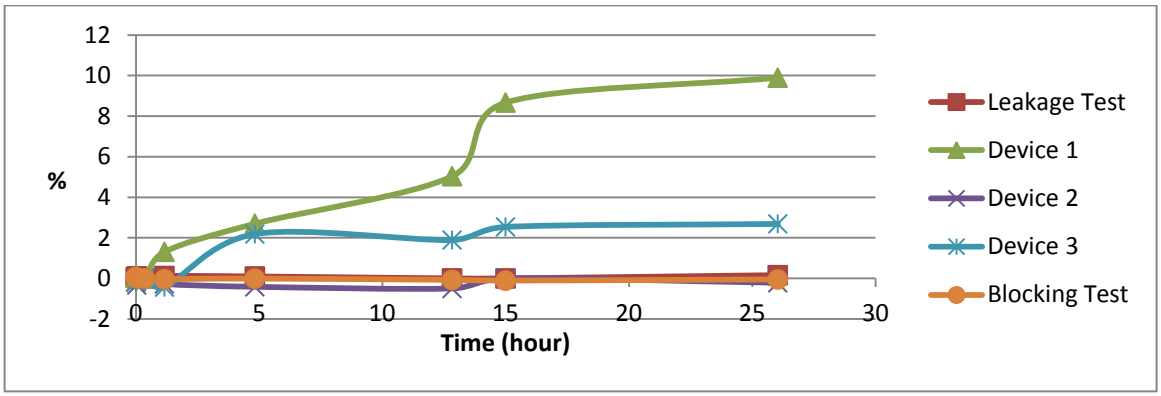

Figure 39 Cumulative NGF (in percentage) release into the receiver chamber in a 25-day NGF release study with PLGA devices

that even without the presence of PVA, the NGF release is slower than the devices. Negative control fit the expectation to have a near-zero release in the 26-day period.

Figure 39 shows the cumulative NGF release percentage in the 26-day period. For the percentage of NGF released into the receiver chamber, both devices 1 and 3 have a cumulative release of less than 10%. It indicates that a lesser concentration of PVA can be used in order to speed up the diffusion rate in the 26-day period. Therefore, in the 25-day NGF release study, PLGA devices will be filled with either 12.5mg/mL or 25mg/mL PVA and 0.05mg/mL or 0.1mg/mL NGF for a faster and higher NGF release.

A 3-week Pilot Animal Study in Rats

Introduction

The purpose for this pilot animal study is to verify the device with the same design of the optimal device in the 25-day NGF release study can promote axonal outgrowth along a given 10mm gap on rat sciatic nerve. Previously experiment shows that the axonal regrowth rate of 1-4mm/day [56], so that this 3-week animal study will not be evaluated by electrophysiology or walking track analysis due to that the repaired axons are not fully extended to innervate the distal muscles, and in this case, gastrocnemius and soleus muscles. Only histology and muscle loss data will be compared in this pilot animal study.

Materials and Methods

The optimal combination of NGF and PVA obtained from the 25-day diffusion test, which is 20-28μL of 0.1mg/mL NGF in 12.5mg/mL PVA, would be used for a 3-week animal study in rats in order to evaluate the outcome of the nerve conduit *in vivo*. In this study, a 10mm gap in the left sciatic nerve would be created in two groups (n=4) of 6-month-old female white Sprague Dawley rats. Before the surgery, PLGA nerve conduits would be sterilized by STERRAD. Then, in the biohood, the desired NGF and PVA would be filled into the device to avoid contamination. PLGA nerve conduits with desired NGF and PVA combination would be implanted into one group (n=4) of rats, and PLGA nerve conduits with empty reservoirs would be implanted into another group (n=4) of rats. After 3 weeks, the rats would be sacrificed, and both the histology of the left sciatic nerve gap with the PLGA nerve conduit and the muscle loss comparison of both gastrocnemius and soleus muscles would be analyzed.

Results and Discussion

No excessive inflammatory response was observed after bridging the 10 mm gaps on the left sciatic nerve of all rats (2 groups, n=4). One rat from the group with NGF supply was sacrificed before the proposed deadline because it consumed its left leg. Therefore, results for muscle loss in gastrocnemius and soleus muscles were obtained from the 7 remaining rats after a 3-week trial. For both gastrocnemius and soleus muscles, Figure 40 shows the group with NGF supply has a lower muscle loss ratio compared to the group without NGF supply. Figure 41 shows the gastrocnemius and soleus muscle loss in each animal model.

Less muscle loss rate in both gastrocnemius and soleus muscles when supplying NGF indicates that the peripheral nerve regenerated faster and some peripheral nerves regenerate across the gap to innervate the muscles. However, because a lower number of animals was used in this pilot animal study, a larger standard deviation value was acquired, as shown in Figure 41. Also, at 3 weeks, most of the peripheral nerves cannot grow long enough to innervate the distal muscles. Therefore, a longer experiment will be conducted in order to verify the muscle loss result appropriately. Walking track analysis will also be conducted to verify the functional recovery of the injured peripheral nerves.

Due to the complex structure of the PLGA device, histology data are difficult to obtain in the way to remain newly-growing neuron cells inside the inner conduit of the PLGA device. No histology data are available at this point, and future PLGA device will be inserted with either a peripheral nerve or a rat tail into the inner conduit for practice histology before being embedded into the animal model.

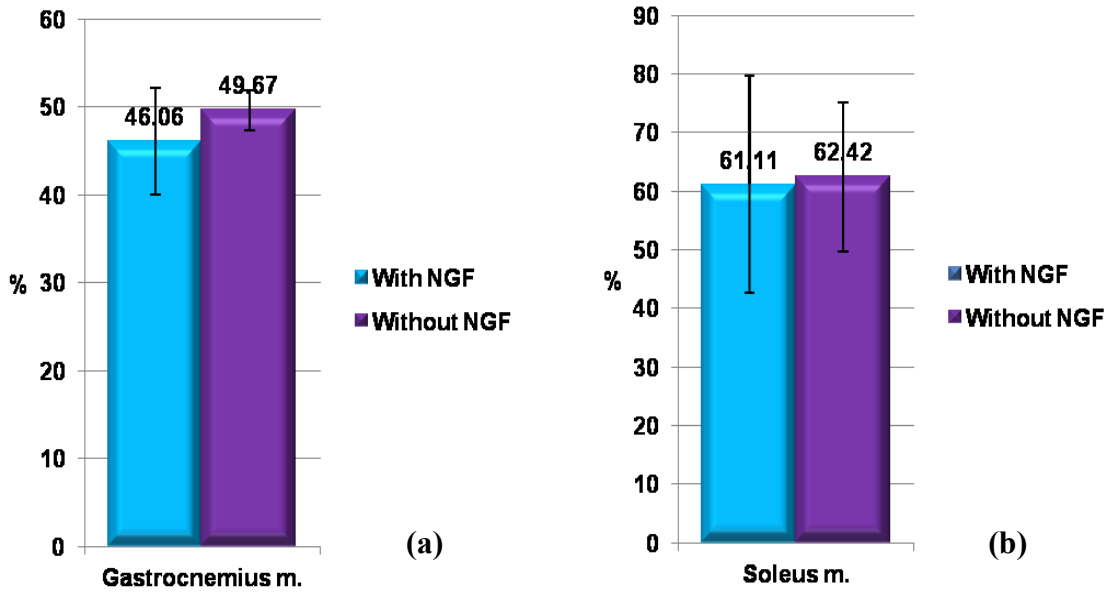

Figure 40 Muscle loss comparison in rats after 3 week pilot animal study. (a) Gastrocnemius muscle loss comparison for groups with and without NGF supply; (b) soleus muscle loss comparison for groups with and without NGF supply

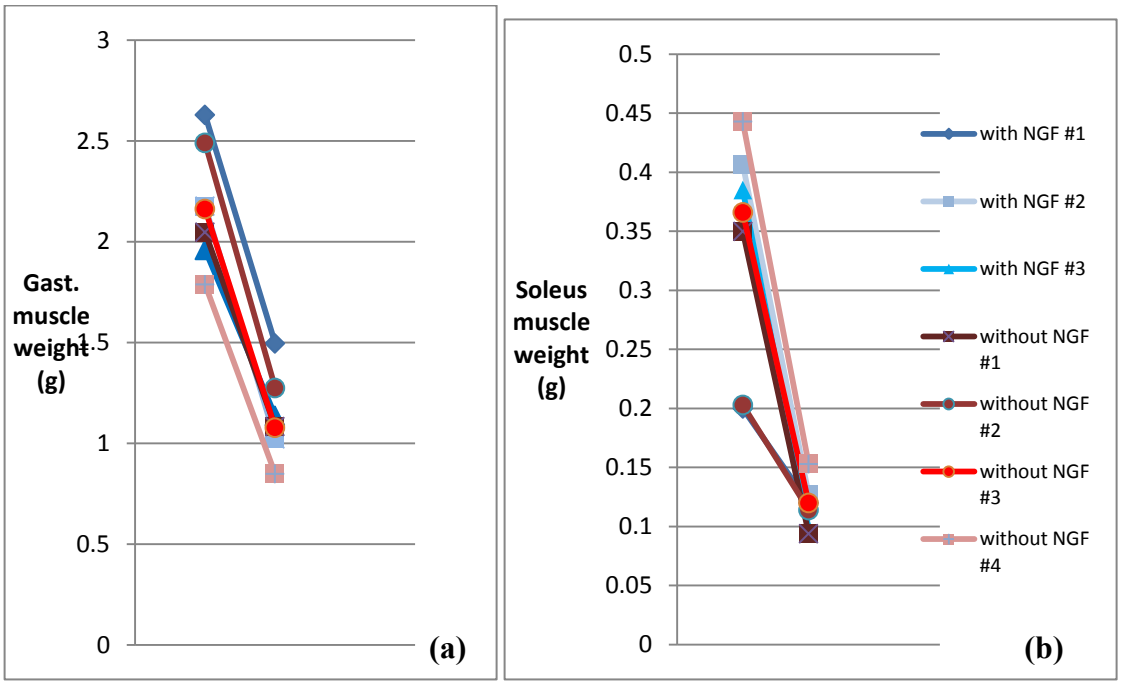

Figure 41 Comparison of muscle loss in each animal model (a) Gastrocnemius and (b) soleus muscle loss comparison in each animal model

Complete PLGA Device Preliminary Study

Introduction

Because the PDMS plug, PES filter membrane and RTV silicone sealant are not biodegradable, a follow-up surgery is required to remove the PLGA device after the nerve gap was bridged at 3 to 6 months postimplantation. This could injure the recovered peripheral nerve. Thus, a PLGA device using only biodegradable material is proposed to eliminate the need for the second surgery.

Materials and Methods

Biodegradable materials with similar functions of the PDMS plug, PES filter membrane and RTV silicone sealant are proposed in this complete PLGA device study. No plug would be used in this complete PLGA device due to the fact that the plug will decrease the volume of the drug reservoir. For replacing the PES filter membrane, a model, which was discussed initially in Chapter 2, will be used to design the corresponding small diffusion holes drilled on the inner conduit of the PLGA device, as shown in Figure 42. Because this is the first time to drill holes using laser on the inner conduit, it is difficult to get a precise dimension of the holes, and the dimension of the holes ranges from 100μm to 300μm. A modeling system for designing NGF release from this complete PLGA device will be discussed in the next section. Contrarily, melted PLGA instead of RTV silicone sealant was used to seal the end of the inner and outer conduit. 75/25 PLGA was heated to 230ºC for 20 minutes on a hot plate (6796-620KIT, Corning), then a needle was used to apply the melted PLGA emulsion to seal the end of the complete PLGA device. A nail clipper was then used to trim the PLGA sealant.

As the improvement for previous filter-based nerve conduit for better consistency,

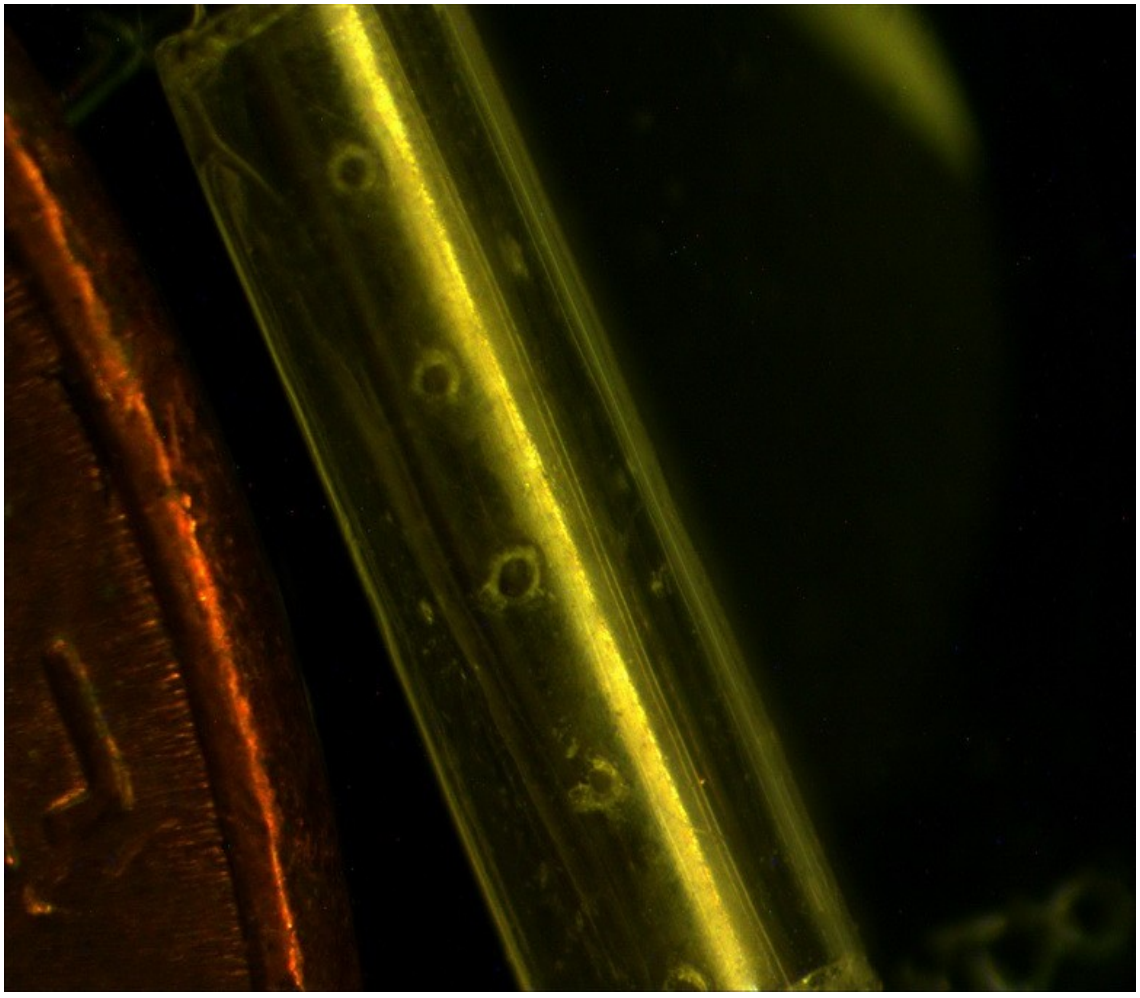

Figure 42 Small diffusion holes drilled on the inner conduit of the complete PLGA device compared to a United States penny

one, approximately 200μm, hole (with plus/minus 100μm) on the inner conduit would be used as the diffusion window for NGF to release into the receiver chamber. Also, because the 1st hour solution in the 25-day NGF release study impeded and killed most of the chick DRG cells in the bioactivity test, no RTV sealant would be used to either seal the end of the PLGA device or attach the PLGA to the bottom of the 12-well plate (serving as the diffusion chamber). Uncured 10:1 PDMS would be used to attach the complete PLGA device to the 12-well plate. In addition, due to the previous contamination in both 25-day and 26-day NGF release study when using DMEM with

10% FBS as the media for the receiver chamber, Amphotericin B (50-0640, Gibco) would be added into the solution of DMEM with 10% FBS.

After sterilizing PLGA devices completely with STERRAD, one group (*n*=3) of PLGA devices would be filled with 30-35μL 0.025mg/mL NGF without PVA in this PLGA device preliminary study. No controls were involved in this preliminary study due to the purpose of this study is to verify the sterilization and the complete PLGA device. These devices were then sealed with melted 75/25 PLGA. One hundred and fifty μL receiver chamber media (DMEM with 10% FBS and 1x Amphotericin B) would be used to flush the inner conduit in order to reduce trapped air in the inner conduit. The device was then attached to the bottom of a 12-well plate by uncured PDMS, following by a 2-hour drying process in the cell culture hood. Then, 5mL of the receiver chamber media was filled into each well. All the steps mentioned in this paragraph are taken in the cell culture hood to minimize the contamination. The receiver chamber was placed in the 37ºC incubator. All the media in the receiver chamber will be replaced with fresh media each time during collection. Samples would be collected every 2 to 3 days in a 20-day period. Collected sample would be stored at -20ºC.

Results and Discussion

Because this is a preliminary study, no NGF ELISA reading was available. Contamination was found at the 20th day, which indicates that a further investigation of the sterilization of the experiment environment has to be conducted prior to the next diffusion test.

Modeling of NGF Release from Complete PLGA Devices

Introduction

There will be two models for predicting the release kinetics. The first model is for predicting both the daily protein delivery rate across the diffusion hole and the local protein concentration before meeting the proximal nerve stump. The second model is to predict the protein concentration in the receiver chamber when the sink method is used. In short, a drug delivery device has to first show that it can deliver the protein at the rate and concentration specified in the first model, then the second model will determine if this design can produce a detectable protein signal in the receiver chamber because each detection method has its detectable range.

One of the purposes for the first model is to predict the daily NGF release and the NGF concentration in the receiver chamber. Literature has shown that a 80ng/day daily NGF supply for 3 weeks has greater sensorimotor recovery compared to all other treatment groups [96]. Another study shows that 10ng/mL NGF will result in the longest axonal outgrowth when compared to the group treated with NGF from 0.01ng/mL to 100ng/mL on chick DRG cells [93]. Though the optimal dosage of NGF differs from different animal model or implantation location, a modeling system was developed to achieve a 10ng/day NGF delivery because smaller animal models (rat, mouse and chick) were used in our release studies.

Another purpose of the first model is to predict the local protein concentration right before exposing to the proximal nerve stump sutured in the inner conduit. A study shows that an optimal axonal growth was found in the environment of 800pg/uL NGF [96], therefore, this model will also aim for producing a 800ng/mL local NGF concentration at

the proximal nerve stump to promote optimal axonal outgrowth.

In contrast, the second model can predict the protein concentration in the receiver chamber when the sink method is used in which the media of the receiver chamber will be replaced each time during collection. This model can ensure that the range is within the detectable range of the preferred detection method, no matter in ELISA, plate reading or other techniques.

First Model: Local Protein Concentration and Daily Delivery Rate

Figure 43 shows the illustration of the PLGA device and a simplified illustration of the complete PLGA device. Four stages were assigned as the following: stage 0 as the donor chamber where the drug reservoir filled with desired protein; stage 1 as the area in the inner conduit near the diffusion hole; stage 2 as the area in the inner conduit at the boundary of the proximal nerve stump; and stage E as 1mm inside the proximal nerve stump where all the protein is "consumed" due to metabolism (or sink method in the diffusion study).

Based on Fick's First Law of Diffusion,

$$J = -D\frac{C_0 - C_1}{\Delta x} \qquad \text{Equation 8}$$

where J is the diffusion flux $(\frac{\mathrm{ng}}{\mathrm{m^2 s}})$; D is the diffusion coefficient $(\frac{\mathrm{m^2}}{\mathrm{s}})$; C is the concentration $(\frac{\mathrm{ng}}{\mathrm{m^3}})$ and Δx is the distance between two stages. Given that the diffusion flux between stages 0-1, 1-2 and 2-E being $J_{0\text{-}1}$, $J_{1\text{-}2}$ and $J_{2\text{-}E}$, respectively; the area for the diffusion filter, inner conduit transverse cross-sectional area, and proximal nerve stump transverse cross-sectional area being $A_{0\text{-}1}$, $A_{1\text{-}2}$ and $A_{2\text{-}E}$, respectively; the concentration at

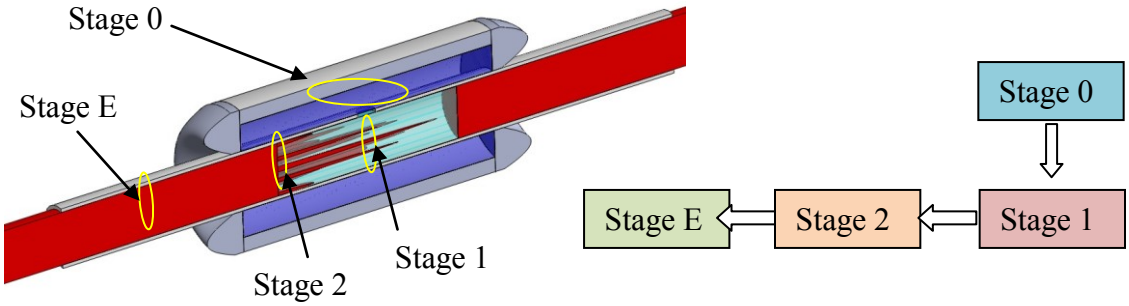

Figure 43 Illustration of the first model to predict both the local protein concentration in the proximal nerve stump and the daily protein diffusion rate across a diffusion hole

stages 0, 1, 2 and E being C_0, C_1, C_2 and C_E, respectively; the distance between stages 0-1, 1-2 and 2-E being $\Delta x_{0\text{-}1}$, $\Delta x_{1\text{-}2}$ and $\Delta x_{2\text{-}E}$, respectively; we can obtain three diffusion equations as:

$$J_{0-1} = -D\frac{C_0 - C_1}{\Delta x_{0-1}} \qquad \text{Equation 9}$$

$$J_{1-2} = -D\frac{C_1 - C_2}{\Delta x_{1-2}} \qquad \text{Equation 10}$$

$$J_{2-E} = -0.5D\frac{C_2 - C_E}{\Delta x_{2-E}} \qquad \text{Equation 11}$$

Diffusion coefficient in the nerve stump is half of the one in the incompressed buffer shown in previous studies [141][142], and was used in Equation 4.

Assume that the diffusion mass flow is the same in stages 0-1, 1-2 and 2-E, we will get:

$$J_{0-1}A_{0-1} = J_{1-2}A_{1-2} = J_{2-E}A_{2-E} \qquad \text{Equation 12}$$

Because a C_2 value of 800ng/mL and a $J_{0\text{-}1}A_{0\text{-}1}$ value of 10ng/day are required, a starting donor chamber concentration of C_0 and the diffusion hole size and number can be acquired when entering the known parameters in Table 17 to Equations 1-5. This model

Table 17 Known parameters in the first model, for the rat and mouse complete PLGA device

Description	**Notation**	**Value (for rat)**	**Value (for mouse)**	**Unit**
Inner conduit cross-sectional area	$A_{1\text{-}2}$	3.14×10^{-6}	7.85×10^{-7}	m^2
Cross-sectional area in the proximal nerve stump	$A_{2\text{-}E}$	2×10^{-6}	6.36×10^{-7}	m^2
Inner conduit wall thickness	$\Delta x_{0\text{-}1}$	200	100	μm
Distance between the diffusion hole to the proximal nerve stump	$\Delta x_{1\text{-}2}$	5	5	mm
Assume the length of the proximal nerve stump in the inner conduit	$\Delta x_{2\text{-}E}$	1	1	mm
Assume the protein concentration is zero in the given distance inside the proximal nerve stump	C_E	0	0	ng/mL
Diffusion coefficient	D	0.00000126 [141] [142]		cm^2/s

calculates in a gap of 1 minute in a 30-day period, and the protein released previously will be deducted from the donor chamber so that a slower and slower release will be expected.

A PLGA device for rats will be designed first, in which an inner conduit with a 2.4mm outer diameter and 2mm inner diameter will be used in order to fit a sciatic nerve with the diameter of 1.6mm. After entering the parameters shown in Table 17, when using a starting concentration of 0.1mg/mL with two 35μm diffusion holes, a daily NGF

delivery rate of 9.9ng/day with a 0.15ng/day standard deviation and a proximal nerve local NGF concentration of 908.8ng/mL with a 14.3ng/mL standard deviation will be acquired for the 30-day period.

For the complete PLGA device implanted into mice, a smaller inner conduit with an outer diameter of 1.2mm and an inner diameter of 1mm will be used to fit a thinner sciatic nerve of the diameter of 0.9mm. After entering the values, shown in Table 17, in the model, when filling the complete PLGA device with a donor chamber concentration of 0.05mg/mL and using three 25μm diffusion holes, an average of 6.8ng/day daily NGF delivery rate with a 0.1ng/day standard deviation and an average proximal nerve stump NGF concentration of 1977.9ng/mL with a 30.1ng/mL standard deviation will be obtained. This model can show the diffusion kinetics and the local protein concentration of any PLGA nerve device for either rats or mice if dimensions of the devices are provided.

Second Model: Protein Concentration in the Receiver Chamber

The second model is to predict the protein concentration in the receiver chamber when the sink method is used. Similar to the first model, a simplified system was used to calculate the protein concentration in the receiver chamber using Fick's First Law of diffusion. Figure 44 shows the concept of this model, in which a donor chamber (stage 0) filled with the desired protein will diffuse through diffusion holes and enter the inner conduit (stage 1). The protein then diffuses from the inner conduit to the receiver chamber (stage 2).

The calculation of drug and protein release is similar to the first model. Two equations based on Fick's First Law of Diffusion are:

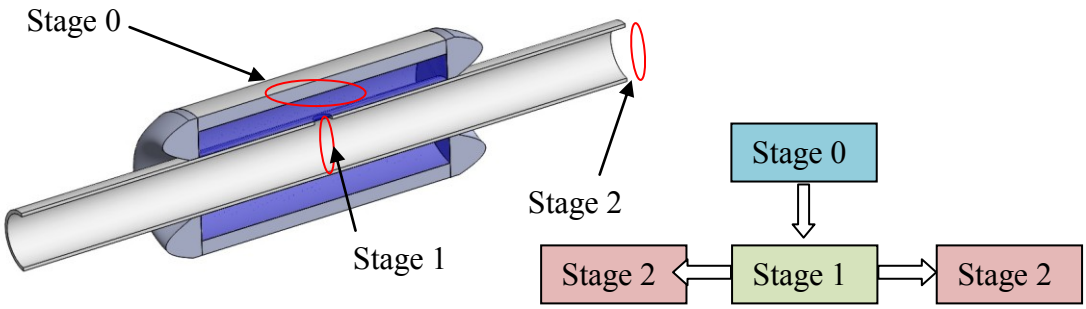

Figure 44 Illustration of the second model to predict the protein concentration in the receiver chamber

$$J_{0-1} = -D\frac{C_0 - C_1}{\Delta x_{0-1}} \qquad \text{Equation 13}$$

$$J_{1-2} = -D\frac{C_1 - C_2}{\Delta x_{1-2}} \qquad \text{Equation 14}$$

where J is the diffusion flux $(\frac{\text{ng}}{\text{m}^2\text{s}})$; D is the diffusion coefficient $(\frac{\text{m}^2}{\text{s}})$; C is the concentration $(\frac{\text{ng}}{\text{m}^3})$ and Δx is the distance between two stages. Given that the diffusion flux between stages 0-1 and 1-2 being $J_{0\text{-}1}$ and $J_{1\text{-}2}$, respectively; the area for the diffusion filter and inner conduit transverse cross-sectional area being $A_{0\text{-}1}$ and $A_{1\text{-}2}$, respectively; the concentration at stages 0, 1 and 2 being C_0, C_1 and C_2, respectively; the distance between stages 0-1 and 1-2 being $\Delta x_{0\text{-}1}$ and $\Delta x_{1\text{-}2}$, respectively; we can obtain three diffusion equations.

Because the diffusion of the inner conduit to the receiver chamber is in two directions from the donor chamber,

$$J_{0-1}A_{0-1} = J_{1-2} \times 2 \times A_{1-2} \qquad \text{Equation 15}$$

Also, net protein increment (in mass) in the receiver chamber equals the net mass flux across the inner conduit in a given time; thus,

$$dC_2 = \frac{-J_{1-2} \times 2A_{1-2} \times dt}{V} \quad \text{Equation 16}$$

where t is the time (second) allowed for diffusion, and V is the volume (m^3) in the receiver chamber.

From these equations, we can get the concentration of the inner conduit (C_1) as:

$$C_1 = \frac{-2D^2 \times A_{0-1} \times A_{1-2} \times t \times C_0 - D \times A_{0-1} \times \Delta x_{1-2} \times V \times C_0}{-2D^2 \times A_{0-1} \times A_{1-2} \times t - D \times A_{0-1} \times \Delta x_{1-2} \times V - 2D \times V \times A_{1-2} \times \Delta x_{0-1}} \quad \text{Equation 17}$$

Then, the concentration in the receiver chamber (C_2) is:

$$C_2 = C_1 + \frac{\Delta x_{1-2} \times J_{1-2}}{D} \quad \text{Equation 18}$$

All calculation was conducted in Microsoft Excel, and after entering the parameters shown in Table 17 and described in the previous sections, the concentrations in the receiver chamber in the 1st day, 5th day, 10th day, 15th day, 20th day, 25th day and 30th day collection with the sink method used are shown in Table 18.

Because the detection range of NGF ELISA is 0.049ng/mL to 15ng/mL, all the data points fit into this range.

These two models will be used to design different complete PLGA devices filled with different protein to fit various applications.

Table 18 The protein (NGF) concentration (ng/mL) in the receiver chamber for rat and mouse models on different collection days

	1st day	**5th day**	**10th day**	**15th day**	**20th day**	**25th day**	**30th day**
Rat	2.1	8.3	10.2	10.1	10.0	10.0	9.9
Mouse	1.5	6.0	7.5	7.4	7.3	7.3	7.2

Conclusion

Several tests related to the nerve conduit project were performed in addition to the ones presented in Chapters 3 and 4, in order to develop the device as well as methodologies for the nerve conduit project in Chapters 3 and 4. These supporting tests are discussed in this chapter.

A 5-day basic VEGF release study from PDMS nerve conduit is the first release experiment of the nerve conduit project, but the results cannot be interpreted due to the design error of the standard VEGF concentration calibration curve. A 6-day BSA release study from PDMS nerve conduit shows that two out of three devices filled with the same amount of BSA have a similar release profile in the 6-day period. Another PDMS device with different design using diffusion holes as the diffusion window was then performed with Dextran as the biomarker. It showed a reasonable release from the devices, but the result of the control is not favorable due to the diffusion chamber setting, thus an improvement design, along with the previous success in 6-day BSA release from the PDMS device, were tested and discussed previously in Chapter 3. After the success of NGF release data in Chapter 3, new material was proposed to better suit the clinical application. PLGA was chosen, and its pilot study were performed in this chapter (Chapter 5) in which a 7-day BSA release study from PLGA nerve conduit shows two out of two devices can release BSA in a 7-day period. A 26-day NGF study from PLGA nerve conduit was then performed in order to achieve an average of 2ng/day NGF delivery, with the comparison between different NGF and PVA concentration. The optimal design consisting of 0.05mg/mL NGF in 50mg/mL PVA has 3.4ng/day average NGF release in the 26-day period. This setting was then modified to become the test

protocol used in Chapter 4, in which PLGA devices with various NGF and PVA concentration were used to achieve 2ng/day daily NGF release. In addition, two models were developed in order to predict the release kinetics of either the PLGA or the PDMS device, and these models were introduced and discussed in both Chapters 3 and 5.

CHAPTER 6

CONCLUSION

This dissertation consists of two medical device projects: intraocular pressure sensors and nerve conduits. The author will conclude the findings for the former project first, followed by a thorough explanation of the later project. The author's contribution will also be addressed in this chapter, followed by the future work proposed for the two medical device projects.

Intraocular Pressure Sensors

Two types of IOP sensors have been designed, fabricated and tested. The subconjunctival IOP sensors possess a more feasible application compared to the intracapsular IOP sensors because of the easiness for both implantation and signal detection. The PMMA intracapsular IOP sensors have a drawback of the immobility of the dye in the channel, resulting in a huge hysteresis when IOP value drops. Also, silicone to PMMA bonding cannot be controlled easily when compared to PDMS to PDMS bonding; so a leakage in the channel is more likely to occur, leading to failure of the device.

Subconjunctival IOP sensors made of PDMS were found to be superior when compared to the intracapsular IOP sensors made of PMMA. Seven out of 70 tested subconjunctival IOP sensors show the ability to detect both rising and falling IOP pressures, with the signal being retrievable with OCT when covered with swine conjunctiva. In order to achieve better signal consistency, additional tests with identical

devices should be performed to acquire more data for the average dye length calibration curves in order to get a more precise prediction of intraocular pressure based on the dye length measurement.

Nerve Conduits for Peripheral Nerve Regeneration

The nerve conduit project started with a concept that concentric tubes storing drugs of interest in the lumen between the two tubes will slowly release the drug into the lumen of the inner lumen and promote local axonal outgrowth at the proximal nerve stump sutured in the inner conduit. In the beginning, a PDMS device with a PCU inner conduit was used to deliver BSA or VEGF through a PES filter membrane. Then, NGF was loaded into this PDMS device for a more directly applicable study and the results showed that all three PDMS devices had different release kinetics in which one PDMS device released nothing, another slowly released NGF, and the other released NGF rapidly in the first 37 hours and nearly nothing for the rest of the 21-day period. Thus, the PDMS devices using the PES filter as the diffusion window had the drawback of inconsistent release kinetics in the same design due to either the application of adhesive on the filter that partially or totally blocks the diffusion window or possibly bubbles forming on the membrane. Another explanation for the poor measurement results might be that the protein adheres to the glass wall after release and is not available to be measured, causing artificially low concentration measurements to occur. Because of these challenges, a different device was designed and different measurement conditions implemented.

Biodegradable PLGA nerve conduits were then developed in this project to hopefully eliminate the need for followup surgery to remove the conduit and to speed up the recovery process. BSA release experiments showed that reasonable release was

achieved in a 7-day study. A 26-day NGF release study using DMEM instead of PBS in the receiver chamber suffered from contamination and some tests had to be stopped in the middle of the 26-day period. A more careful 25-day NGF release study with a higher dosage of NGF in order to acquire higher NGF concentration in the receiver chamber was performed and showed more consistent release kinetics than in the previous PLGA device release study, and the NGF released from the PLGA device was shown to be bioactive even after being stored in the PLGA device for 20 days, which was verified with DRG cells. A pilot 3-week animal study in rats was conducted and showed that the device was generally biocompatible *in vivo*. The optimal design was then used in a 3-week *in vivo* animal study in rats that again showed good biocompatibility, but was not long enough to show any significant difference in muscle loss protection from nerve regrowth.

The PDMS and PLGA devices using filter membranes to release protein showed poor consistency in release results due to the possible blockage of filter membranes by the application of the adhesive. A model using Fick's First Law of Diffusion was proposed in Chapter 3, and 75 % of the PDMS devices with diffusion holes fit the modeling results in Dextran release percentage in a 10-day study. This not only indicates that using diffusion holes instead of filter membranes can result in a more consistent release, but also validates that the model is useful for predicting the release kinetics of the device.

Contribution

The author made the following contributions to the IOP sensor project:

- Developed a hydraulic pressure testing station to mimic intraocular environment.

- Modified the intracapsular IOP sensor.
- Developed the subconjunctival IOP sensor.
- Developed a PDMS partially cured bonding method for 20μm PDMS membrane attachement.
- Tested and characterized 60 intracapsular IOP sensors and 70 subconjunctival IOP sensors.
- Introduced reservoirs for storing trapped air.
- Introduced a protective layer for minimizing applied pressure on the sensing channel.
- Published one conference paper: MicroTAS 2012 poster.
- Journal paper ready for submission

The author contributed the following items to the nerve conduit project:

- Helped acquire the initial funding (University of Utah Research Foundation Seed Grant): $32k for 1 year.
- Helped acquire more funding for expanding the study:
    - Department of Defense (DOD) Congressionally Directed Medical Research Program (CDMRP): $186k for 1.5 years.
    - DOD CDMRP: $744k for 3 years.
- Developed the whole process from design, manufacture and verification the drug released *in vitro*.
- Developed the PDMS device.
- Developed the PLGA device.
- Developed the complete PLGA device.

- Proposed using holes instead of using a filter. Conducted preliminary fabrication using the laser etching machine.
- Proposed several PLGA sealing methods, including PLGA glue and heat sealing.
- Invented the PLGA outer conduit manufacturing process.
- Developed the diffusion chamber for PLGA device release studies.
- Invented methods for making PLGA sheets and PLGA disks for use in the device manufacture.
- Developed modeling systems to predict:
    - Drug release kinetics from the donor chamber to the receiver chamber. (Detectability)
    - Drug release kinetics from the donor chamber to the proximal nerve stump. (Dosage)
- Published 3 conference papers:
    - IEEE EMBC 2012
    - BMES 2013
    - ACS-Utah 2013
- Two journal papers ready for submission

Future work

Intraocular Pressure Sensors

In order to achieve better signal consistency, more results matching the error zone of the average dye length calibration curve should be acquired in order to get a precise prediction of intraocular pressure based on the dye length measurement. Also, human

conjunctiva should be harvested and placed on top of the subconjunctival IOP sensor to see if a better OCT signal could be achieved. Furthermore, hysteresis in the subconjunctival sensors should be solved in order to get a repeatable signal reading.

Nerve Conduits for Peripheral Nerve Regeneration

A procedure for turning the design concepts into prototypes is proposed in order to accelerate the development process of the nerve conduits in the future. This procedure includes the following steps:

1. Obtaining the clinical needs in material, dimension and drugs of interest.
2. Acquiring the dimension of the diffusion holes and the dosage of the drug filled in the drug reservoir by performing design characterization using the first model (proposed in Chapter 5) to verify if the drug delivery dosage to the proximal nerve stump meets expectations.
3. Ensuring the dimension of the diffusion holes and the dosage of the drug filled in the drug reservoir is detectable by perform design characterization using the second model introduced in both Chapters 3 and 5.
4. Fabricating the device with dimension obtained from the two models.
5. Testing the integrity of the device in a sealing test using Dextran with a similar molecular weight to the drug of interest.
6. Testing the consistency of the drug release kinetics in a 30-day release study using Dextran with a similar molecular weight to the drug of interest.
7. Practicing the histology techniques for the proposed device with a biological tissue inserted into the device.
8. Testing the consistency of the drug release kinetics in a 30-day release study

using the drug of interest.

9. Verifying the bioactivity of the collected sample in the 30-day release study on DRG cells.
10. Verifying the function of the device in a 1-month pilot animal study.
11. Verifying the function of the device in a 6-month full animal study.

Following these procedures, a complete PLGA device will be fabricated, and a dual-chambered device will also be developed to deliver multiple neurotrophins at once in order to fit different applications. These PLGA devices will be designed using the modeling results in order to acquire an optimal delivery and release kinetics to not only be bioactive and detective but also be clinically preferred. A diffusion test with the sink method will be started to verify the integrity and release kinetics of the complete PLGA device (single or dual chambers); then, an *ex vivo* study in DRG cells will be conducted to verify the bioactivity of the neurotriphin released from the devices. If both the release kinetics and the bioactivity have been confirmed, a pilot 30-day *in vivo* test will be conducted in rats, followed by a 6-month full animal test in mice in order to inspect the electrophysiology, histomorphometry and walking track analysis data compared to the group bridged with autografts.

REFERENCES

[1] K. C. Katuri, S. Asrani, and M. K. Ramasubramanian, “Intraocular pressure monitoring sensors,” *IEEE Sens. J.*, vol. 8, no. 1, pp. 9–16, Jan. 2008.

[2] L. Mowatt, J. Nelson-Imoru, and G. Gordon-Strachan, “Glaucoma medication compliance issues in a Jamaican hospital eye clinic,” *West India Med. J.*, vol. 60, no. 5, pp. 541–547, 2011.

[3] P. Boudes, “Drug compliance in therapeutic trials: a review,” *Control. Clin. Trials*, vol. 19, no. 3, pp. 257–68, Jun. 1998.

[4] R. L. Stamper, “A history of intraocular pressure and its measurement,” *Optom. Vis. Sci.*, vol. 88, no. 1, pp. E16–28, Jan. 2011.

[5] L. W. Herndon, “Measuring intraocular pressure-adjustments for corneal thickness and new technologies,” *Curr. Opin. Ophthalmol.*, vol. 17, no. 2, pp. 115–9, Apr. 2006.

[6] G. A. Lee, P. T. Khaw, L. A. Ficker, and P. Shah, “The corneal thickness and intraocular pressure story: where are we now?” *Clin. Experiment. Ophthalmol.*, vol. 30, no. 5, pp. 334–7, Oct. 2002.

[7] M. A. Zarbin, C. Montemagno, J. F. Leary, and R. Ritch, “Nanotechnology in ophthalmology,” *Can. J. Ophthalmol.*, vol. 45, no. 5, pp. 457–476, Oct. 2010.

[8] D. Touboul, C. Roberts, J. Kérautret, C. Garra, S. Maurice-Tison, E. Saubusse, and J. Colin, “Correlations between corneal hysteresis, intraocular pressure, and corneal central pachymetry,” *J. Cataract Refract. Surg.*, vol. 34, no. 4, pp. 616–22, Apr. 2008.

[9] T. Schlote and H. Landenberger, “Intraocular pressure difference in Goldmann applanation tonometry versus a transpalpebral tonometer TGDc-01‘PRA’ in glaucoma patients,” *Klin. Monbl. Augenheilkd.*, vol. 222, no. 2, pp. 123–31, Feb. 2005.

[10] M. Neuburger, A. Rosentreter, T. S. Dietlein, and J. F. Jordan, “Techniques of intraocular pressure measurement,” *Klin. Monbl. Augenheilkd.*, vol. 228, no. 2, pp. 118–24, Feb. 2011.

[11] M. Amm and J. Hedderich, “Transpalpebral tonometry with a digital tonometer in healthy eyes and after penetrating keratoplasty,” *Ophthalmologe*, vol. 102, no. 1, pp. 70–6, Jan. 2005.

[12] K. Mansouri and T. Shaarawy, “Continuous intraocular pressure monitoring with a wireless ocular telemetry sensor: initial clinical experience in patients with open angle glaucoma,” *Br. J. Ophthalmol.*, vol. 95, no. 5, pp. 627–9, May 2011.

[13] P. Auvray, L. Rousseau, G. Lissorgues, F. Soulier, O. Potin, S. Bernard, F. Dieuleveult, E. Scorsone, P. Bergonzo, L. Chicaud, S. Picaud, and J. a. Sahel, “A passive pressure sensor for continuously measuring the intraocular pressure in glaucomatous patients,” *IRBM*, pp. 1–6, Mar. 2012.

[14] M. Leonardi, P. Leuenberger, D. Bertrand, A. Bertsch, and P. Renaud, “First steps toward noninvasive intraocular pressure monitoring with a sensing contact lens,” *Invest. Ophthalmol. Vis. Sci.*, vol. 45, no. 9, pp. 3113–7, Sep. 2004.

[15] M. Leonardi, E. M. Pitchon, A. Bertsch, P. Renaud, and A. Mermoud, “Wireless contact lens sensor for intraocular pressure monitoring: assessment on enucleated pig eyes,” *Acta Ophthalmol.*, vol. 87, no. 4, pp. 433–7, Jun. 2009.

[16] A. K. C. Lam and W. A. Douthwaite, “The effect of an artificially elevated intraocular pressure on the central corneal curvature,” *Ophthalmic Physiol. Opt.*, vol. 17, no. 1, pp. 18–24, Jan. 1997.

[17] C.-K. Tseng, Y.-C. Huang, S.-W. Tsai, G.-T. Yeh, C.-H. Chang, and J.-C. Chiou, “Design and fabricate a contact lens sensor with a micro-inductor embedded for intraocular pressure monitoring,” *2012 IEEE Sensors*, pp. 1–4, Oct. 2012.

[18] W. P. Eaton and J. H. Smith, “Micromachined pressure sensors: review and recent developments,” *Smart Mater. Struct.*, vol. 6, no. 5, pp. 530–539, Oct. 1997.

[19] A. V. Chavan and K. D. Wise, “Batch-processed vacuum-sealed capacitive pressure sensors,” *J. Microelectromechanical Syst.*, vol. 10, no. 4, pp. 580–588, 2001.

[20] Y. Shih, T. Shen, and B. P. Otis, “A 2 . 3 W wireless intraocular pressure / temperature monitor,” *IEEE J. Solid-State Circuits*, vol. 46, no. 11, pp. 2592–2601, 2011.

[21] G. Jiang, “Design challenges of implantable pressure monitoring system,” *Front. Neurosci.*, vol. 4, no. February, p. 29, Jan. 2010.

[22] R. M. Haque and K. D. Wise, “A 3D implantable microsystem for intraocular pressure monitoring using a glass-in-silicon reflow process,” in *2011 IEEE 24th International Conference on Micro Electro Mechanical Systems*, 2011, pp. 995–998.

[23] R. M. Haque and K. D. Wise, “An intraocular pressure sensor based on a glass reflow process,” in *SolidState Sensors Actuators and Microsystems Workshop*, 2010, pp. 49–52.

[24] G. Chen, H. Ghaed, R. Haque, M. Wieckowski, Y. Kim, G. Kim, D. Fick, D. Kim, M. Seok, K. Wise, D. Blaauw, and D. Sylvester, “A cubic-millimeter energy-autonomous wireless intraocular pressure monitor,” in *2011 IEEE International Solid-State Circuits Conference*, 2011, pp. 310–312.

[25] D. Ha, W. N. de Vries, S. W. M. John, P. P. Irazoqui, and W. J. Chappell, “Polymer-based miniature flexible capacitive pressure sensor for intraocular pressure (IOP) monitoring inside a mouse eye,” *Biomed. Microdevices*, vol. 14, no. 1, pp. 207–15, Feb. 2012.

[26] C. Yang, E. Y. Chow, P. P. Irazoqui, and W. J. Chappell, “RF powering for embedded glaucoma sensors in miniature packages,” in *RF Powering For Embedded Glaucoma Sensors in Miniature Packages*, 2008.

[27] E. Y. Chow, D. Ha, T.-Y. Lin, W. N. Devries, S. W. M. John, W. J. Chappell, and P. P. Irazoqui, “Sub-cubic millimeter intraocular pressure monitoring implant to enable genetic studies on pressure-induced neurodegeneration,” in *Conference Proceedings: Annual International Conference of the IEEE Engineering in Medicine and Biology Society. IEEE Engineering in Medicine and Biology Society. Conference*, 2010, vol. 2010, pp. 6429–32.

[28] R. P. Dresher and P. P. Irazoqui, “A compact nanopower low output impedance CMOS operational amplifier for wireless intraocular pressure recordings,” *Conf. Proc. IEEE Eng. Med. Biol. Soc.*, vol. 2007, pp. 6056–9, Jan. 2007.

[29] E. Y. Chow, A. L. Chlebowski, and P. P. Irazoqui, “A miniature-implantable RF-wireless active glaucoma intraocular pressure monitor,” *IEEE Trans. Biomed. Circuits Syst.*, vol. 4, no. 6, pp. 340–349, Dec. 2010.

[30] D. Ha, T.-Y. Lin, W. N. de Vries, B. Kim, A. L. Chlebowski, S. W. M. John, P. P. Irazoqui, and W. J. Chappell, “A compact-size packaged third-order harmonic tag for intraocular pressure (IOP) monitoring inside a mouse eye,” in *2012 IEEE/MTT-S International Microwave Symposium Digest*, 2012, pp. 1–3.

[31] C. Smith, “Piezoresistance effect in germanium and silicon,” *Phys. Rev.*, vol. 94, no. 1, pp. 42–49, 1954.

[32] R. N. Rizq, W. H. Choi, D. Eilers, M. M. Wright, and B. Ziaie, “Intraocular pressure measurement at the choroid surface: a feasibility study with implications for implantable microsystems,” *Br. J. Ophthalmol.*, vol. 85, no. 7, pp. 868–71, Jul. 2001.

[33] F. Piffaretti, D. Barrettino, P. Orsatti, L. Leoni, and P. Stegmaier, “Rollable and implantable intraocular pressure sensor for the continuous adaptive management of glaucoma,” *Conf. Proc. IEEE Eng. Med. Biol. Soc.*, vol. 2013, pp. 3198–201, Jan. 2013.

[34] N. Xue, S. Member, S. Chang, J. Lee, and S. Member, “A SU-8-based microfabricated implantable inductively coupled passive RF wireless intraocular pressure sensor,” *J. Microelectromechanical Syst.*, vol. 21, no. 6, pp. 1338–1346, 2012.

[35] E. F. Price, “A miniature spiral bourdon tube pressure transducer,” Royal Aircraft Establishment, Farnborough, United Kingdom, 1964.

[36] P.-J. Chen, D. C. Rodger, R. Agrawal, S. Saati, E. Meng, R. Varma, M. S. Humayun, and Y.-C. Tai, “Implantable micromechanical parylene-based pressure sensors for unpowered intraocular pressure sensing,” *J. Micromechanics Microengineering*, vol. 17, no. 10, pp. 1931–1938, Oct. 2007.

[37] E. Meng, P.-J. Chen, D. Rodger, Y. Tai, and M. Humayun, “Implantable parylene MEMS for glaucoma therapy,” in *3rd Annual International IEEE EMBS Conference on Microtechnologies in Medicine and Biology*, 2005, no. May, pp. 116–119.

[38] P.-J. Chen, C.-Y. Shih, and Y.-C. Tai, “Design, fabrication and characterization of monolithic embedded parylene microchannels in silicon substrate,” *Lab Chip*, vol. 6, no. 6, pp. 803–10, Jun. 2006.

[39] P. Chen, D. Roger, M. Humayun, and Y. Tai, “Unpowered spiral-tube parylene pressure sensor for intraocular pressure sensing,” *Sensors Actuators A Phys.*, vol. 127, no. 2, pp. 276–282, Mar. 2006.

[40] P.-J. Chen, D. C. Rodger, E. Meng, M. S. Humayun, and Y.-C. Tai, “Implantable unpowered parylene MEMS intraocular pressure sensor,” *2006 Int. Conf. Microtechnologies Med. Biol.*, pp. 256–259, May 2006.

[41] S. A Molokhia, H. Sant, J. Simonis, C. J. Bishop, R. M. Burr, B. K. Gale, and B. K. Ambati, “The capsule drug device: novel approach for drug delivery to the eye,” *Vision Res.*, vol. 50, no. 7, pp. 680–5, Mar. 2010.

[42] G. Ciardelli and V. Chiono, “Materials for peripheral nerve regeneration,” *Macromol. Biosci.*, vol. 6, no. 1, pp. 13–26, Jan. 2006.

[43] A. C. Lee, V. M. Yu, J. B. Lowe, M. J. Brenner, D. a Hunter, S. E. Mackinnon, and S. E. Sakiyama-Elbert, “Controlled release of nerve growth factor enhances sciatic nerve regeneration,” *Exp. Neurol.*, vol. 184, no. 1, pp. 295–303, Nov. 2003.

[44] C. T. Chalfoun, G. A Wirth, and G. R. D. Evans, “Tissue engineered nerve constructs: where do we stand?” *J. Cell. Mol. Med.*, vol. 10, no. 2, pp. 309–17, 2006.

[45] B. Nicholson and S. Verma, “Comorbidities in chronic neuropathic pain,” *Pain Med.*, vol. 5 Suppl 1, pp. S9–S27, Mar. 2004.

[46] R. S. Taylor, “Epidemiology of refractory neuropathic pain,” *Pain Pract.*, vol. 6, no. 1, pp. 22–6, Mar. 2006.

[47] D. Ha, B. G. Kim, T. Lin, Y. Ouyang, P. P. Irazoqui, and W. J. Chappell, “3D packaging technique on liquid crystal polymer (LCP) for miniature wireless biomedical sensor,” in *2010 IEEE MTT-S International Microwave Symposium*, 2010, pp. 612–615.

[48] E. Y. Chow, C. Yang, Y. Ouyang, A. L. Chlebowski, P. P. Irazoqui, and W. J. Chappell, “Wireless powering and the study of RF propagation through ocular tissue for development of implantable sensors,” *IEEE Trans. Antennas Propag.*, vol. 59, no. 6, pp. 2379–2387, Jun. 2011.

[49] J. Noble, C. A. Munro, V. Prasad, and R. Midha, “Analysis of upper and lower extremity peripheral nerve injuries in a population of patients with multiple injuries,” *J. Trauma*, vol. 45, no. 1, pp. 116–122, 1998.

[50] B. Rosén and G. Lundborg, “A model instrument for the documentation of outcome after nerve repair,” *J. Hand Surg. Am.*, vol. 25, no. 3, pp. 535–43, May 2000.

[51] S. Sunderland, “A classification of peripheral nerve injuries producing loss of function,” *Brain*, vol. 74, no. 4, pp. 491–516, 1951.

[52] R. Deumens, A. Bozkurt, M. F. Meek, M. A. E. Marcus, E. A. J. Joosten, J. Weis, and G. A. Brook, “Repairing injured peripheral nerves: bridging the gap,” *Prog. Neurobiol.*, vol. 92, no. 3, pp. 245–76, Nov. 2010.

[53] L. de Medinaceli, M. Prayon, and M. Merle, “Percentage of nerve injuries in which primary repair can be achieved by end-to-end approximation: review of 2,181 nerve lesions,” *Microsurgery*, vol. 14, no. 4, pp. 244–246, 1993.

[54] N. Danielsen, B. Pettmann, H. L. Vahlsing, M. Manthorpe, and S. Varon, “Fibroblast growth factor effects on peripheral nerve regeneration in a silicone chamber model,” *J. Neurosci. Res.*, vol. 20, no. 3, pp. 320–30, Jul. 1988.

[55] K.-M. Lin, H. J. Sant, B. K. Gale, and J. P. Agarwal, “New approaches to bridge nerve gaps: development of a novel drug-delivering nerve conduit,” in *2012*

Annual International Conference of the IEEE Engineering in Medicine and Biology Society, 2012, pp. 747–750.

[56] G. R. D. Evans, "Peripheral nerve injury : a review and approach to tissue engineered constructs," *J. Neurosci. Res.*, vol. 404, no. January, pp. 396–404, 2001.

[57] L. a Pfister, M. Papaloïzos, H. P. Merkle, and B. Gander, "Nerve conduits and growth factor delivery in peripheral nerve repair," *J. Peripher. Nerv. Syst.*, vol. 12, no. 2, pp. 65–82, Jun. 2007.

[58] S. J. Archibald, J. Shefner, C. Krarup, and R. D. Madison, "Monkey median nerve repaired guide tube by nerve graft or collagen nerve," *J. Neurosci.*, vol. 15, no. May, pp. 4109–4123, 1995.

[59] X. Jiang, S. H. Lim, H.-Q. Mao, and S. Y. Chew, "Current applications and future perspectives of artificial nerve conduits," *Exp. Neurol.*, vol. 223, no. 1, pp. 86–101, May 2010.

[60] E. O. Johnson and P. N. Soucacos, "Nerve repair: experimental and clinical evaluation of biodegradable artificial nerve guides," *Injury*, vol. 39 Suppl 3, pp. S30–6, Sep. 2008.

[61] S. Madduri, K. Feldman, T. Tervoort, M. Papaloïzos, and B. Gander, "Collagen nerve conduits releasing the neurotrophic factors GDNF and NGF," *J. Control. Release*, vol. 143, no. 2, pp. 168–74, Apr. 2010.

[62] D.-Y. Lee, B.-H. Choi, J.-H. Park, S.-J. Zhu, B.-Y. Kim, J.-Y. Huh, S.-H. Lee, J.-H. Jung, and S.-H. Kim, "Nerve regeneration with the use of a poly(l-lactide-co-glycolic acid)-coated collagen tube filled with collagen gel," *J. Craniomaxillofac. Surg.*, vol. 34, no. 1, pp. 50–6, Jan. 2006.

[63] D. Ceballos, X. Navarro, N. Dubey, G. Wendelschafer-Crabb, W. R. Kennedy, and R. T. Tranquillo, "Magnetically aligned collagen gel filling a collagen nerve guide improves peripheral nerve regeneration," *Exp. Neurol.*, vol. 158, no. 2, pp. 290–300, Aug. 1999.

[64] T. Kiyotani, M. Teramachi, Y. Takimoto, T. Nakamura, Y. Shimizu, and K. Endo, "Nerve regeneration across a 25-mm gap bridged by a polyglycolic acid-collagen tube: a histological and electrophysiological evaluation of regenerated nerves," *Brain Res.*, vol. 740, no. 1–2, pp. 66–74, Nov. 1996.

[65] T. Toba, T. Nakamura, a K. Lynn, K. Matsumoto, S. Fukuda, M. Yoshitani, Y. Hori, and Y. Shimizu, "Evaluation of peripheral nerve regeneration across an 80-mm gap using a polyglycolic acid (PGA)--collagen nerve conduit filled with laminin-soaked collagen sponge in dogs," *Int. J. Artif. Organs*, vol. 25, no. 3, pp. 230–7, Mar. 2002.

[66] L. J. Chamberlain, I. V Yannas, H. P. Hsu, G. Strichartz, and M. Spector, "Collagen-GAG substrate enhances the quality of nerve regeneration through collagen tubes up to level of autograft," *Exp. Neurol.*, vol. 154, no. 2, pp. 315–29, Dec. 1998.

[67] S. Yoshii and M. Oka, "Peripheral nerve regeneration along collagen filaments," *Brain Res.*, vol. 888, no. 1, pp. 158–162, Jan. 2001.

[68] J. S. Belkas, C. a Munro, M. S. Shoichet, and R. Midha, "Peripheral nerve regeneration through a synthetic hydrogel nerve tube," *Restor. Neurol. Neurosci.*, vol. 23, no. 1, pp. 19–29, Jan. 2005.

[69] R. Midha, C. a Munro, P. D. Dalton, C. H. Tator, and M. S. Shoichet, "Growth factor enhancement of peripheral nerve regeneration through a novel synthetic hydrogel tube," *J. Neurosurg.*, vol. 99, no. 3, pp. 555–65, Sep. 2003.

[70] Y. Katayama, R. Montenegro, T. Freier, R. Midha, J. S. Belkas, and M. S. Shoichet, "Coil-reinforced hydrogel tubes promote nerve regeneration equivalent to that of nerve autografts," *Biomaterials*, vol. 27, no. 3, pp. 505–518, Jan. 2006.

[71] A. Piotrowicz and M. S. Shoichet, "Nerve guidance channels as drug delivery vehicles," *Biomaterials*, vol. 27, no. 9, pp. 2018–27, Mar. 2006.

[72] R. A. Weber, W. C. Breidenbach, R. E. Brown, M. E. Jabaley, and D. P. Mass, "A randomized prospective study of polyglycolic acid conduits for digital nerve reconstruction in humans," *Plast. Reconstr. Surg.*, vol. 106, no. 5, pp. 1036–45; discussion 1046–8, Oct. 2000.

[73] M. J. O. E. Bertleff, M. F. Meek, and J.-P. a Nicolai, "A prospective clinical evaluation of biodegradable neurolac nerve guides for sensory nerve repair in the hand," *J. Hand Surg. Am.*, vol. 30, no. 3, pp. 513–8, May 2005.

[74] G. R. D. Evans, K. Brandt, S. Katz, P. Chauvin, L. Otto, M. Bogle, B. Wang, R. K. Meszlenyi, L. Lu, A. G. Mikos, and C. W. Patrick, "Bioactive poly(L-lactic acid) conduits seeded with Schwann cells for peripheral nerve regeneration," *Biomaterials*, vol. 23, no. 3, pp. 841–8, Feb. 2002.

[75] G. R. Evans, K. Brandt, a D. Niederbichler, P. Chauvin, S. Herrman, M. Bogle, L. Otta, B. Wang, and C. W. Patrick, "Clinical long-term in vivo evaluation of poly(L-lactic acid) porous conduits for peripheral nerve regeneration," *J. Biomater. Sci. Polym. Ed.*, vol. 11, no. 8, pp. 869–78, Jan. 2000.

[76] S. Wang, a C. Wan, X. Xu, S. Gao, H. Q. Mao, K. W. Leong, and H. Yu, "A new nerve guide conduit material composed of a biodegradable poly(phosphoester)," *Biomaterials*, vol. 22, no. 10, pp. 1157–69, May 2001.

[77] X. Xu, H. Yu, S. Gao, H.-Q. Ma, K. W. Leong, and S. Wang, "Polyphosphoester microspheres for sustained release of biologically active nerve growth factor," *Biomaterials*, vol. 23, no. 17, pp. 3765–72, Sep. 2002.

[78] X. Xu, W.-C. Yee, P. Y. . Hwang, H. Yu, A. C. . Wan, S. Gao, K.-L. Boon, H.-Q. Mao, K. W. Leong, and S. Wang, "Peripheral nerve regeneration with sustained release of poly(phosphoester) microencapsulated nerve growth factor within nerve guide conduits," *Biomaterials*, vol. 24, no. 13, pp. 2405–2412, Jun. 2003.

[79] D. J. Bryan, a H. Holway, K. K. Wang, a E. Silva, D. J. Trantolo, D. Wise, and I. C. Summerhayes, "Influence of glial growth factor and Schwann cells in a bioresorbable guidance channel on peripheral nerve regeneration," *Tissue Eng.*, vol. 6, no. 2, pp. 129–38, Apr. 2000.

[80] T. Hadlock, C. Sundback, D. Hunter, M. Cheney, and J. P. Vacanti, "A polymer foam conduit seeded with Schwann cells promotes guided peripheral nerve regeneration," *Tissue Eng.*, vol. 6, no. 2, pp. 119–27, Apr. 2000.

[81] S. H. Oh, J. H. Kim, K. S. Song, B. H. Jeon, J. H. Yoon, T. B. Seo, U. Namgung, I. W. Lee, and J. H. Lee, "Peripheral nerve regeneration within an asymmetrically porous PLGA/Pluronic F127 nerve guide conduit," *Biomaterials*, vol. 29, no. 11, pp. 1601–9, Apr. 2008.

[82] T. B. Bini, S. Gao, X. Xu, S. Wang, S. Ramakrishna, and K. W. Leong, "Peripheral nerve regeneration by microbraided poly(L-lactide-co-glycolide) biodegradable polymer fibers," *J. Biomed. Mater. Res. A*, vol. 68, no. 2, pp. 286–95, Feb. 2004.

[83] D. Yin, X. Wang, Y. Yan, and R. Zhang, "Preliminary studies on peripheral nerve regeneration using a new polyurethane conduit," *J. Bioact. Compat. Polym.*, vol. 22, no. 2, pp. 143–159, Mar. 2007.

[84] X. Wang, T. Cui, Y. Yan, and R. Zhang, "Peroneal nerve regeneration using a unique bilayer polyurethane-collagen guide conduit," *J. Bioact. Compat. Polym.*, vol. 24, no. 2, pp. 109–127, Mar. 2009.

[85] P. H. Robinson, B. Van Der Lei, H. J. Hoppen, J. W. Leenslag, A. J. Pennings, and P. Nieuwenhuis, "Nerve regeneration through a two-ply biodegradable nerve guide in the rat and the influence of ACTH4-9 nerve growth factor," *Microsurgery*, vol. 12, no. 6, pp. 412–419, 1991.

[86] L. Ghasemi-Mobarakeh, M. P. Prabhakaran, M. Morshed, M. H. Nasr-Esfahani, H. Baharvand, S. Kiani, S. S. Al-Deyab, and S. Ramakrishna, "Application of conductive polymers, scaffolds and electrical stimulation for nerve tissue engineering," *J. Tissue Eng. Regen. Med.*, vol. 5, no. 4, pp. e17–35, Apr. 2011.

[87] J. S. Belkas, C. a. Munro, M. S. Shoichet, M. Johnston, and R. Midha, "Long-term in vivo biomechanical properties and biocompatibility of poly(2-hydroxyethyl methacrylate-co-methyl methacrylate) nerve conduits," *Biomaterials*, vol. 26, no. 14, pp. 1741–1749, May 2005.

[88] X. M. Lam, E. T. Duenas, and J. L. Cleland, "Encapsulation and stabilization of nerve growth factor into poly(lactic-co-glycolic) acid microspheres," *J. Pharm. Sci.*, vol. 90, no. 9, pp. 1356–65, Sep. 2001.

[89] J. M. Péan, M. C. Venier-Julienne, F. Boury, P. Menei, B. Denizot, and J. P. Benoit, "NGF release from poly(D,L-lactide-co-glycolide) microspheres. Effect of some formulation parameters on encapsulated NGF stability," *J. Control. Release*, vol. 56, no. 1–3, pp. 175–87, Dec. 1998.

[90] M. Borkenhagen, R. C. Stoll, P. Neuenschwander, U. W. Suter, and P. Aebischer, "In vivo performance of a new biodegradable polyester urethane system used as a nerve guidance channel," *Biomaterials*, vol. 19, no. 23, pp. 2155–65, Dec. 1998.

[91] A. Wang, Z. Tang, I.-H. Park, Y. Zhu, S. Patel, G. Q. Daley, and S. Li, "Induced pluripotent stem cells for neural tissue engineering," *Biomaterials*, vol. 32, no. 22, pp. 5023–32, Aug. 2011.

[92] G. Lundborg, "A 25-year perspective of peripheral nerve surgery: evolving neuroscientific concepts and clinical significance," *J. Hand Surg. Am.*, vol. 25, no. 3, pp. 391–414, May 2000.

[93] S. Madduri, M. Papaloïzos, and B. Gander, "Synergistic effect of GDNF and NGF on axonal branching and elongation in vitro," *Neurosci. Res.*, vol. 65, no. 1, pp. 88–97, Sep. 2009.

[94] C. E. Henderson, H. S. Phillips, R. a Pollock, a M. Davies, C. Lemeulle, M. Armanini, L. Simmons, B. Moffet, R. a Vandlen, and L. Simmons, "GDNF: a potent survival factor for motoneurons present in peripheral nerve and muscle," *Science*, vol. 266, no. 5187, pp. 1062–4, Nov. 1994.

[95] W. Sun, C. Sun, H. Zhao, H. Lin, Q. Han, J. Wang, H. Ma, B. Chen, Z. Xiao, and J. Dai, "Improvement of sciatic nerve regeneration using laminin-binding human NGF-beta," *PLoS One*, vol. 4, no. 7, p. e6180, Jan. 2009.

[96] S. W. P. Kemp, A. a Webb, S. Dhaliwal, S. Syed, S. K. Walsh, and R. Midha, "Dose and duration of nerve growth factor (NGF) administration determine the extent of behavioral recovery following peripheral nerve injury in the rat," *Exp. Neurol.*, vol. 229, no. 2, pp. 460–70, Jun. 2011.

[97] K. M. Rich, J. R. Luszczynski, P. a Osborne, and E. M. Johnson, "Nerve growth factor protects adult sensory neurons from cell death and atrophy caused by nerve injury," *J. Neurocytol.*, vol. 16, no. 2, pp. 261–8, Apr. 1987.

[98] X. S. Wu and N. Wang, "Synthesis, characterization, biodegradation, and drug delivery application of biodegradable lactic/glycolic acid polymers. Part II: Biodegradation," *J. Biomater. Sci. Polym. Ed.*, vol. 12, no. 1, pp. 21–34, Jan. 2001.

[99] J. Calamia, "The sun's in your eyes: a solar-powered sensor could monitor the eyeball's pressure," *IEEE Spectrum*, p. 18, 2011.

[100] D. C. Rodger and M. S. Humayun, "Implantable parylene-based wireless intraocular pressure sensor," in *2008 IEEE 21st International Conference on Micro Electro Mechanical Systems*, 2008, pp. 58–61.

[101] J. C.-H. Lin, P.-J. Chen, B. Yu, M. Humayun, and Y.-C. Tai, "Minimally invasive parylene dual-valved flow drainage shunt for glaucoma implant," in *2009 IEEE 22nd International Conference on Micro Electro Mechanical Systems*, 2009, pp. 196–199.

[102] D. C. Rodger, S. Saati, and M. S. Humayun, "Microfabricated implantable parylene-based wireless passive intraocular pressure sensors," *J. Microelectromechanical Syst.*, vol. 17, no. 6, pp. 1342–1351, Dec. 2008.

[103] K.-M. Lin, C. Bishop, H. Sant, B. Ambati, and B. Gale, "Refilling mechanism to stabilize a free-floating intraocular capsule drug ring (CDR)," in *AIChE Annual Meeting*, 2010, p. 568v.

[104] K. Atsuta, H. Noji, and S. Takeuchi, "Micro patterning of active proteins with perforated PDMS sheets (PDMS sieve)," *Lab Chip*, vol. 4, no. 4, pp. 333–6, Aug. 2004.

[105] J. L. Tan, J. Tien, D. M. Pirone, D. S. Gray, K. Bhadriraju, and C. S. Chen, "Cells lying on a bed of microneedles: an approach to isolate mechanical force," *Proc. Natl. Acad. Sci. U. S. A.*, vol. 100, no. 4, pp. 1484–9, Mar. 2003.

[106] Akorn, "Akorn IC-Green (IC-G)," Lake Forest, IL, 2008.

[107] Akorn, "Akorn AK-Fluor (fluorescein injection, USP) 10% dyes and tests," Lake Forest, IL, 2008.

[108] M. A. Eddings, M. A. Johnson, and B. K. Gale, "Determining the optimal PDMS–PDMS bonding technique for microfluidic devices," *J. Micromechanics Microengineering*, vol. 18, no. 6, p. 067001, Jun. 2008.

[109] S. K. Lee and S. W. Wolfe, “Peripheral nerve injury and repair,” *J. Am. Acad. Orthop. Surg.*, vol. 8, no. 4, pp. 243–252, 2000.

[110] F. Stang, G. Keilhoff, and H. Fansa, “Biocompatibility of different nerve tubes,” *Materials (Basel).*, vol. 2, no. 4, pp. 1480–1507, Sep. 2009.

[111] S. Madduri, K. Feldman, T. Tervoort, M. Papaloïzos, and B. Gander, “Collagen nerve conduits releasing the neurotrophic factors GDNF and NGF,” *J. Control. Release*, vol. 143, no. 2, pp. 168–74, May 2010.

[112] A. M. Moore, M. D. Wood, K. Chenard, D. a Hunter, S. E. Mackinnon, S. E. Sakiyama-Elbert, and G. H. Borschel, “Controlled delivery of glial cell line-derived neurotrophic factor enhances motor nerve regeneration,” *J. Hand Surg. Am.*, vol. 35, no. 12, pp. 2008–17, Dec. 2010.

[113] V. B. Doolabh, M. C. Hertl, and S. E. Mackinnon, “The role of conduits in nerve repair: a review,” *Rev. Neurosci.*, vol. 7, no. 1, pp. 47–84, 1996.

[114] R. Meirer, R. Gurunluoglu, and M. Siemionow, “Neurogenic perspective on vascular endothelial growth factor: review of the literature,” *J. Reconstr. Microsurg.*, vol. 17, no. 8, pp. 625–30, Nov. 2001.

[115] J. S. Belkas, M. S. Shoichet, and R. Midha, “Peripheral nerve regeneration through guidance tubes,” *Neurol. Res.*, vol. 26, no. 2, pp. 151–60, Mar. 2004.

[116] K.-M. Lin, H. J. Sant, B. K. Gale, and J. P. Agarwal, “New approaches to bridge nerve gaps: development of a novel drug-delivering nerve conduit,” *Conf. Proc. IEEE Eng. Med. Biol. Soc.*, vol. 2012, pp. 747–50, Jan. 2012.

[117] K.-M. Lin, B. K. Gale, H. Sant, J. Shea, W. Sanders, C. M. Terry, and J. P. Agarwal, “BSA-filled PLGA nerve conduits for potential applications in nerve regeneration,” in *Biomedical Engineering Society (BMES) Annual Meeting*, 2013.

[118] W. M. Saltzman, M. W. Mark, M. J. Mahoney, E. T. Duenas, and J. L. Cleland, “Intracranial delivery of recombinant nerve growth factor: release kinetics and protein distribution for three delivery systems,” *Pharm. Res.*, vol. 16, no. 2, pp. 232–240, 1999.

[119] R. Herrero-vanrell, L. Ramirez, A. Fernandez-carballido, and M. F. Refojo, “Loaded with ganciclovir for intraocular administration. Encapsulation technique, in vitro release profiles, and sterilization process,” *Pharm. Res.*, vol. 17, no. 10, pp. 1323–1328, 2000.

[120] T. C. Amu, “Activation enthalpy of diffusion for well fractionated dextrans in aqueous solutions,” *Biophys. Chem.*, vol. 16, no. 4, pp. 269–273, Dec. 1982.

[121] S. Y. Fu and T. Gordon, “The cellular and molecular basis of peripheral nerve regeneration,” *Mol. Neurobiol.*, vol. 14, no. 1–2, pp. 67–116, Jan. 1977.

[122] T. Mimura, M. Dezawa, H. Kanno, H. Sawada, and I. Yamamoto, “Peripheral nerve regeneration by transplantation of bone marrow stromal cell-derived Schwann cells in adult rats,” *J. Neurosurg.*, vol. 101, no. 5, pp. 806–12, Nov. 2004.

[123] M. I. Hobson, C. J. Green, and G. Terenghi, “VEGF enhances intraneural angiogenesis and improves nerve regeneration after axotomy,” *J. Anat.*, vol. 197 Pt 4, pp. 591–605, Nov. 2000.

[124] M. D. Wood, D. Hunter, S. E. Mackinnon, and S. E. Sakiyama-Elbert, “Heparin-binding-affinity-based delivery systems releasing nerve growth factor enhance sciatic nerve regeneration,” *J. Biomater. Sci. Polym. Ed.*, vol. 21, no. 6, pp. 771–87, Jan. 2010.

[125] P. Camarata, R. Suryanarayanan, D. Turner, R. Parker, and Timothy Ebner, “Sustained release of nerve growth factor from biodegradable polymer microspheres,” *Neurosurgery*, vol. 30, no. 3, pp. 313–319, 1992.

[126] X. Cao and M. S. Schoichet, “Delivering neuroactive molecules from biodegradable microspheres for application in central nervous system disorders,” *Biomaterials*, vol. 20, no. 4, pp. 329–39, Feb. 1999.

[127] K. J. Lampe, A. L. Antaris, and S. C. Heilshorn, “Design of three-dimensional engineered protein hydrogels for tailored control of neurite growth,” *Acta Biomater.*, vol. 9, no. 3, pp. 5590–9, Mar. 2013.

[128] C. E. Astete and C. M. Sabliov, “Synthesis and characterization of PLGA nanoparticles,” *J. Biomater. Sci. Polym. Ed.*, vol. 17, no. 3, pp. 247–89, Jan. 2006.

[129] N. Csaba, L. González, A. Sánchez, and M. J. Alonso, “Design and characterisation of new nanoparticulate polymer blends for drug delivery,” *J. Biomater. Sci. Polym. Ed.*, vol. 15, no. 9, pp. 1137–51, Jan. 2004.

[130] C. E. Holy, C. Cheng, J. E. Davies, and M. S. Shoichet, “Optimizing the sterilization of PLGA scaffolds for use in tissue engineering,” *Biomaterials*, vol. 22, no. 1, pp. 25–31, Jan. 2001.

[131] M. H. Lee, H.-L. Kim, C. H. Kim, S. H. Lee, J. K. Kim, S. J. Lee, and J.-C. Park, “Effects of low temperature hydrogen peroxide gas on sterilization and cytocompatibility of porous poly(d,l-lactic-co-glycolic acid) scaffolds,” *Surf. Coatings Technol.*, vol. 202, no. 22–23, pp. 5762–5767, Aug. 2008.

[132] A. L. Thangawng, R. S. Ruoff, M. a Swartz, and M. R. Glucksberg, “An ultra-thin PDMS membrane as a bio/micro-nano interface: fabrication and characterization,” *Biomed. Microdevices*, vol. 9, no. 4, pp. 587–95, Aug. 2007.

[133] S. L. Peterson, A. McDonald, P. L. Gourley, and D. Y. Sasaki, “Poly(dimethylsiloxane) thin films as biocompatible coatings for microfluidic devices: cell culture and flow studies with glial cells,” *J. Biomed. Mater. Res. A*, vol. 72, no. 1, pp. 10–8, Jan. 2005.

[134] E. Ostuni, R. Kane, C. S. Chen, D. E. Ingber, and G. M. Whitesides, “Patterning mammalian cells using elastomeric membranes,” *Langmuir*, vol. 16, no. 20, pp. 7811–7819, Oct. 2000.

[135] Y. Xia and G. M. Whitesides, “Soft lithography,” *Annu. Rev. Mater. Sci.*, vol. 28, no. 12, pp. 153–84, 1998.

[136] J. C. Mcdonald, D. C. Duffy, J. R. Anderson, D. T. Chiu, H. Wu, O. J. A. Schueller, and G. M. Whitesides, “Fabrication of microfluidic systems in poly(dimethylsiloxane),” *Electrophoresis*, vol. 21, pp. 27–40, 2000.

[137] M. A. Eddings and B. K. Gale, “A PDMS-based gas permeation pump for on-chip fluid handling in microfluidic devices,” *J. Micromechanics Microengineering*, vol. 16, no. 11, pp. 2396–2402, Nov. 2006.

[138] L.M. Fouldsa, L. Leversha, F.J. Morgan, M.T.W. Hearn, H.G. Burger, R.E.H. Wettenhall and D.M. de Kretsera, “Isolation of inhibin from bovine follicular fluid,” *Biochem. Biophys. Res. Commun.*, vol. 126, no. 1, pp. 220–226, 1985.

[139] S. K. Kassim, E. M. El-Salahy, S. T. Fayed, S. A. Helal, T. Helal, E. E. Azzam, and A. Khalifa, “Vascular endothelial growth factor and interleukin-8 are associated with poor prognosis in epithelial ovarian cancer patients,” *Clin. Biochem.*, vol. 37, no. 5, pp. 363–9, May 2004.

[140] H. Yan, F. Zhang, M. B. Chen, and W. C. Lineaweaver, “Chapter 10: Conduit luminal additives for peripheral nerve repair,” *Int. Rev. Neurobiol.*, vol. 87, pp. 199–225, Jan. 2009.

[141] W. M. Saltzman, M. W. Mak, M. J. Mahoney, E. T. Duenas, and J. L. Cleland, “Intracranial delivery of recombinant nerve growth factor: release kinetics and protein distribution for three delivery systems,” *Pharm. Res.*, vol. 16, no. 2, pp. 232–40, Feb. 1999.

[142] M. Stroh, W. R. Zipfel, R. M. Williams, W. W. Webb, and W. M. Saltzman, “Diffusion of nerve growth factor in rat striatum as determined by multiphoton microscopy,” *Biophys. J.*, vol. 85, no. 1, pp. 581–8, Jul. 2003.